CLRTO PERFORMANCE MONITORING, DIAGNOSING AND ENHANCEMENT

MONITORING, DIAGNOSING AND ENHANCING THE PERFORMANCE OF LINEAR CLOSED-LOOP REAL-TIME OPTIMIZATION SYSTEMS

by

DANIELLE ZYNGIER, B.Sc., M.Sc.

A Thesis Submitted to the School of Graduate Studies
in Partial Fulfillment of the Requirements
for the Degree

Doctor of Philosophy

McMaster University

Abstract

Linear Programming (LP) has a wide range of industrial applications, including closed-loop systems such as real-time optimization and the steady-state economic optimization at each execution of Model Predictive Controllers. This thesis presents new metrics for monitoring the performance of linear closed-loop real-time optimization systems, as well as new methods for improving their performance when necessary. A novel diagnostic method for ranking parameter importance with respect to the objective function is also presented.

Many standard methods are available for estimating the effects of parameter uncertainty on the objective function without a basis change, and more powerful existing methods require enumeration or sampling. This work introduces new sensitivity methods in LP problems with uncertain coefficients that can be correlated, appear in equality and inequality constraints, and have uncertainties with large enough magnitudes to lead to basis changes.

The new monitoring approach measures the uncertainty effect as the range between the maximum and minimum profit in the plant under closed-loop optimization, termed the *Profit Gap*, and both its maximum and expected values can be determined.

If the monitoring indicates a substantial Profit Gap could exist, the improvement step designs experiments to reduce parametric uncertainty. The unique experimental design maximizes the total profit during and after the experiment to the end of a production run.

Both the monitoring and improvement methods involve the solution of bilevel optimization problems, which include complementarity constraints. Results of application to a closed-loop gasoline-blending problem demonstrate the power of the methods. The

studies include typical uncertainties and measurement noise and show the economic benefits possible through the application of real-time monitoring and improvement.

Acknowledgements

First of all, I would like to thank my advisor, Dr. Thomas Marlin, for his patience and understanding. His enthusiasm has always been a source of inspiration to me. I would also like to thank Dr. Marlin for sharing his insight and for giving me the opportunity to experience first-hand the teaching profession through the teaching assistantship position in his Process Control course for several terms.

Thank you to Dr. Andrew Hrymak and Dr. George Wesolowsky for their comments during my committee meetings.

I am very appreciative of the lectures from Dr. Tamás Terlaky and Dr. John MacGregor, who introduced me to the world of Optimization and Multivariate Statistics. They are wonderful teachers.

Over the course of my stay at McMaster, several faculty members were particularly receptive and helpful in many occasions. In special, I would like to thank (in alphabetical order) Dr. Hrymak, Dr. Kourti, Dr. Loutfy, Dr. MacGregor, Dr. Marlin, Dr. Swartz and Dr. Terlaky.

I have been fortunate enough to have made some good friends during my stay at McMaster, with whom I have had many technical and non-technical discussions. We had a real good time. Thank you all for making these years so enjoyable.

Dale Mudt from Sunoco Canada has provided me with very helpful information on gasoline-blending processes. More recently, Andrew Chin, Jeff Kelly and Randy Wagler from Honeywell have also offered me information on several industry-related topics. I thank them all for that.

I would also like to thank Lynn Falkiner, Kathy Goodram, Andrea Vickers, Julie Birch and Lara for always helping me out.

Words would not be enough to thank my husband, Leonardo, for being there for me all along, in good and bad times. His love and support have made this whole journey extraordinary. Special thanks to Olivia, for coming into our lives during the course of this work and for being a great source of inspiration and joy ever since.

To my parents, Sonia and Felix, and to my brother, Ivan, thank you very much for always having been encouraging and supportive of all of my projects.

Table of Contents

DOCTOR OF PHILOSOPHY (2006) McMaster University

(Chemical Engineering) Hamilton, Ontario, Canada

TITLE:	Monitoring, Diagnosing and Enhancing the Performance of Linear Closed-Loop Real-Time Optimization Systems
AUTHOR:	Danielle Zyngier, B.Sc., M.Sc. (Federal University of Rio de Janeiro)
SUPERVISOR:	Professor Thomas E. Marlin
NUMBER OF PAGES:	xvii, 202

List of Figures

List of Tables

Chapter 1
Introduction

1.1 . Optimization in the Process Industries

Optimization has been successfully applied in the process industries since the beginning of mathematical programming and digital computation (e.g., Symonds, 1955). Because of the many degrees of freedom in complex process applications, optimization can improve solutions obtained through experience or heuristics. Because of the large cash flows, the economic benefits are often substantial. Typical optimization applications involve models that contain uncertain parameters; therefore, the benefits of optimization can be eroded because of model uncertainty. This study develops methods for monitoring the performance of process optimization and for improving the performance when severe degradation is possible due to uncertainty.

1.1.1 . General properties of optimization problems

An optimization problem comprises an objective function which is to be minimized or maximized. In some cases, inequality and equality constraints must be added to the optimization problem. Inequality constraints may be of two types, Bounds or General. Bounds are used when the decision variables in the problem must be limited by upper and/or lower values. For example, in a process plant, individual flowrates cannot have negative values or be above the maximum pumping capacity. General constraints are used where some function of the variables (e.g. summation of flowrates) must be limited (Williams, 1999). Equality constraints define the relationship between dependent and independent variables, such as in the case where the production rate has to be exactly equal to the demand.

There are two methods for optimizing an existing physical system. One method is through continuous perturbation of process variables in the plant, which is called Evolutionary Operations (EVOP) (Box and Draper, 1998). Besides requiring continual perturbations of the system, EVOP does not ensure satisfying process constraints in the dependent variables, and scales poorly with the number of manipulated variables. The second method is by optimizing a mathematical model of the system and implementing the results in the system. Since mismatch will undoubtedly exist between the model and the real system, measurements can be used to provide updated estimates of model parameters. This research investigated the performance of model-based optimization.

The optimization systems addressed in this thesis include feedback of measured variables for model correction, which is a common optimization approach used in the process industries. Optimization models can be used in either an open-loop or closed-loop manner. These two approaches are briefly explained in the following two subsections.

1.1.2 . Open-Loop Optimization

In open-loop optimization systems, the model-based optimization results are implemented in the process, and no information from the process is used to update or correct the model or calculated results (Figure 1.1a). In automatic control, this approach would be termed feedforward. We note that the decisions from open-loop optimization could be implemented automatically or could rely on a person for implementation. Naturally, the performance of an open-loop optimization can be strongly affected by model mismatch, but it is sometimes the only possible approach when timely measurements are not available.

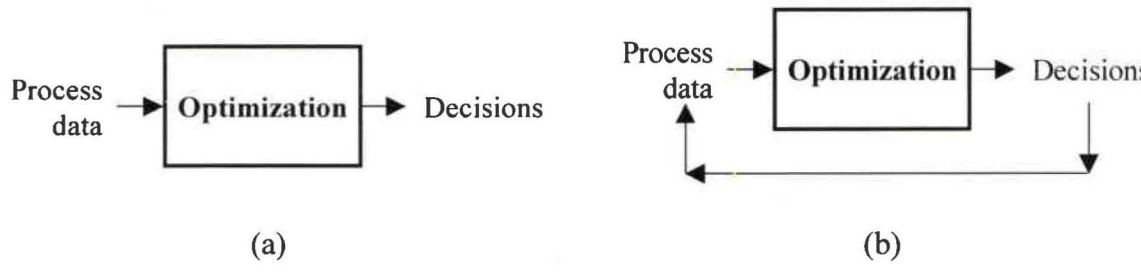

Figure 1.1. (a) Open-Loop and (b) Closed-Loop Optimization

There are several typical applications of open-loop optimization problems in industry. As an example, one application is in plant design problems, in which one must determine what is the best set of design variables – e.g., tank volumes, number of trays in a column, and so on – in a process.

1.1.3 . Closed-Loop Optimization

Closed-loop optimization is the term used to describe a system that contains some form of feedback information that modifies subsequent optimization calculations (Figure 1.1b). In plant operations, the information is provided by real-time sensors to measure selected physical variables. Naturally, the feedback has the potential for reducing the effects of model mismatch and disturbances, but in general, feedback cannot eliminate their effects.

A wide variety of approaches are possible for using measurements to update the model used in the optimization. The approach used in this study involves the Model-Predictive Control (MPC) structure, which is widely employed in the process industries. In MPC, future values of selected manipulated variables are determined to optimize an objective function, which includes controlled and manipulated variables. The measured values of the controlled variables are used for the feedback. This control structure has several excellent properties; primary among these are zero-steady-state offset from the

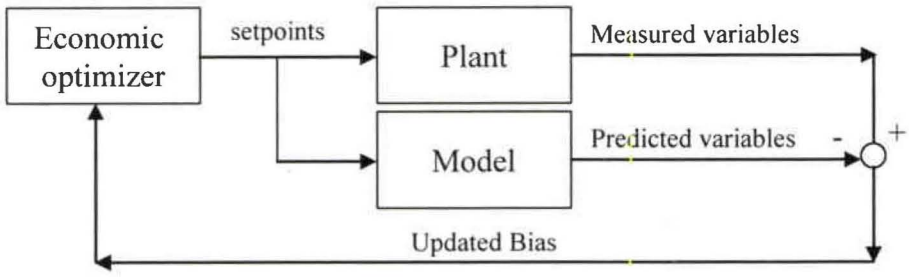

Figure 1.2. Structure of a Model Predictive Controller (MPC)

setpoints (reference values) and flexible feedback compensation that is not restricted by a fixed control law, such as PID or other algorithm. The structure of an MPC controller can be seen in Figure 1.2, and details of the structure are given in Appendix A.

As we will see, the applications in this study involve quasi-steady-state processes (note that the system is dynamic, because it takes several iterations to reach steady-state), so that dynamic performance is less of an issue

This thesis concentrates on Closed-Loop Real-Time Optimization (CLRTO) using the MPC structure. In Real-Time Optimization (RTO), the economic optimization of a system is achieved by adjusting manipulated variables, which often are setpoints of controllers. The calculations involved in the feedback compensation in model updating will be presented in subsequent chapters. The extension to open-loop optimization is presented with examples in Appendix E.

1.2 . Linear Programming

Many optimization problems in the process industries are based on linear equations; thus, linear programming is the natural choice for these optimization problems. Although processes are nearly always nonlinear, adequate optimization results can often be obtained by careful modelling, e.g., disjunctive, separable, base-delta, etc. (Williams, 1999) and restricting operations within the linear region. Linear programming has mathematical properties that make it attractive for use in closed-loop optimization, where obtaining rapid and reliable solutions is important.

This thesis concentrates on linear programming because of its importance in the process industries. While the selection might appear limiting, CLRTO using linear programming contains some of the most challenging aspects of the research project, which are monitoring the performance of *closed-loop* optimization of uncertain processes with the possibility of *changing active inequality constraints*. The extension of results to nonlinear problems is briefly introduced in Appendix E.

1.3 . Monitoring the Performance of Economic Optimization

Optimizing a complex process using linear programming will perform well, i.e., achieve nearly the best possible objective in the real process, when model mismatch is small. Therefore, monitoring the performance of an optimizer involves determining a metric that measures the effect of model mismatch. Performance monitoring is complicated by the typical situation in which the objective achieved in the real plant cannot be measured exactly because of sensor inaccuracies and in some cases, missing measurements. Therefore, monitoring requires two key elements: a description of the potential model mismatch, i.e., the uncertainty, and a metric of the effect of uncertainty on optimization performance.

Model mismatch can result from structural mismatch between the model and true plant and from parametric mismatch between the model and in the true plant. No structural mismatch between model and plant is considered in this work. All plant/model mismatch originates from the difference between parameters in the true plant and in the model. In this work, the parameter uncertainties are described using two different approaches: (1) interval model parameter uncertainty, which is used whenever there is little or no knowledge about the correlation structure of the system, and (2) ellipsoidal model parameter uncertainty, which uses the variance-covariance matrix of the system that represents either correlated or independent parameter variations. Ellipsoidal uncertainty could result from a multivariate normal distribution, where parameters are assumed to vary within an ellipsoid with confidence regions delimited by the chi-square statistic. In some formulations in this work, only the boundary of this ellipse was taken

into consideration, whereas in other formulations, an approximation of the parameter probability distribution was considered.

The performance metric addresses the objective function. In process examples, the objective function is the profit of the operation, and if secondary items are important, such as changes to the manipulated variables, they can be included either in the objective function or as variable bounds. As previously noted, the objective function value in the true plant cannot be obtained in the general situation. A potential straightforward approach for improving the model would involve perturbing the process to compare the responses of the model and true plant; however, continual perturbations would be very costly. Therefore, this work presents monitoring methods that do *not require plant perturbations*. The monitoring method develops scalar measures on the performance of the uncertain system; for example, the greatest possible loss in profit due to mismatch or the expected value of the loss due to mismatch.

When monitoring performance, the user must decide a critical value that distinguishes "good" from "poor" performance. Since the objective function is the metric in the monitoring method, the critical value will be profit, which is expressed in $/day in the examples in this work. The critical value is *problem dependent*. However, one generally would not strive for a metric value of $0.0/day because the effort for further improvement would not be worth the gain and because the monitoring methods provide only an estimate of the improvements, which are not exact. In this work, we will use a critical value of roughly $100/day for the maximum tolerable profit loss due to mismatch. When the metric is below the critical value, the system is deemed to be functioning acceptably. The threshold value should be defined based on the trade-off between the inherent achievable accuracy given the available sensors (which would be very significant for a production with a large cash flow), the true costs of changing operation, and organizational barriers.

1.4. Optimizer Performance Diagnosis and Enhancement

When the metric indicates unacceptable performance, the engineer would like to improve the performance of the CLRTO system, which requires reducing the model

mismatch. There are a few approaches for improving parameter estimates. First, one can measure each uncertain parameter by onstream analysis or by sampling with subsequent offline analysis. These approaches definitely increase the process cost. Besides, onstream measurement might even be impossible, depending on the system. Second, a more accurate first-principles model can be developed in order to achieve better estimates of the model parameters. However, when the more accurate model is not readily available, it is expensive to develop and might not provide the required accuracy. Finally, a third option is to re-estimate model parameters by running designed experiments in the plant, which can be costly. This thesis presents novel experimental designs that minimize total cost, so that the experiment yields the optimum tradeoff between the costs of experimentation and the benefits of future (improved) operation after the experiment.

In some systems, it is useful to obtain diagnostic information about the relative importance of parameter uncertainty with respect to the optimizer performance. This information can help in sensor location problems or in focusing fundamental model improvement efforts. This thesis presents a method for determining the relative importance of parameters with respect to the objective function that does not require a constant active constraint set.

1.5 . The Major Case Study and a Motivating Example

The methods are developed for application to any CLRTO using linear programming. The case studies in this work demonstrate the efficacy of the methods on an industrial process. The blending of petroleum products to manufacture gasoline has been selected because it has the basic properties of the process systems being considered in this research, namely:

- The process can be modeled with reasonable accuracy using linear programming;
- CLRTO has been applied to many industrial gasoline blending processes using the MPC structure;
- The process has significant uncertainty in constraint parameters that multiply variables, i.e., left-hand side coefficients in a linear program;

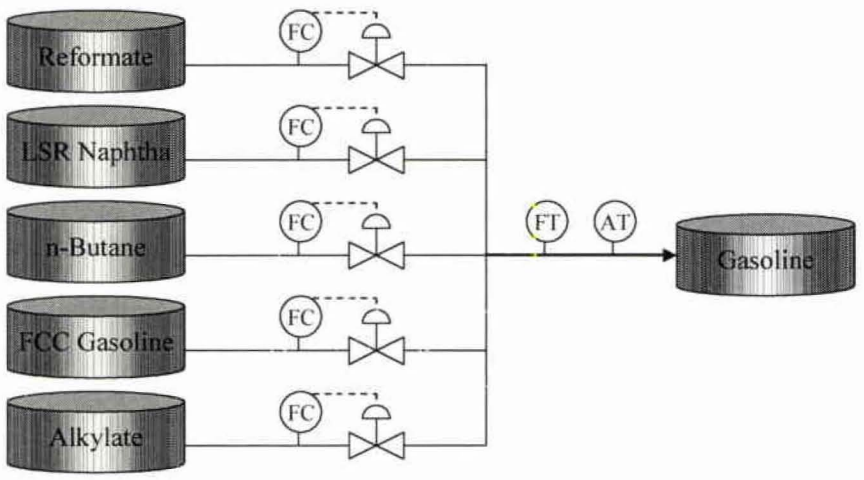

Figure 1.3. Gasoline Blending Process

- The process is economically important and has opportunity for further improvements via monitoring and diagnosis;
- The process is representative of other CLRTO systems using an LP.

In an oil refinery, there are several important blending processes, such as the blending of crude oil, gasoline and fuel oil. Most of the case studies in this thesis refer to the gasoline-blending process, which has great economic incentive for optimizer performance improvement.

In the gasoline-blending process considered in this work, five components are blended to form the final gasoline product: Reformate, Light-Straight Run (LSR) Naphtha, n-Butane, FCC Gasoline and Alkylate (Figure 1.3). There are two property specifications that are very relevant to customers: octane number and Reid vapour pressure (RVP). These properties are only measured online for the final product.

The five components are either purchased or obtained from upstream operation that has variable operating conditions, and are stored in large tanks; therefore, short-term violations of component properties are allowed. The component properties are only measured very infrequently, e.g., once a week (Mudt, 2005; Kelly, 2006). Also, due to occasional shortage of storage capacity, components may be pre blended into component

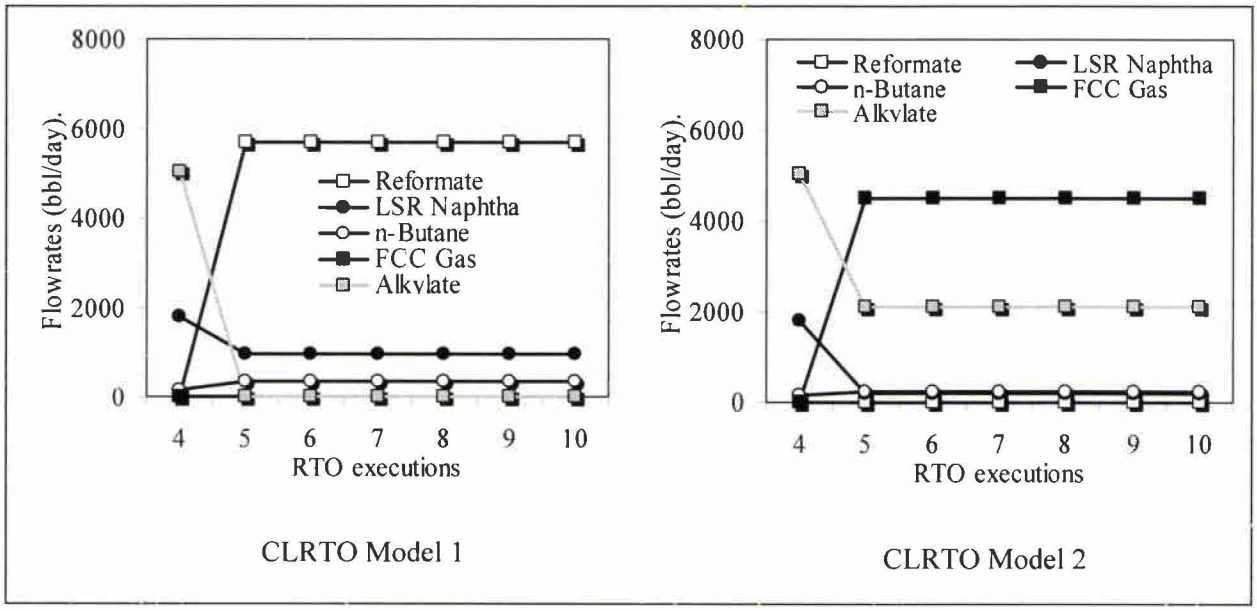

Figure 1.4. Result of Parametric Mismatch on CLRTO operation

tanks (Kelly, 2006; Chin, 2006). Therefore, the octane numbers and RVP for each of the components are a significant source of uncertainty to this CLRTO system. Details on this process can be found in Appendix A.

The closed-loop implementation of RTO has limited feedback information, since only the right-hand side of the constraints ("bias") is updated (Figure 1.2). This is a common feedback structure in industrial applications, such as MPC systems. The bias-updating method, however, is only guaranteed to lead the system to the true plant optimum if the parametric mismatch between model and plant is small enough; Forbes and Marlin (1994) provide the mathematical definition for the needed size of uncertainty. If the parametric mismatch is too large, the CLRTO may operate at an optimum different from the true plant.

To demonstrate the effect of parametric mismatch, Figure 1.4 shows the flowrates of gasoline components to the final blend during a blending batch. These flowrates were calculated by the CLRTO system for the *same* plant parameters using *different* CLRTO models; i.e., linear models with different parameter values. The octane number and RVP quality specifications of the final product are met for both CLRTO models. However,

only one of the two models results in a system achieving its true plant optimum. With no additional information about this system, how is it possible to know which operation is better or whether either is close to the true plant optimum? Which model parameters should be re-estimated in order to achieve potentially more profitable operation? How should the parameters be re-estimated in order not to have major disruptions in plant operation? Such questions are answered by using the methods developed in this work.

1.6 . Importance and Contributions

Perhaps the major question for the reader is: "Is this work important?" The value can be evaluated based on the importance for applications and on the contributions to technology. Both are addressed briefly in this section.

1.6.1 . Useful applications

In process industries, LP has been used in many applications, such as planning and scheduling models, which assign, time, size and sequence operations in production. Yet another application of LPs is in selected CLRTO systems when the linear(ized) model provides adequate accuracy. This generally occurs when the optimum is known to occur at a corner point of the feasible region, which is assured in the LP solution. Linear CLRTO blending systems exist, for example, in cement manufacture and in coal mixing for use as fuel. The approaches in this research are tailored for application to CLRTO, and two important applications of LP-based CLRTO are discussed in this section.

One of the earliest applications of closed-loop linear programming was to gasoline blending (Birchfield, 2002), which resulted from the enormous economic importance of this process. For example, the average gasoline demand in the USA is about 3.8×10^8 gal/day (Oak Ridge National Laboratory, 2004). At the current cost of gasoline (about 2.50 $/gal), the total cost to the US consumer is about 3.5×10^{11} (350 billion) $/year! Clearly, even small percentage improvements in the blending process can have significant benefit to refining companies and consumers.

In addition, the LP in the widely used Model Predictive Controller (MPC) has the same structure as the systems considered in this thesis, so that the results of this work are

applicable to the steady-state optimization of MPC systems. Linear models are used in steady-state optimization to give the final conditions for MPC controllers (Qin and Badgwell, 1997). The final steady-state solution is required for (1) open-loop unstable processes, and (2) non-square control systems, where extra degrees of freedom are used to improve the profitability of the plant operation. Besides blending processes, MPCs are a very significant application of the technology, since there are approximately 4,000 MPC controllers currently installed worldwide, and MPC implementation growth rates are expected to increase in the next few years with the recent rise in oil prices and due to growth in China, Eastern Europe, India and the Middle East (Wagler, 2006). Since MPC implementation costs for a single refinery process unit may range from $250,000 to $500,000 (Wagler, 2006), it is clear that methods are required to monitor the performance of the LP in the MPC, and that improve it if necessary.

The formulations in this thesis were tailored to linear CLRTO systems, and were applied to a 5-manipulated-variable blending process. The extension of the methods to open-loop linear optimization problems is straightforward. Nonlinear optimization problems may also benefit from the technology, although some post-solution checks must be made. The extensions to open-loop linear and nonlinear problems are discussed in Appendix E. The computational aspects of the application of the methods to larger optimization problems (20+ variables) should be evaluated in the future.

1.6.2 . Technical contributions

This work concentrates on optimization of uncertain systems. The importance of this topic was identified by a recent NSF-funded workshop on Statistics and Operations Research (Robinson, 2005), where some of the key issues in these fields were identified. Amongst those issues selected as high priority were (1) the design of profit-based experiments to reduce the uncertainty in key parameters, and (2) screening the uncertain model parameters to determine their importance on optimizer performance. This research addresses these two issues, along with a performance monitoring method to identify when these two technologies are needed for a specific application.

The work described in this thesis presents the following new technical contributions.

- Modelling the behaviour of the LP-based closed-loop real-time optimization system (CLRTO) in one simultaneous equation set
- Modelling the effect of uncertainty in CLRTO system on plant profit
- Evaluating several metrics for the effect of parameter mismatch on CLRTO performance, i.e., profit
- Developing a diagnostic method for ranking the effects of uncertain parameters
- Designing novel, profit-based experimental designs appropriate for enhancing CLRTO performance in operating plants
- Applying the methods to several cases of an industrially-relevant blending process
- Extending the monitoring methods to open-loop linear problems and to a preliminary study of nonlinear problems

A new sequential procedure for implementing the monitoring and enhancement of closed-loop linear RTO systems was also developed. The method is designed to monitor and diagnose CLRTO performance without plant perturbations. The sequential nature of the procedure enables its interruption whenever performance is deemed satisfactory. Also, it ensures that the cost-effective experiments are implemented only when necessary.

1.7 . Overview of the Thesis

The thesis is outlined as follows:

- Chapter 2 gives an overview of technology related to this work, including related optimization problems and solution strategies.
- Chapter 3 presents CLRTO performance monitoring approaches. One approach is based on the number of corner points, and four approaches are based on the Profit Gap. Monitoring CLRTO performance determines if model enhancements are necessary.

- Chapter 4 contains different experimental design strategies for when there is the need for CLRTO model enhancement. Experiments are designed in a cost-efficient manner. This chapter also presents the diagnostic method for determining key model parameters whose uncertainty should be reduced in order to achieve a better RTO performance metric.
- Chapter 5 presents a sequential procedure for implementing the CLRTO monitoring and enhancement strategy, so that model/plant mismatch is assessed and the plant is perturbed (only if needed) by profit-based experiments.
- Finally, Chapter 6 summarizes the work with conclusions and future extensions to the technology developed in this thesis.

A **Nomenclature** section contains all the symbols used throughout this thesis.

1.8. Thesis Conventions

In this work, **closed-loop real-time optimization (CLRTO)** and **real-time optimization (RTO)** refer to a steady-state constrained economic optimizer operated under closed-loop, where the term **real time** refers to how measurements are obtained (as opposed to computing). **True** plant properties refer to properties that occur in the real process, and that are not known by operating personnel. **Model** (or **RTO** or **CLRTO**) **parameters or properties** are properties used in the RTO model.

Optimizer performance measures the potential economic loss due to parametric uncertainty. The **Profit Gap** is defined as the difference between CLRTO operation under perfect knowledge of parameter values and CLRTO operation using nominal parameter values. It is an indication of the cost of uncertainty in a system.

Optimizer Performance Enhancement aims at reducing the parameter uncertainty in order to decrease the potential economic loss (Profit Gap) in the optimization problem. In the extensions to open-loop problems, there are references to **best-case (worst-case) properties**. These properties are those that yield the best (worst) objective function value in an optimization problem (for instance, highest (lowest) profit).

Chapter 2

Technology Survey

Model-based optimization employs a mathematical model of a process when determining feasible values of the variables that yield the best objective function value. As a result, the performance of model-based optimization depends on the accuracy of the model. This research develops methods for quantifying the potential loss in performance, i.e., deviation in the true plant objective function from its optimum value, due to model errors. This chapter reviews the relevant state-of-the-art in formulation of optimization problems under uncertainty and solution methods.

Linear programming problems have found wide application in the process industries, such as in blending processes and in the steady-state optimization within Model Predictive Control systems. Due to their practical importance, linear closed-loop RTO systems were considered in this work. More details are presented in Section 2.4.

If the performance of a CLRTO system is deemed unacceptable, parameter uncertainty should be reduced. One of the ways to achieve this is through designed experiments in the plant. The formulations in this thesis differ from state-of-the-art experimental design strategies in that they take the cost of experimentation into account, as well as the CLRTO monitoring metric of choice. More details can be seen in Section 2.2.2.

Once plant data has been obtained, parameters should be re-estimated in order to improve CLRTO model accuracy. The parameter-updating method of choice was Bayesian estimation, since prior information about parameter uncertainty can be included (Section 2.2.3). This information is obtained from historical data from previous processing runs.

Finally, several formulations in this work involve bilevel optimization problems. Solving these problems is computationally very challenging, requiring special reformulations. An overview of this field is given in Section 2.3.3.

2.1. Sensitivity Analysis

The work in this thesis concentrates on the sensitivity of the objective function with respect to parameter uncertainty, which may originate in any of the coefficients of the problem (including left-hand side coefficients of constraints). The parameter uncertainty may cause the active set to change, and the objective function values are compared at different optimal bases without the need for enumerative procedures.

A natural topic when dealing with uncertain systems is to evaluate how much the problem is affected by parameter uncertainty. This is the goal of sensitivity analysis (SA). SA evaluates the sensitivity of the problem to changes in variables *after* the decisions have been made, and therefore are not appropriate methods for integration into the optimization decisions.

Traditional sensitivity analysis methods for linear programming provide valuable information about changes in selected single parameters (Winston, 1994; Nash and Sofer, 1996). They give the effect on the objective of changes in the right-hand side of inequalities and changes in cost coefficients. In addition, they give ranges for each coefficient over which the optimal basis (active set) does not change. Limited results are available for multiple coefficient changes via the 100% rules that give the maximum total changes for multiple coefficients for which the basis is guaranteed not to change. These methods find wide application in applied optimization.

Unfortunately, these traditional methods are not applicable to the problems posed in this research. First, in addition to cost and right-hand side uncertainty, the problems in this research have uncertainty in the left-hand side coefficients, i.e. those that are multiplied by variables in the constraint equalities and inequalities. Second, many parameters have uncertainty simultaneously. Third, a key issue in this research is the evaluation of changes in parameters when the optimal basis changes.

Chinneck and Ramadan (2000) determined the sensitivity of LP problems to parametric interval uncertainty. They use interval mathematics to determine the worst-case (best-case) value of each parameter, and then, they solve the resulting LP for the worse-case (best-case) objective value. Chinneck and Ramadan solve problems similar to those in this research; however, substantial differences exist. First, they address "open-loop" systems without feedback correction. Second, they allow only independent parameter variations, *i.e.*, no correlation among parameters is considered. Third, their solution method requires a combinatorial procedure to deal with uncertainty in equality constraints. However, the problems of Chinneck and Ramadan are of practical interest and therefore the solution methods developed in this research were applied to their problems to demonstrate the advantages of these new formulations. The results can be found in Appendix E.

Finally, the effect of parameter variation can be determined by introducing changes to relevant parameters and re-solving the optimization problem. This approach might be attractive when few, discrete candidates are to be evaluated. However, the uncertain parameters are continuous within a defined region; therefore, a large number of cases would be required to estimate the effect of uncertainty (Sen and Higle, 1999). In addition, the evaluation of many cases, each requiring an LP solution, would be problematic when embedded in a sub-problem on a multi-level optimization, as discussed in Section 2.3.3.

2.2. Problem Definition

The problem defined in Section 1.5 is a linear optimization problem, with limited feedback. Model and plant are assumed to differ only in the parameter values, since no structural mismatch is considered. We seek a steady-state solution that is feasible, if possible, and at or close to the optimum of the true plant.

Two descriptions of parameter uncertainty were used in this work: (1) Interval, where parameters vary within upper and lower bounds, and is used when there is no information about parameter distribution, and (2) Ellipsoidal, where the parameters are

assumed to be normally distributed, and vary within a multidimensional ellipsoid described by:

$$(Q-Q_0)^T \mathbf{V}^{-1}(Q)(Q-Q_0) \leq \chi^2_{\alpha,dof} \qquad (2.1)$$

In the ellipsoidal description of uncertainty, parameters Q lie within the ellipsoidal contour defined by their variance-covariance matrix $V(Q)$ at a given confidence level (α). The number of degrees of freedom (*dof*) for the chi-square distribution is equal to the number of uncertain parameters (Rooney and Biegler, 2003; Draper and Smith, 1998). This description of uncertainty allows for the incorporation of correlation among parameters.

An important class of optimization problems under uncertainty is Stochastic Programming, which is discussed below.

2.2.1. Stochastic Programming

Stochastic Programming enables the integration of uncertainty into the solution of an optimization problem. Stochastic Programming can be classified into two main types of problems: Probabilistic Programming and Recourse Problems (Sahinidis, 2004).

Probabilistic Programming

Probabilistic Programming incorporates uncertainty by the use of chance constraints (Charnes and Cooper, 1963). Chance constraints occur in both steady-state and dynamic optimization problems. An example of a chance-constrained problem can be seen below.

$$\begin{aligned} &\min \quad cx \\ &\text{s.t.} \quad P(Ax \geq b) \geq p \end{aligned} \qquad (2.2)$$

In Problem (2.2), the constraint $Ax \geq b$ is satisfied with a probability of at least p. As examples of steady-state chance-constraint applications, there is the work of Charnes and Cooper (1963) that considers independent uncertainty in the right-hand side coefficients. More recent works related to robust feasibility are Ben-Tal and Nemirovski (2000) and Lin *et al.* (2004), which take the uncertainty in the left-hand side coefficients (A) into account. These methods, however, cannot handle closed-loop systems directly.

Dynamic robust MPC problems, on the other hand, consider the feedback structure of the problem when incorporating parameter uncertainty to ensure that constraints remain feasible during transient operation (Kothare *et al.*, 1996; Warren and Marlin, 2004). Even though robust MPC technology guarantees a feasible trajectory to the final steady-state, it does not ensure that the final point of the trajectory is the true plant optimum because it is not part of the robust control definition.

In this thesis, an inherently dynamic system is considered, but only the steady-state performance is monitored. The trajectory that leads to steady-state operation is allowed to be infeasible due to the integrating properties of batch processes with only end-point objectives. If necessary, the formulations developed in robust control technology could be applied to the dynamic transient system to ensure feasibility throughout the trajectory leading to steady-state operation. In fact, the combination of steady-state optimization with dynamic trajectory optimization is an example of this combined approach, although uncertainty has not been considered in this coordinated system to date.

Recourse Problems

The probabilistic programming approaches described previously limit the probability of infeasibility of an optimization problem. Another approach to optimization under uncertainty is to model the future response (recourse) of a model to the realizations of the uncertain parameters (Sen and Higle, 1999). In the two-stage recourse problem, the variables are named according to when they have to be implemented within the decision-

making process: the decisions that have to be made before the realization of the uncertain variables are called first-stage decision variables, whereas the decisions that can be made after the realization of the uncertain variables are called second-stage decision variables.

The classical case of recursion assumes "perfect" information about the second-stage (inner) variables of the uncertain optimization problems. An example of a two-stage recourse problem is seen below (Sen and Higle, 1999).

$$
\begin{aligned}
\min_{x_1} \quad & c_1 x_1 + E\left(\tilde{h}(x_1)\right) \\
\text{s.t.} \quad & A_1 x_1 = b_1 \\
& x_{1,\min} \le x_1 \le x_{1,\max} \\
& h_s(x_1) = \min_{x_{2s}} \; c_{2s} x_{2s} \\
& \qquad \textbf{s.t.} \; A_{2s} x_{2s} + B_s x_1 = b_{2s} \\
& \qquad\quad x_{2,min} \le x_{2s} \le x_{2,max}
\end{aligned}
\tag{2.3}
$$

In Problem (2.3), x_1 and x_2 are the first- and second stage decision variables, respectively. The subscript s corresponds to each of the S scenarios used in the evaluation, and $E\left(\tilde{h}(x_1)\right)$ is the expected value of the random variable $\tilde{h}(x_1)$. The expected value of this variable also known as the recourse function. From Problem (2.3), it is possible to see that the inner problem ($h_s(x_1)$) depends on the realization of the outer problem (x_1), *i.e.*, the decisions x_2 are only made after deciding on x_1.

There are two types of models associated with Recourse Programming: the Here-and-Now (HAN) and the Wait-and-See (WAS) models. HAN models relate to the first stage decision variables, where the decision must be made before knowing the outcome of the uncertain parameters in the second stage problems. If nominal parameter values are assumed for the second stage variables, the HAN solution may be infeasible for the uncertain problem (Sen and Higle, 1999). Therefore, one of the methods for handling HAN models by reformulating second stage decisions as chance constraints, as seen below.

$$\begin{aligned} \min \quad & cx \\ \text{s.t.} \quad & A_1 x \geq b_1 \\ & P(A_2 x \geq b_2) \geq p \\ & x_{\min} \leq x \leq x_{\max} \end{aligned} \qquad (2.4)$$

In WAS models, perfect information of parameter values is assumed when the optimization problem is performed, which corresponds to the optimization of the second stage variables. WAS models often require the solution of several scenarios for the different realizations of the second stage variables (Sen and Higle, 1999). Decision Analysis literature has WAS models in the form of, for example, Regret problems (Averbakh, 2000), which will be addressed in more detail in Section 2.5. Many applications of WAS models only consider interval uncertainty (with the exception of Rooney and Biegler, 2003). Most of the work in the literature can only handle inequality constraints, and the parameter space is usually discretized to solve the inner problems. These shortfalls were overcome with the methods presented in this thesis.

Ierapetritou *et al.* (1996) studied the effect of uncertainty in a production planning problem through the use of the Expected Value of Perfect Information (EVPI). In Ierapetritou *et al.* (1996), EVPI is described as the difference between the HAN and the WAS model decisions. EVPI is further addressed in Section 2.5.

The work in this thesis is a combination of HAN and WAS models in Recourse Programming. The HAN-model concept of making a decision before the realization of the uncertain variables in known is used. However, differently from the WAS approach of enumerating the different realizations, or from the chance-constrained approach of "backing-off" from constraints to ensure feasibility, feedback information was incorporated directly into the model by a novel modeling approach in order to predict the closed-loop response of the system. In addition, the systems in this research have "limited feedback', so that the uncertainty in some parameters is not reduced in spite of multiple recursion.

Other Related Problems in Stochastic Programming

There are other problems in the literature of Optimization under Uncertainty that relate to the work in this thesis. Grossmann and Sargent (1978) developed a minmax optimization strategy to solve an open-loop plant design problem under uncertainty. The idea was to minimize the sum of design and operational costs subject to keeping process constraints feasible given the worst-case parameter disturbances. In their work, they assumed interval parameter uncertainty without any correlation. Equality constraints were eliminated from the problem, and the constraints that were monotonic with respect to the parameters were fixed at the worst-case parameter bounds in order to eliminate the inner optimization problem.

In another plant design problem, Rooney and Biegler (2003) considered uncertain model parameters and variable process parameters (disturbances). They suggested an iterative procedure for solving the design and feasibility problems, in which the (full) parameter space was discretized in the design stage, and then, for a fixed set of design variables, the problem was solved again for feasibility. A new set of critical (worst-case) parameters that yield the largest constraint violation was identified and added to the set of discretized parameters. The procedure continued until no constraint violation was found in the feasibility stage. In their work, complementarity constraints were replaced by a smoothing function, and ellipsoidal confidence regions were used. The complementarity constraints originated from replacing the bilevel optimization problems in their formulation with the corresponding optimality conditions. Even with efficient sampling, the problem complexity grows rapidly. Furthermore, their methodology was only applied to open-loop problems in which there were no explicit equality constraints.

2.2.2. Model Improvement

In Chapter 3, methods for monitoring CLRTO performance are presented. When the RTO performance metric indicates that the RTO is performing poorly, model

parameters should be re-estimated in order to reduce their uncertainty. Experiments are performed to obtain better parameter estimates. Note that the methods are not intended to discriminate between different model structures, since no structural mismatch is assumed.

Traditional (fractional) factorial design of experiments (Montgomery and Runger, 1994) predetermines the condition and size of experiments. This method tends to use extreme values of the variables during experiments, and no cost of experimentation is considered. As a result, there is likely an excessive number of (unfocused) experiments.

In an attempt to reduce the number of experiments needed in the plant, "alpha"-optimal design of experiments (such as A-optimal and D-optimal) focus on reducing the uncertainty in parameters such that the some metric of the parameter confidence region (volume, largest axis, etc.) becomes smaller (Fraleigh, 1999). These methods, however, do not take the cost of experimenting into account, and they may therefore result in very expensive experiments.

Other methods for model improvement have been proposed that do not require drastic changes in operation. One of these strategies is Dual Control (Wittenmark, 2002). This technology enables the controller (or CLRTO) to reach the desired setpoint while also improving the model by minimizing the expected loss over the remainder of the control horizon. However, the calculations can be very intensive because of the nested calculation of conditional expectation in the optimization. Evolutionary Operations (EVOP) (Box and Draper, 1969), on the other hand, continually excites the plant with small perturbations in order to continually improve the model. Both Dual Control and EVOP may introduce unnecessary perturbations in the plant because they do not include a monitoring phase; i.e., there is no established threshold on performance at which plant perturbation stops.

Pinto (2001) recognized the importance of incorporating the cost of parameter uncertainty into the experimental design framework. In his work, the objective function in the experimental design procedure was characterized as the cost of not operating at the true plant optimum due to uncertainty, and it was based on profit Hessian information and variances of the manipulated variables and parameters. Besides only being applicable

to nonlinear problems, this method only considers open-loop optimization problems and independent parameter variations, and does not have a straightforward extension to constrained optimization problems.

Yip and Marlin (2001) included the cost of experimentation into the design of experiments for nonlinear constrained RTO systems. The objective function for the design of experiments was subdivided in three parts: RTO profit given the current nominal model, profit during experimentation, and profit after experimentation. In his work, however, a constant active set was assumed. The method was limited to nonlinear RTO systems with second-order derivative information, and there was no possibility of incorporating constraints during the experiment.

In this thesis, a profit-based experimental design strategy was developed for linear CLRTO systems. This method chooses experimental conditions to achieve the desired uncertainty bounds after experimentation, while obeying process constraints during the experiment.

2.2.3. Parameter Estimation

Once there is process data available for updating the model, a parameter estimation strategy must be chosen. A traditional method of estimating parameters is Least-Squares regression (Montgomery and Runger, 1994; Robertson and Lee, 2002). In this method, the sum of squares of the deviations between measured and predicted outputs are minimized, weighted by the inverse of the measurement variance-covariance matrix. Least-squares estimation, however, assumes error-free input variables. In order to account for errors in the input variables of a system, the Error-in-Variables method (EVM) was developed (Keeler and Reilly, 1992).

Kalman filtering is an online recursive method for updating states, which could be physical variables or model parameters. For linear systems, the Kalman filter and the least-squares estimator are equivalent if the weighting matrices are tuned appropriately (Robertson *et al.*, 1996). Since it is very difficult to incorporate constraints in a Kalman filter, it is not often used in CLRTO applications.

When updating a model with (very) limited amounts of data, Least-Squares and EVM should be used with caution: even though the parameter estimates may be closer to the true plant parameters, the estimates of parameter variances will be very large until a sufficient number of data points are considered. In an operating production unit, however, there may be prior knowledge (from past operation) on the "usual" variability of some process parameters. Even when there is no information available from previous operation, prior information can be obtained from using efficient sampling techniques, such as Latin Hypercube. This information on the prior parameter distributions can be incorporated into the parameter estimation in order to decrease the number of experiments needed to bring the parameters to a small uncertainty region.

The incorporation of the prior distributions can be done by using Bayesian estimation (Box and Tiao, 1973). In this technique, the prior knowledge about the parameter distribution is multiplied by the likelihood of the new observation in order to obtain the new parameter distribution. Reilly (1973) derived the Least-Squares parameter estimation in a Bayesian framework. Due to its ability to incorporate prior knowledge, the Bayesian approach to least-squares estimation was used to update parameters in this thesis.

When parameters are initially assumed unknown (*i.e.*, with an "infinite-valued" variance-covariance matrix, or in traditional least-squares estimation), the system is very susceptible to ill-conditioned parameter estimates. This occurs due to the inversion of the variance-covariance matrix of parameters in the estimation procedure. Because the Bayesian approach to Least Squares incorporates (reasonable, slightly greater-than-expected-value) prior variances of the uncertain parameters, the parameter estimation becomes numerically more stable. More details on Bayesian Estimation can be found in Appendix B.

2.3. Solution Methods

In order to solve an optimization problem, there are two common solution approaches: model-based and direct-search methods. Model-based optimization is based

on using a model of the system and its curvature information (from derivatives) in order to find a search direction. In direct-search optimization methods, the manipulated (optimization) variables in a system are perturbed, and the objective function value is assessed for improved values. In the following subsections, some model-based and direct-search methods are briefly discussed. For a more detailed discussion on each of the optimization methods described below, the reader is referred to Appendix D.

2.3.1. Model-Based Optimization

This section briefly presents the optimization methods used in this work. One of the first model-based optimization methods for finding a search direction for nonlinear optimization models was the Newton method (Nash and Sofer, 1996). It is based on finding the next point in the search by approximating a function by its tangent line at the current point.

Many optimization methods are based on Newton's method. One of them is Sequential Quadratic Programming (SQP), in which the Lagrangian of the original problem is approximated by a quadratic function, and the original constraints are linearized. The "approximated" quadratic programming (QP) problem is then solved by either an active set-based method, or by an interior-point method. One of the commercial solvers with an active set-based SQP is Matlab's *fmincon* solver (Mathworks, 1999).

Active-set methods are based on considering only the active inequality constraints at each iterate of the QP subproblem in order to compute a search direction based on an equality-constrained problem (Wächter, 2002). Interior-point methods, as its name suggests, ensure that the iterates will remain in the interior of the feasible region. One of the methods used in interior-point algorithms are barrier methods, in which the constraints $g(x) \geq 0$ are satisfied at every iteration by making constraint violations infeasible. This is done by adding a barrier function – such as inverse ($1/ g(x)$) or the logarithm ($\log(g(x))$) operator – in the objective function of the original problem.

IPOPT-C is a solver based on solving the internal QP of the SQP algorithm by an interior point method (Raghunathan and Biegler, 2003; Wächter, 2002). In path-

following interior point methods such as the one used in IPOPT-C, a trust region is assigned around the starting point, and a search direction is found within that region. Then, a (Newton) step is taken along the central path and the procedure is repeated around the new point (Nash and Sofer, 1996). More details on SQP and IPOPT-C can be found in Appendix D.

2.3.2. Direct-Search Optimization

Direct search methods were first proposed in the 1950's and continued being used since the 1960's (Wright, 1996). Although having been available for a few decades, no theoretical results on the convergence properties of these methods were available until 1980's, with the thesis of Torczon (1989) on multidirectional searches. This interest was sparked 20 years after the initial development of direct search methods due to the possibility of parallel computing.

Direct-search methods are based on finding the maximum or minimum of a (possibly) nonlinear and non-smooth function, using only function evaluations. There is no need for calculating derivatives or Hessians. Direct-search methods can be useful when the function evaluations are computationally very expensive, and/or when derivatives either do not exist or are not continuous over the feasible region.

One of the most famous and widely used direct-search methods is the Nelder-Mead simplex method. It is based on defining a sequence of $(n+1)$-dimensional simplexes that adapt to the surface of the n-dimensional function. The simplexes may reflect, expand, contract (outside or inside) or shrink at each step. In the Nelder-Mead simplex, an iteration succeeds when it finds a point that has a better objective function than the worst simplex vertex. It was shown that, even for relatively well-behaved functions, convergence to a local optimum for a Nelder-Mead simplex method can be slow (Wright, 1996).

Dennis and Torczon (1991) proposed a Parallel Direct Search algorithm to take advantage of parallel computing environments. Each iteration of this algorithm succeeds whenever it finds a better point than the *best* vertex of the simplex, which is a stronger

assumption than the one in the Nelder-Mead simplex method. However, this multidirectional search method requires a larger number of (expensive) iterations.

In order to reduce the number of evaluations needed in the optimization, Conn *et al.* (1996) developed a Derivative-Free Optimization (DFO) method, which exploits (but does not require) smoothness in the objective function. DFO is based on approximating the objective function by a (simpler) smooth, quadratic surrogate model within a trust region, and then optimizing the surrogate model to obtain an improved point. A more detailed description of DFO can be found in Appendix D. Due to its good reported performance and global convergence characteristics, DFO was used in this work (see Chapter 4).

2.3.3. Bilevel Optimization

Multilevel programming problems are structured in such a way that there is a decision-making hierarchy defined. An example of a bilevel programming problem can be seen below.

$$\min_{x_1} f_1(x_1, x_2) \qquad (2.5)$$

$$\text{s.t.} \quad g_1(x_1, x_2) \le 0$$

$$x_2 \in arg\min_{x_2} f_2(x_1, x_2)$$

$$\text{s.t.} \quad g_2(x_1, x_2) \le 0$$

The upper-level decision variables (x_1) affect not only the objective functions, but also the feasible set of the lower-level decision variables (x_2), and vice-versa. An extensive survey of bilevel programming applications is given by Vicente and Calamai (1994).

Bilevel optimization problems are mathematically very challenging due to this interacting nature between variables in different levels. One of the complicating characteristics of this class of problems is that even if each one of the levels is a convex

optimization problem, the overall bilevel formulation is inherently non-convex due to the optimality conditions of the lower-level problem (Clark and Westerberg, 1990). This implies that there is no guarantee of global optimality, unless a global optimization method is used.

One of the methods to solve bilevel optimization problems is to substitute the inner problem by algebraic equations that correspond to its Karush-Kuhn-Tucker (KKT) optimality conditions. If the inner problem of Problem (2.5) is substituted by its KKT conditions, the following (single-level) optimization problem is obtained:

$$\min_{x_1} f_1(x_1, x_2) \tag{2.6a}$$

$$\text{s.t.} \quad g_1(x_1, x_2) \le 0 \tag{2.6b}$$

$$\nabla_{x_2} f_2(x_1, x_2) + \lambda \nabla_{x_2} g_2(x_1, x_2) = 0 \tag{2.6c}$$

$$g_2(x_1, x_2) \le 0 \tag{2.6d}$$

$$\lambda \ge 0 \tag{2.6e}$$

$$\lambda \cdot g_2(x_1, x_2) = 0 \tag{2.6f}$$

It is known that inequality constraints that are not at their bounds must have zero Lagrange multipliers (λ) associated with them. This is the origin of equation (2.6f), also known as a *complementarity constraint*, where either $g_2(x_1,x_2)$ or λ must be equal to zero. Due to its discontinuous characteristic, these constraints introduce a type of nonlinearity that leads to nonconvexity of the overall problem, and that most NLP solvers cannot handle easily due to degeneracy. In linear programming, degeneracy occurs when some basic variable is at one of its bound values (INFORMS, 2006).

Algorithms to solve bilevel problems usually differ in the manner in which the complementarity constraints in equation (2.6f) are handled (Clark and Westerberg, 1990). For example, mixed-integer programming reformulations may be used to define the active set. However, these reformulations may result in very large computation times.

Another method for solving bilevel optimization problems is by enumerating scenarios or by using sampling approaches (Averbakh, 2000). However, a prohibitively large number of scenarios (or samples) is needed as the problem size increases. If a direct-search method is used on the overall problem, the inner optimization problem can be viewed as an expensive, discontinuous function with unavailable derivatives.

Parametric programming (Ryu *et al.*, 2004) transforms the bilevel problems into many single-level optimization problems, which are solved at once. Clearly, this approach results in a very large optimization problem. Furthermore, the parameterization depends upon the (single level) LP problem formulation, which may change frequently.

Raghunathan and Biegler (2003) developed a method for handling complementarity constraints based on an interior point solver (IPOPT-C). Their method relaxes the equality constraints to $g_2(x_1,x_2).\lambda \leq \varepsilon$, so that they are satisfied to successively smaller tolerances ε until the user-specified tolerance is achieved. So far, IPOPT-C has been reported to handle problems with up to 1,748 complementarity constraints (Raghunathan and Biegler, 2003). Due to ability to handle complementarity constraints in a computationally-efficient manner, IPOPT-C was applied extensively to the formulations in this work.

2.4. Closed-Loop Blending Technology

The choice of LP blending processes as case studies in this research was made because they have numerous and important industrial applications. In the petroleum industry, gasoline, diesel, fuel oils and lubricating oils are blended from multiple intermediate products. Some of the earliest applications of linear programming were to gasoline blending (Symonds, 1955).

Optimal blending is also important in other industries. Some examples include iron ore processing (Long, 1981; Zhou *et al.*, 2003), coal processing (Shih and Frey, 1993; Liao *et al.*, 2005) and in the cement industry (Sakr et al., 1988, ABB, 2006). In fact, one of the very early published papers on industrial closed-loop LP blending optimization describes an application to cement blending (Bay *et al.*, 1969). Therefore,

the monitoring and improvement of closed-loop LP optimization can have wide application in many industries.

It is very often the case where the component properties blend linearly (e.g., % lumps and fines in mineral processing, °Brix in fruit juice processing). In other cases, such as gasoline blending, the relationship between flow ratios and product qualities is nonlinear. There are nonlinear blend models available for calculating the octane properties of the final blend, such as the Ethyl RT-70 method (Healy *et al.*, 1959), the DuPont interaction method (Snee, 1981) and the Mobil transformation method (Rusin *et al.*, 1981). Even when nonlinear blend laws are used, the solution will be at the corner point of the feasible region for economic reasons; *i.e.*, the blend properties and total production rate will be at their upper or lower bounds. Some component flowrates will be between their bounds to satisfy the quality and production constraints, while the remaining ones will be at their bounds. Therefore, the nonlinear blend models can be linearized around the current operation, resulting in a linear blending model that can be used for octane ranges of up to around ±0.4 octane numbers (Snee, 1981). If the variation range of component properties is larger, there can be several linear models available, one for each region of interest.

Many technology vendors provide hardware and software for closed-loop optimal blending, *e.g.*, Yokogawa (Sasaki *et al.*, 1997), ABB's Optimize^{IT} Raw Mix Preparation (ABB, 2006), Invensys's Blend Optimization and Supervisory System - BOSS (Foxboro, 2006), Aspen Technology's ASPEN BLEND (AspenTech, 2006), Honeywell's OpenBPC (Open Blend Property Control) (Honeywell, 2006). In all cases, the structure of the optimizer is the same as the MPC structure described in Chapter 1 and Appendix A, where the manipulated variables are the component flows (or flow ratios) and the measured output variables are blend product properties. In no case are the component qualities measured or estimated from the measured component flow rates and product qualities. As demonstrated in this research, the data from typical plant operation does not have sufficient information, *i.e.*, variation, to enable the estimation of component compositions.

The models used in these commercial blending applications vary from linear to nonlinear. For example, Honeywell's OpenBPC uses nonlinear models directly. In contrast, others use a nonlinear model to provide the composition coefficients in the LP coefficient matrix. These systems usually solve an LP at each iteration (Vermeer *et al.*, 1996). As the system converges, the step where the LP coefficients are calculated based on the current blend ratios does not change the coefficients. Therefore, the optimizer is an LP when converged to a steady state, even though the qualities used for each component in the linearized model are calculated in a (separate) nonlinear optimization. Because a linear programming problem is commonly applied in gasoline-blending systems, linear blend models were considered in this study. For more details on the gasoline-blending process model, data, and on-line optimizer, the reader is referred to Appendix A.

At the present time, we know of no systematic manner for monitoring or diagnosing the performance of closed-loop blending optimization available in either industrial practice or technical publications. One heuristic approach is to determine whether the active set of inequality constraints in the plant operation conforms to guidelines based on experience (Chin, 2006). This approach has shortcomings. First, the proper active set depends upon the scenario, which changes daily. Second, the active set of output (quality and production rate) variables does not uniquely determine the operation or profit. Third, the heuristic does not estimate the cost for not achieving the expected good operation.

2.5. Relationship to Decision Analysis Theory

Decision Analysis (DA) literature poses questions that are very relevant to the work in this thesis. The most relevant topics from Decision Analysis for this research address the effect of uncertainty on decision making and introduce the concepts of Regret and Expected Value of Information. These concepts are used throughout the thesis to monitor, diagnose and improve closed-loop optimization systems.

Regret is defined as the opportunity loss identified after the uncertain variable realizations have been determined. In other words, Regret can be seen as the deviation of

the current objective function value from the one that would have been achieved if the information on the realization of the uncertain variables of a system had been known at the time of the decision-making (Averbakh, 2000). The Maximum Regret, therefore, is the decision based on the worst possible parameter realization in the system. For each realization j of the uncertain variables, the Regret (r) with respect to the decision $i \in D$ can be defined as (Drezner, 2001):

$$r_{ij} = \max_{i \in D}(a_{ij}) - a_{ij} \qquad (2.7)$$

In equation (2.7), a_{ij} corresponds to the payoff of decision i; *i.e.*, the objective function value, which is maximized.

The Expected Value of Perfect Information (EVPI) is similar to Regret in that it is also a measure of the cost of uncertainty in a system. EVPI can be interpreted as the expected objective function improvement if the information on the future realization of uncertain variables (including the probability p_j of each realization) were known in advance (Drezner, 2001).

$$EVPI = \sum_{j=1}^{p} p_j \max_{i \in D}(a_{ij}) - \max_{i \in D}\left(\sum_{j=1}^{p} p_j a_{ij}\right) \qquad (2.8)$$

The Expected Value of Sample Information (EVSI) evaluates the potential benefits (in terms of objective function value) of a sample that provides improved information about a system (Winston, 1994). If the EVSI is less than the cost for gaining new information to reduce (eliminate) uncertainty, e.g., by performing a test or measurement, such an evaluation is not performed. In traditional Decision Analysis literature, the cost of obtaining the information is known (e.g., cost of performing a market evaluation or of taking samples to a laboratory), as is the improvement in information content due to the added information. This is a realistic description of many decision-making systems, but the scenario in this research is very different. In the real-

time optimization system, the current scenario and the experimental design affect the cost of experimentation. Also, the improvement after the experiment depends upon the problem scenario and the experimental design. Therefore, the evaluation of the EVSI in this research is more challenging.

Finally, Decision Analysis often optimizes over a set of discrete options that are the decision variables. These could be laboratory analysis, hiring a consultant, etc. In the real-time optimizer, the decision variables are continuous and the uncertain parameters are continuous over known regions. Therefore, the solution approaches required to evaluate the problems in this thesis are significantly different from, and more challenging than, those in common use in Decision Analysis.

2.6. Summary

This chapter presented the aspects of optimization literature that are relevant to this work. The methods for diagnosing and enhancing CLRTO performance developed in this work cover technological gaps in the Model Improvement and Screening Experiments areas. The following table shows some of the challenges of state-of-the-art optimization technology, and summarizes the contributions made by this thesis.

Table 2.1. Challenges in State-of-the-Art Optimization Technology

2.1. Sensitivity Analysis		
	State-of-the-Art	This Thesis
Monitoring and Diagnosing Optimization Systems	Sensitivity analysis literature, restricted to a single active set of constraints, or requiring enumeration of scenarios.	Not restricted to a constant active set. Solution is obtained in a single optimization run.
	Sensitivity Analysis has not been applied to closed-loop optimization systems.	Closed-loop optimization systems are considered, with "limited feedback" information
	Regret, EVPI and EVSI used in decision analysis	Novel diagnostics method that ranks parameters with respect to effect on objective function, calculated in few optimization runs.

Table 2.1. Challenges in State-of-the-Art Optimization Technology (continued)

2.2.1 Model Formulation / Stochastic Programming

	State-of-the-Art	This Thesis
Types of Optimization Problems	Chance constraint established for open-loop optimization with uncertainty Recursion methods for perfect information and sampling uncertainty well established Existing worst-case techniques concentrate on formulations for open-loop optimization	Closed-loop optimization systems are considered, in which the best- and worst-case parameter realizations are obtained as a "byproduct" of the performance evaluation
Sources of Parameter Uncertainty	Many techniques do not handle all possible sources of parameter uncertainty (especially left-hand side coefficients and coefficients in equality constraints)	All sources of parameter uncertainty are considered: left- and right-hand side coefficients of any constraint type and objective function coefficients. Parameter correlation is also handled.
Continuous Parameter Distributions	Currently, there is great reliance on sampling and scenarios to represent continuous distributions	No evaluation of scenarios or sampling.

2.2.2 Model Enhancement

	State-of-the-Art	This Thesis
Experimental Design	Experimental design technology based on information (parameter variance) is mature. However, a gap exists in considering the cost of experimentation	Cost of (possibly constrained) experimentation is considered explicitly. Experiment improves the new performance metric.

Table 2.1. Challenges in State-of-the-Art Optimization Technology (continued)

2.3. Solution Methods		
	State-of-the-Art	This Thesis
Solver Technology	Extensive range of technology and software packages available	Because of diverse problems, LP, SQP, IPM, and direct search methods are employed. No novel contribution is made to the algorithms in this work
2.4. Closed-Loop Optimization		
	State-of-the-Art	This Thesis
LP-Based CLRTO	Mature technology widely applied to blending processes and to optimizing the steady-state for MPC dynamic controllers	Novel, integrated five-step procedure for monitoring, diagnosing and enhancing developed that is compatible with the installed base of CLRTO

Chapter 3
RTO Performance Monitoring

This chapter introduces new methods for performance monitoring in process optimization. The basic scenario considered involves a nominal model, uncertain plant parameters and estimates for the uncertainty regions of these parameters. In all but one short example in Appendix E, the model structure is linear, thus yielding a linear programming optimization problem. The uncertain parameters can appear anywhere in the linear program, i.e., the objective, equalities and inequalities, right hand side bounds, and the left hand side coefficients multiplied by the variables. The uncertainty descriptions can be either individual intervals or correlated ellipsoidal regions.

The goal of the monitoring is to determine the effect of the parameter uncertainty on the optimization solution when it is implemented in the true plant, which is not known exactly. The results of the monitoring analysis determine whether the true plant optimum is achieved, or if it is not achieved, these results give a measure of the deviation from the true plant optimum; the deviation measure is different depending on the method applied, as described in the chapter.

The methods in this chapter are designed to provide capabilities beyond current technology, specifically: sensitivity analysis allowing changes in the active set of inequality constraints, automatic selection of worst-case plant parameter realizations without guidance from the engineer, and assessment of uncertainty for closed-loop systems. Importantly, the methods achieve their results in the numerical solution of one optimization problem, rather than through Monte Carlo procedures. This feature not only greatly speeds the solution to the problems addressed in this chapter, but it also is essential for these methods to be effectively integrated with the diagnostic and

improvement methods introduced in Chapter 4. In addition, monitoring is achieved without interfering with typical plant operation.

Several monitoring methods are presented in this chapter, with each subsequent method providing more valuable information at the cost of more computation. The first method in Section 3.2 determines whether or not the true plant optimum will be achieved for all realizations of the uncertain parameters. The second method in Section 3.3 determines the maximum decrease in profit due to interval uncertainty. Then, this method is extended to ellipsoidal uncertainty in Section 3.4. Since the problem is stochastic in nature, Sections 3.5 and 3.6 introduce methods for evaluating the expected value of the cost of uncertainty. Finally, in Appendix E, the methods are applied to monitoring the performance of open-loop optimization for both linear and nonlinear models.

A Pentium 4, 1700MHz, 523 Gb was used in the simulations. All problems in the thesis were solved to the 10^{-8} tolerance levels of IPOPT-C (version 2.0.1) solver. In *fmincon* (Mathworks, 1999) (in Matlab version 6.5.0.180913a Release 13), tolerances of 10^{-3} for constraint violations and absolute values of the variables and objective function values were set. All of the closed-loop optimization methods will be applied to an industrially important, closed-loop blending system. Therefore, we begin with a description of the gasoline-blending process in the next section.

3.1. Gasoline-Blending Case Study

One of the first industrial applications of real-time optimization was the gasoline blending processes (Birchfield, 2002). Since these processes have a very high throughput, even small improvements in operation have a large economic impact. The components that are blended to form the final gasoline product come from very large storage tanks, so that fluctuations in their (unmeasured) properties can be assumed to be much slower than the RTO execution periods. Nevertheless, since the components are made from variable upstream refinery operations or are purchased from suppliers, their properties vary from one batch to another, justifying the need for real-time optimization. Since this is a batch blending process, transient violations of blended properties can be compensated for, if

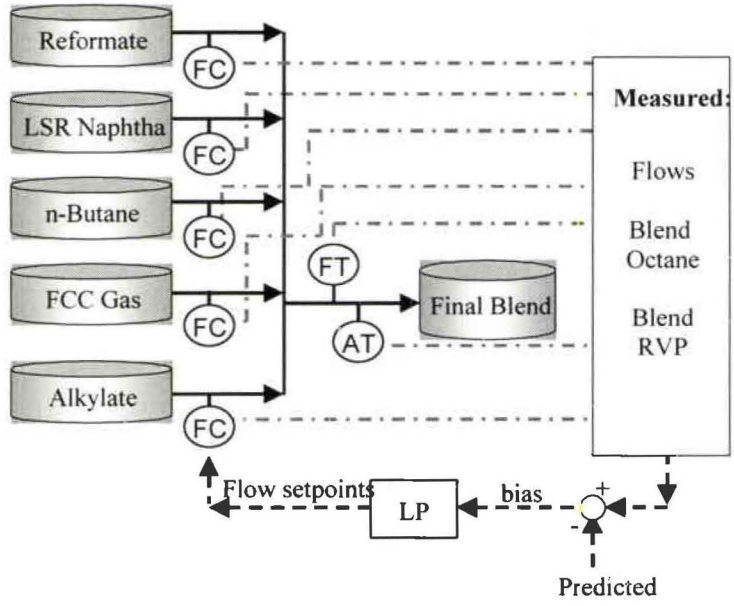

Figure 3.1. Gasoline Blending Process

necessary. Very large deviations from the specifications should be avoided, however, since stratification of material can occur due to the large volume of gasoline stored in the product tank, which is not mixed.

In the gasoline-blending process considered in this work, five components (Reformate, LSR Naphtha, n-Butane, FCC Gasoline and Alkylate) are blended to form the final gasoline product. Component properties are assumed to blend linearly due to the use of blending indexes. A schematic of this process can be seen in Figure 3.1.

All uncertainty in this system is parametric and occurs in the octane and Reid vapour pressure (RVP) properties of the five components in the tanks, which are not measured. The parameter uncertainty is described by either intervals (Sections 3.2 and 3.3) or ellipsoids (Sections 3.4 and 3.5). In Sections 3.2 to 3.5, the parameters are assumed to lie within intervals of ± 1.0 (octane numbers or psi) for the interval description of uncertainty, or to have variances of 0.0546 (octane numbers^2 or psi^2) for ellipsoidal description of uncertainty. For parameter values used in the case studies and

more detailed information about the gasoline-blending process, the reader is referred to Appendix A.

In many industrial blending applications of RTOs, bias updating is chosen as the model updating strategy, since it leads the model to the true plant optimum whenever the parametric mismatch is sufficiently small (Diaz and Barsamian, 1996; Vermeer *et al.*, 1996; Forbes and Marlin, 1994; Zahed *et al.*, 1993). The closed-loop RTO that uses a bias-updating strategy obeys the set of equations described in Problem 3.1.

Problem 3.1: Closed-Loop RTO

$$Pr_{nom,CL} = \max_{F_{i,nom}} \sum_{i=1}^{n} (value - cost_i) F_{i,nom}$$

s.t.

$$\sum_{i=1}^{n} F_{i,nom} (Q_{i,nom}^{j} + \varepsilon^{j}) \geq Q_{blend,min}^{j} \sum_{i=1}^{n} F_{i,nom} \qquad j = oct,\ RVP$$

$$\sum_{i=1}^{n} F_{i,nom} (Q_{i,nom}^{j} + \varepsilon^{j}) \leq Q_{blend,max}^{j} \sum_{i=1}^{n} F_{i,nom}$$

$$F_{blend,\min} \leq \sum_{i=1}^{n} F_{i,nom} \leq F_{blend,\max}$$

$$0 \leq F_{i,nom} \leq F_{i,\max}$$

where the bias term ε^{j} is constant during the optimization. This term corrects the model prediction of each product quality and is calculated prior to the optimization at each CLRTO execution using the following equation.

$$\varepsilon^{j} \sum_{i=1}^{n} F_{i,nom} = \sum_{i=1}^{n} F_{i,nom} \left(Q_{i}^{j,plant} - Q_{i,nom}^{j} \right) \qquad j = oct,\ RVP \qquad (3.1)$$

In cases where the model mismatch in the component quality parameters is large, the closed-loop system will converge to a corner point that is different from the true plant optimum. In the following sections in this chapter, monitoring methods for the performance of CLRTO systems are developed that do not rely on any information about the true plant optimum.

3.2. Method Based on the Number of Optimal Corner Points

As an initial monitoring criterion of a CLRTO system, the Maximum Achievable Profit (*MAP*) is calculated by solving the following problem.

Problem 3.2

$$MAP = \max_{F_i, Q_i^{j,plant}} \sum_{i=1}^{n} (value - \cos t_i) F_i$$

s.t.

$$\sum_{i=1}^{n} F_i Q_i^{j,plant} \geq Q_{blend,\min}^{j} \sum_{i=1}^{n} F_i \qquad j = oct,\ RVP$$

$$\sum_{i=1}^{n} F_i Q_i^{j,plant} \leq Q_{blend,\max}^{j} \sum_{i=1}^{n} F_i$$

$$F_{blend,\min} \leq \sum_{i=1}^{n} F_i \leq F_{blend,\max}$$

$$F_{i,\min} \leq F_i \leq F_{i,\max}$$

$$Q_{i,\min}^{j} \leq Q_i^{j,plant} \leq Q_{i,\max}^{j}$$

This metric indicates the optimum operation for the best possible scenario of component qualities in the plant, given the parameter uncertainty. If the current profit achieved by the CLRTO is close in value to *MAP*, the system is deemed to be functioning properly. If not, the possibility of improvement exists, and a subsequent monitoring metric needs to be calculated. This additional metric is based on determining if more than

one corner point is possible given the parameter uncertainty, and is presented in Section 3.2.1.

3.2.1. Point-Wise Model Adequacy

If only one corner point is possible within the parameter uncertainty, such a corner point corresponds to the true plant optimum, because the parameter uncertainty is small enough so that the bias-updating strategy of the CLRTO will be able to achieve the true plant optimum (Forbes and Marlin, 1994). Forbes and Marlin (1994) have defined the point-wise model accuracy for RTO models. Consider the following optimization problem.

Problem 3.3:

$$\max_{F_i} Pr(F_i)$$

$$s.t.$$

$$h(F_i, Q_i^J) - \beta_1 = 0$$

$$g_A(F_i, Q_i^J) - \beta_{2,A} = 0$$

$$g_I(F_i, Q_i^J) - \beta_{2,I} < 0$$

In Problem 3.3, h, g_A and g_I correspond to equality constraints, active inequality constraints and inactive inequality constraints, respectively. For this problem, the model is deemed point-wise adequate if, at the true process optimum, there exists a vector of adjustable bias parameter values β (the difference between measured and predicted values) for which the optimality conditions are satisfied (Forbes and Marlin, 1994).

$$\nabla_F Pr - \lambda^T \nabla_F g_A = 0 \quad (3.2a)$$

$$h(F_i, Q_i^J) - \beta_1 = 0 \quad (3.2b)$$

$$g_I(F_i, Q_i^J) - \beta_{2,I} < 0 \quad (3.2c)$$

$$g_A(F_i, Q_i^J) - \beta_{2,A} = 0 \quad (3.2d)$$

$$\lambda_i \geq 0 \quad (3.2e)$$

The optimality conditions are given in the set of equations (3.2), where the Lagrange multipliers λ_i are for the active inequality constraints of the original CLRTO model. By using the bias-updating strategy, the adjustable parameters β (which are equivalent to the bias terms ε^j in equation (3.1)) only play a part in ensuring feasibility of the solution (equations (3.2b) to (3.2d)), but do not influence its optimality (equation (3.2a)). The parameters that influence the optimality are the uncertain parameters in the model-based optimizer, Q_i^j, which appear in the first-order optimality condition, equation (3.2a). Note that no feedback terms β appear in this equation.

If the model is adequate for a given uncertainty region, the Lagrange multipliers λ_i will be positive at the solution, since this indicates that the same optimal bases is maintained. This verification can be done by using the following formulation.

Problem 3.4:

$$\delta = \min_i \begin{pmatrix} \min\limits_{\lambda, Q^j} \lambda_i \\ s.t. \\ \nabla_{F^*} \Pr|_F - \boldsymbol{\lambda}^T \nabla_{F^*} g_A|_F = 0 \\ Q^j_{i,\min} \le Q^j_i \le Q^j_{i,\max} \end{pmatrix}$$

Problem 3.4 is the basis of the first monitoring strategy developed in this chapter: if the smallest Lagrange multiplier is positive over the range of uncertain parameters, only one corner point is optimal. This criterion is used to determine whether there is a possibility of different optimal bases occurring in the system given the uncertainty information.

In order to compute δ, the minimization sub-problem in Problem 3.4 was solved successively for each element i in the vector of Lagrange multipliers. This sub-problem was solved using the *fmincon* software in Matlab. For more details on *fmincon* and SQP, the reader is referred to Appendix D. The following section illustrates the results of applying this monitoring strategy to the gasoline-blending process.

Table 3.1. Solution of Problem 3.2

	$Q_i^{oct,plant}$ (octane)	$Q_i^{RVP,plant}$ (psi)	F_i (bbl / day)
Reformate	94.10	1.70	5258.2
LSR Naphtha	65.30	9.90	1353.0
n-Butane	93.50	137.00	388.8
FCC Gas	84.78	6.26	0.0
Alkylate	96.62	6.68	0.0
CPU seconds (IPOPT) :	< 1e-3		
# obj fun / constr evals :	14		

3.2.2. Case Study

We begin by determining whether the current profit is close to the maximum achievable profit. By using the nominal parameter values in Tables A.1 to A.3 (Appendix A) with an interval uncertainty of ±1.0 octane or psi for each of the ten parameters in Table A.3, a Maximum Achievable Profit (*MAP*) of $ 14,090.4 / day is obtained from the solution of Problem 3.2. The component properties at the steady-state solution of Problem 3.2 (from "perfect" RTO) can be seen in Table 3.1.

Since Problem 3.2 is nonconvex due to the bilinear terms in the inequality equations, solutions of this problem from different starting points were compared (Table 3.2). A starting point of $Q_i^{j,0} = Q_{i,nom}^j$ was used in both cases. The same value of *MAP* ($ 14,090.4/day) was obtained by using Starting Point 1 or Starting Point 2, but different values for FCC Gasoline and Alkylate octane and RVP properties were found at the solution. This is because there are infinite combinations of values for these component properties and flow rates that will yield the same objective function value. The existence of alternative solutions in this problem does not affect the analysis, as expected, because the assessment is based on the objective function.

Table 3.2. Starting Points Used in Problem 3.2

	Starting Point 1 = (1/5)*$F_{blend,max}$	Starting Point 2 := current CLRTO operation
	F_i^0 (bbl/day)	F_i^0 (bbl/day)
Reformate	1,400.0	5,695.6
LSR Naphtha	1,400.0	942.5
n-Butane	1,400.0	361.0
FCC Gas	1,400.0	0.0
Alkylate	1,400.0	0.0

Suppose that the CLRTO has reached a steady-state operation yielding a profit of $10,257.2/day. Since the current profit is significantly lower than the *MAP*, Problem 3.4 is used to check if multiple optima are possible in this system. When assessing alternative optimal bases within the uncertainty description of the parameters, a value of δ = -0.7665 $/bbl/day was obtained in 5.7 CPU seconds. Since δ is negative, more than one optimal basis for the CLRTO exists given the parameter uncertainty description. For example, given "true" plant parameters of 92.3 and 64.0 octane for Reformate and LSR, respectively, different nominal model parameter values for these properties in the RTO model (within the uncertainty description) will yield two different optimal bases at the closed-loop steady state operation reached by the CLRTO after 10 executions. Table 3.3 contains the "true" plant parameters, while Table 3.4 shows the two different bases that result from solving Problem 3.1 with different nominal parameter values in the RTO model for Reformate and LSR octane numbers. The nominal model parameters for the remaining components and properties used in this comparison are the same as the true plant parameters in Table 3.3.

Table 3.3. Values of $Q_i^{j,plant}$ used in the Case Study

	$Q_i^{oct,plant}$ (octane)	$Q_i^{RVP,plant}$ (psi)
Reformate	92.30	2.70
LSR Naphtha	64.00	10.90
n-Butane	92.50	138.00
FCC Gas	84.60	6.40
Alkylate	96.60	6.70

Table 3.4. Two Different Optimal Bases within Uncertainty Description

	Wrong Basis F_i (bbl / day) $Q_{Ref,nom}^{oct}$ = 93.1 octane $Q_{LSR,nom}^{oct}$ = 64.3 octane	Correct Basis F_i (bbl / day) $Q_{Ref,nom}^{oct}$ = 92.9 octane $Q_{LSR,nom}^{oct}$ = 64.0 octane
Reformate	5,695.6	3,212.7
LSR Naphtha	942.5	0.0
n-Butane	361.9	324.4
FCC Gas	0.0	3,463.0
Alkylate	0.0	0.0
$Pr_{nom,CL}$	\$ 10,257.2 / day	\$ 10,680.1 / day

The CLRTO profit at each of these two different optimal bases ($Pr_{nom,CL}$) is lower than *MAP* because the latter represents the best possible plant scenario (Reformate octane = 94.1 octane), which in this case does not correspond to the true plant parameter realization (Reformate octane = 92.3 octane) considered in this case study. The transient flowrates and blended qualities can be seen in Figure 3.2(a-c).

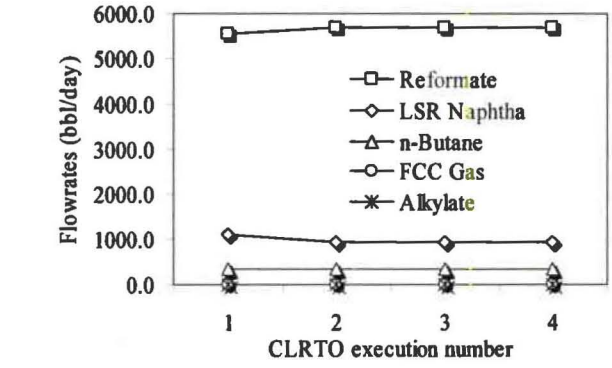

(a)

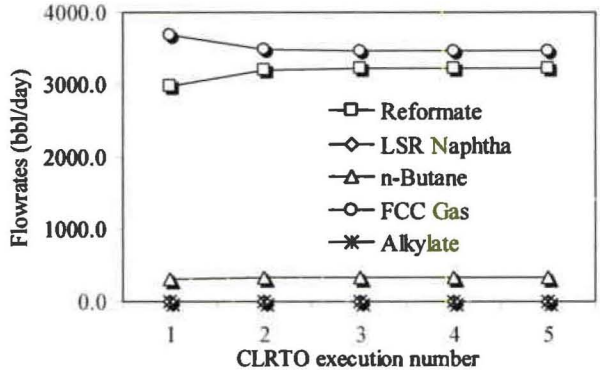

(b)

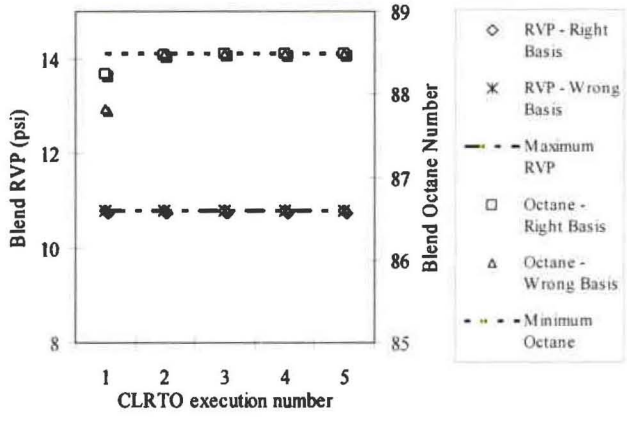

(c)

Figure 3.2. Transient CLRTO behaviour for the case with two possible corner points: (a) Flowrates converging to the wrong basis; (b) Flowrates converging to the correct basis; (c) Blend properties for both cases

Table 3.5. Values of $Q_i^{j,plant}$ used in the Comparison

	$Q_i^{oct,plant}$ (octane)	$Q_i^{RVP,plant}$ (psi)
Reformate	93.12	2.70
LSR Naphtha	64.30	10.90
n-Butane	92.50	138.00
FCC Gas	84.60	6.40
Alkylate	96.60	6.70

In order to further illustrate the monitoring procedure, a different case study is presented (Table 3.5). In this case, all the parameter intervals are defined as ±0.02 (octane or psi), which is smaller than the original case of ±1.0 (octane or psi). The Maximum Achievable Profit (*MAP* from Problem 3.2*)* in this case, is equal to $ 11,385.1/day, whereas the current profit is $11,354.4/day. The variable values at the solution can be seen in Table 3.6. The same two starting points were used as in the previous case studies.

Since *MAP* is very close to the current profit (within $30/day), no further diagnostics would be needed. However, for illustration purposes, Problem 3.4 was solved to determine if other optimal bases existed. This problem yielded a value of δ of +0.00735 $/bbl/day in 3.1 CPU seconds. Since δ is positive, only one optimal basis exists given the parameter uncertainty (Table 3.7), indicating that the CLRTO is performing adequately, i.e., the CLRTO system is achieving the maximum profit achievable in the plant, as expected. The results can be seen in Figure 3.3.

Table 3.6. Solution of Problem 3.2

	$Q_i^{oct,plant}$ (octane)	$Q_i^{RVP,plant}$ (psi)	F_i (bbl/day)
Reformate	93.12	2.68	5,531.9
LSR Naphtha	64.32	10.88	1,115.6
n-Butane	92.52	137.98	352.5
FCC Gas	84.60	6.40	0.0
Alkylate	96.60	6.70	0.0
CPU seconds (IPOPT) :	<1e-3		
# obj fun / constr evals :	12		

Table 3.7. One Optimal Basis within Uncertainty Description

	F_i (bbl / day) $Q^{oct}_{Ref,nom}$ = 93.1 octane $Q^{oct}_{LSR,nom}$ = 64.3 octane
Reformate	5,537.5
LSR Naphtha	1,110.7
n-Butane	351.8
FCC Gas	0.0
Alkylate	0.0
$Pr_{nom,CL}$	\$ 11,354.4 / day
$(MAP - Pr_{nom,CL})$	\$ 30.7 / day

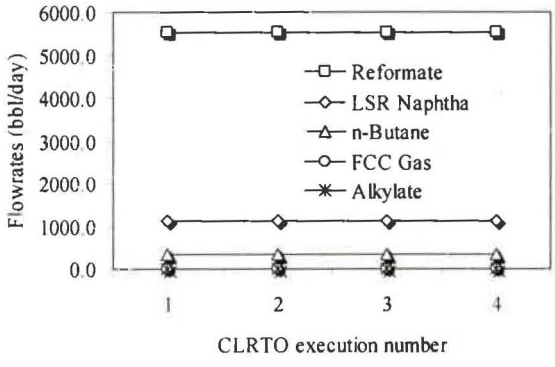

(a)

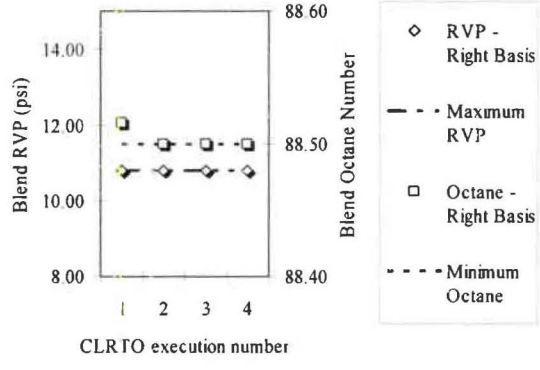

(b)

Figure 3.3. Closed-Loop RTO behaviour for the case with one possible corner point: (a) Transient behaviour of the flowrates; (b) Transient blend properties.

3.2.3. Conclusions

The monitoring method described in this section provides the definitive answer regarding achieving the maximum plant profit; if only one corner point exists, the system is at its best possible operation. However, this method is only applicable to linear programming problems, since it is based on corner point information.

Furthermore, there is no indication of the number of alternative corner points when the smallest Lagrange multiplier found by solving Problem 3.4 is negative, or of how large the difference in profit between the alternative corner points is. If the profit difference is small, the system may already be operating very close to the best possible operation. A negative Lagrange multiplier in Problem 3.4 could trigger overly aggressive model improvement actions, as shown in the Chapter 4. Therefore, a method that determines the profit loss that can occur due to model mismatch is shown in Section 3.3.

3.3. Method Based on the Largest Profit Gap – Interval Uncertainty ($MaxGap_{int}$)

Since the method in Section 3.2 does not evaluate RTO performance based on profit information, it is likely that in some cases, model enhancement will be performed – possibly with substantial costs to operation -- with only very small (or no) performance improvement possible.

In this section, the potential profit loss due to mismatch is considered. It can be represented by the maximum profit difference (gap) between the "best case" and "worst case" CLRTO operations. The best case involves a CLRTO with no model mismatch, so that it achieves the true plant optimum for the given parameter values. The worst case involves a CLRTO using a nominal model, which differs from the true plant in a manner that yields the largest profit loss. Recall that the feedback affects the "biases" in the model, so that the behaviour is determined by Problem 3.1 with the nominal model used by the CLRTO controller and the plant model having parameters within the uncertainty description.

- Best CLRTO - Since the best performance occurs with no model error, the model of the CLRTO in Problem 3.1 can be simplified. The feedback error is always zero for no mismatch, and the CLRTO can be modelled as an optimization without feedback.

- Nominal CLRTO - Because of model mismatch between plant and (nominal) model parameters, the closed-loop RTO using nominal parameter values can result in an operation (component flows) that yields a profit that is lower than the true plant optimum. The worst-case scenario occurs when the component qualities in the true plant maximize the profit difference due to plant/model mismatch.
- Uncertainty - In this sub-section, the model uncertainty is represented by intervals for each model parameter.

The difference between best CLRTO and nominal CLRTO is the maximum benefit than can be achieved for reducing CLRTO model mismatch. This is the measure used for performance monitoring, with a small value being good and a large value being bad.

The formulation for evaluating the largest profit gap given interval parameter uncertainty description is presented in the following problem.

Problem 3.5:

$$MaxGap_{int} = \max_{Pr_{BC}, Pr_{nom,CL}, \varepsilon^j, Q_i^j} (Pr_{BC} - Pr_{nom,CL})$$

subject to

$$Pr_{nom,CL} = \max_{F_{i,nom}} \sum_{i=1}^{n} (value - cost_i) F_{i,nom}$$

s.t.

$$\sum_{i=1}^{n} F_{i,nom} (Q_{i,nom}^j + \varepsilon^j) \geq Q_{blend,min}^j \sum_{i=1}^{n} F_{i,nom}$$

$$\sum_{i=1}^{n} F_{i,nom} (Q_{i,nom}^j + \varepsilon^j) \leq Q_{blend,max}^j \sum_{i=1}^{n} F_{i,nom}$$

$$F_{blend,\min} \leq \sum_{i=1}^{n} F_{i,nom} \leq F_{blend,\max}$$

$$F_{i,\min} \leq F_{i,nom} \leq F_{i,\max}$$

Nominal CLRTO for any plant realization Q_i^j

$$\varepsilon^j \sum_{i=1}^{n} F_{i,nom} = \sum_{i=1}^{n} F_{i,nom} (Q_i^j - Q_{i,nom}^j)$$

$$Pr_{BC} = \max_{F_{i,BC}} \sum_{i=1}^{n} (value - cost_i) F_{i,BC}$$

s.t.

$$\sum_{i=1}^{n} F_{i,BC} \cdot Q_i^j \geq Q_{blend,min}^j \sum_{i=1}^{n} F_{i,BC}$$

$$\sum_{i=1}^{n} F_{i,BC} \cdot Q_i^j \leq Q_{blend,max}^j \sum_{i=1}^{n} F_{i,BC}$$

$$F_{blend,\min} \leq \sum_{i=1}^{n} F_{i,BC} \leq F_{blend,\max}$$

$$F_{i,\min} \leq F_{i,BC} \leq F_{i,\max}$$

Best result for CLRTO for any plant realization Q_i^j

$$Q_{i,\min}^j \leq Q_i^j \leq Q_{i,\max}^j$$

Interval bounds

We note that the best- and nominal CLRTO cases are evaluated at the same values of the uncertain plant parameters, so that the optimal value of $MaxGap_{int}$ is *due entirely to model mismatch.* Also, we note that Problem 3.5 maximizes the difference between the results of two optimizations; therefore, Problem 3.5 is a bilevel optimization problem. Problem 3.5 was solved by replacing the inner optimization problems Pr_{BC} and $Pr_{nom.CL}$ with their respective optimality conditions. This formulation can be seen in Appendix F. The resulting nonlinear optimization problem was solved using an interior-point solver tailored to handle complementarity constraints, IPOPT-C (Raghunathan and Biegler, 2003). Details on this interior-point method can be found in Appendix D.

3.3.1. Case Study

Problem 3.5 was applied to the gasoline-blending case study using the nominal parameter values in Tables A.1 to A.3. All parametric intervals for the uncertain plant qualities in Table A.3 were equal to ± 1.0 (octane or psi) around the nominal values. In this case, a value of $MaxGap_{int}$ = $ 3,024.9/day is found, where Pr_{BC} = $11,845.1/day and $Pr_{nom.CL}$ = $ 8,820.2/day. $MaxGap_{int}$ corresponds to the largest potential profit loss due to model mismatch under the parametric uncertainty assumptions. The variable values at the solution are given in Table 3.8.

Since Problem 3.5 is nonconvex, there is no guarantee of global optimality of the solution when standard nonlinear solvers are used. In order to search for better local optima, different starting points were used to solve this problem, as can be seen in Table 3.9.

Table 3.8. Parameter Values and Flowrates at the Solution of Problem 3.5

	Q_i^{oct} (octane numbers)	Q_i^{RVP} (psi)	$F_{i,BC}$ (bbl/day)	$F_{i,nom}$ (bbl/day)
Reformate	92.10	3.70	2,731.1	5,791.5
LSR Naphtha	63.30	11.90	0.0	890.5
n-Butane	93.50	137.00	322.5	318.1
FCC Gas	85.60	5.40	3,946.4	0.0
Alkylate	96.58	6.72	0.0	0.0

Table 3.9. Starting points for Problem 3.5

	$F_{i,1}^0$ = (1/5)*$F_{blend,max}$ (bbl/day)	$F_{i,2}^0$ = current CLRTO operation (bbl/day)
Reformate	1,400.0	5,695.6
LSR Naphtha	1,400.0	942.5
n-Butane	1,400.0	361.0
FCC Gas	1,400.0	0.0
Alkylate	1,400.0	0.0

The results found by solving Problem 3.5 for different starting points can be seen in Table 3.10. Initial quality values $Q_i^{j,0}$ were assumed equal to $Q_{i,nom}^j$. In this table, λ_{nom} are the Lagrange multipliers obtained from the initial CLRTO system (with mismatch) after it converges to steady operation. "Good" solutions correspond to the same local optimum as the one found in Table 3.8, whereas "Bad" solutions correspond to the (worse) local optimum of $MaxGap_{int} = 0$. Since the same two solutions were found given four different initial starting points, the procedure was considered completed, and the results, valid. Again, since this is a nonconvex optimization problem, there is no guarantee that the solutions found correspond to global optima.

As previously mentioned, Problem 3.5 was solved using an interior point solver, IPOPT-C (Raghunathan and Biegler, 2003). When the reduction in the barrier parameter in the interior point solver is too aggressive and the solution approaches corner points of the optimization prematurely (where Lagrange multipliers switch from zero to non-zero values, or vice versa), and depending on the initial points and initial value of the

Table 3.10. Computational Results for Problem 3.5

Starting Points	CPU sec	# func. eval	# restarts	Solution
$F_{i,BC}^0 = F_{i,nom}^0 = F_{i,1}^0$; $\lambda_{BC}^0 = \lambda_{nom}^0 = \mathbf{0}$	1.16	570	0	Good
$F_{i,BC}^0 = F_{i,nom}^0 = F_{i,1}^0$; $\lambda_{BC}^0 = \lambda_{nom}^0 = \lambda_{nom}$	6.45	12,682	0	Good
$F_{i,BC}^0 = F_{i,nom}^0 = F_{i,2}^0$; $\lambda_{BC}^0 = \lambda_{nom}^0 = \mathbf{0}$	0.75	460	0	Bad
$F_{i,BC}^0 = F_{i,nom}^0 = F_{i,2}^0$; $\lambda_{BC}^0 = \lambda_{nom}^0 = \lambda_{nom}$	3.86	13,310	0	Bad

barrier parameter, IPOPT-C sometimes fails, and the optimization is aborted (Nocedal *et al.*, 2005). Even though different values of the barrier parameter and line search (using a merit function) were tuned, this problem could not be eliminated. In order to overcome this failure, the optimization problem was warm-started at the point at which it failed, initializing the barrier parameter at its default initial (larger) value. This procedure provides the algorithm with a broader search space, since the complementarity constraints are relaxed. Very recently, Nocedal *et al.* (2005) developed an improved (adaptive) barrier reduction strategy that may be able to avoid such a problem from occurring. Nocedal's new method, however, was not tested in this work.

3.3.2. Conclusions

By using the $MaxGap_{int}$ approach for a defined parameter uncertainty, a one-step optimization determines the largest profit gap possible and the values of the parameters and variables for the cases giving the $MaxGap_{int}$. This approach handles closed-loop optimization systems, equality and inequality constraints and uncertainty in any model coefficient directly, and it is computationally efficient for the case study in this work.

There are a few drawbacks to the use of this approach. Problem 3.5 is a nonconvex optimization problem, so global optimal solutions cannot be guaranteed unless a global solver is used. For large-scale problems, the formulation may become computationally expensive due to the increasing number of complementarity constraints. So far, IPOPT-C has been reported to handle up to 1,748 complementarity constraints (Raghunathan and Biegler, 2003).

Also, the method in this section uses interval description of uncertainty, which is simple and easily defined but may not accurately represent parameter uncertainty where the physics and chemistry dictate correlation in parameter variation. The interval description can only be extended to deterministic relationships between parameters (e.g., $a_{11} = 0.5*a_{12}$) but cannot address statistical correlation among parameters. In order to address this challenge, a method based on ellipsoidal description of uncertainty was developed and is presented in Section 3.4.

3.4. Method Based on the Largest Profit Gap – Ellipsoidal Uncertainty ($MaxGap_{ell}$)

In order to overcome the difficulties associated with the interval uncertainty in $MaxGap_{int}$, a monitoring method using an ellipsoidal description of parameter uncertainty ($MaxGap_{ell}$) was developed. This allows for the incorporation of correlation among parameters, which often occurs in process models. The formulation for calculating $MaxGap_{ell}$ is shown in Problem 3.6.

One should note that the number of equations in Problem 3.6 is smaller than in Problem 3.5, since the parameter region in Problem 3.6 can be represented by a single ellipsoid equation instead of requiring $2*P$ bound constraints as in Problem 3.5 (where P is the number of uncertain parameters).

As in Problem 3.5, the potential profit loss due to mismatch is calculated as the maximum profit gap between the "best case" and "worst case" CLRTO operations. As previously mentioned, the "best case" CLRTO has the same parameters as the true plant (no mismatch), whereas the "worst case" CLRTO uses a nominal model that differs from the true plant and thus a smaller profit than the "best case" CLRTO may be achieved.

- Best CLRTO – Similarly to Problem 3.5, the feedback term in Problem 3.1 is always zero for the "best case" CLRTO (no mismatch), and therefore the CLRTO can be modelled as an optimization without feedback.
- Nominal CLRTO – Also as in Problem 3.5, model mismatch between plant and (nominal) model parameters may result in CLRTO profit that is lower than the true plant optimum. The worst-case scenario occurs when the component qualities in the true plant maximize the profit difference due to plant/model mismatch.
- Uncertainty - In this sub-section, an ellipsoidal description of model uncertainty is used.

Problem 3.6:

$$MaxGap_{ell} = \max_{Pr_{BC}, Pr_{nom,CL}, \varepsilon^j, Q_i^j} (Pr_{BC} - Pr_{nom,CL})$$

subject to

$$Pr_{nom,CL} = \max_{F_{i,nom}} \sum_{i=1}^{n} (value - cost_i) F_{i,nom}$$

s.t.

$$\sum_{i=1}^{n} F_{i,nom} (Q_{i,nom}^j + \varepsilon^j) \geq Q_{blend,min}^j \sum_{i=1}^{n} F_{i,nom}$$

$$\sum_{i=1}^{n} F_{i,nom} (Q_{i,nom}^j + \varepsilon^j) \leq Q_{blend,max}^j \sum_{i=1}^{n} F_{i,nom}$$

$$F_{blend,\min} \leq \sum_{i=1}^{n} F_{i,nom} \leq F_{blend,\max}$$

$$F_{i,\min} \leq F_{i,nom} \leq F_{i,\max}$$

Nominal CLRTO for any plant realization Q_i^j

$$\varepsilon^j \sum_{i=1}^{n} F_{i,nom} = \sum_{i=1}^{n} F_{i,nom} (Q_i^j - Q_{i,nom}^j)$$

$$Pr_{BC} = \max_{F_{i,BC}} \sum_{i=1}^{n} (value - cost_i) F_{i,BC}$$

s.t.

$$\sum_{i=1}^{n} F_{i,BC} \cdot Q_i^j \geq Q_{blend,min}^j \sum_{i=1}^{n} F_{i,BC}$$

$$\sum_{i=1}^{n} F_{i,BC} \cdot Q_i^j \leq Q_{blend,max}^j \sum_{i=1}^{n} F_{i,BC}$$

$$F_{blend,\min} \leq \sum_{i=1}^{n} F_{i,BC} \leq F_{blend,\max}$$

$$F_{i,\min} \leq F_{i,BC} \leq F_{i,\max}$$

Best result for CLRTO for any plant realization Q_i^j

$$(Q - Q_{nom})^T \mathbf{V}^{-1}(Q)(Q - Q_{nom}) \leq \chi^2_{\alpha,dof}$$

Ellipsoidal uncertainty bounds

3.4.1. Case Study

Problem 3.6 was applied to the gasoline-blending case study using the nominal parameter values in Tables A.1 to A.3. The uncertainty region was assumed to be that of a 10-dimensional distribution with independent parameter variances of 0.0546 (octane^2 of psi^2). Therefore, at 95% confidence levels, the *largest variation possible* for each individual parameter would be ±1.0 octane or psi. In this case, the chi-squared statistic used in Problem 3.6 is equal to 18.31 (with $\alpha = 0.95$ and 10 degrees-of-freedom). For the independent parameter case evaluated in this section, the parameter variance-covariance matrix V(Q) = 0.0546*I_{10}, where I_{10} is the 10-dimensional identity matrix.

When applying Problem 3.6 to this case study, a value of $MaxGap_{ell}$ = \$1,314.0/day is found, where Pr_{BC} = \$ 11,813.7/day and $Pr_{nom,CL}$ = \$ 10,499.7/day. The variable values at the solution of Problem 3.6 are presented in Table 3.11.

As in Section 3.3, different starting points were used, and the computational experience can be found in Tables 3.12 and 3.13. For these cases, the nominal parameter values ($Q^j_{i,nom}$) were used as starting points for the component qualities. Again, "good" solutions correspond to the same solution found in Table 3.11, and "bad" solutions correspond to the optimum at which $MaxGap_{ell}$ = \$0/day.

Table 3.11. Case Study Results (Problem 3.6)

	Q_i^{oct} (octane)	Q_i^{RVP} (psi)	$F_{i,BC}$ (bbl/day)	$F_{i,nom}$ (bbl/day)
Reformate	92.74	3.04	2,696.1	5,622.9
LSR Naphtha	64.15	11.02	0.0	1,035.8
n-Butane	92.51	138.00	316.9	341.3
FCC Gas	85.31	5.94	3,987.0	0.0
Alkylate	96.60	6.70	0.0	0.0

Table 3.12. Starting Points for Problem 3.6

	$F^0_{i,1}$ = (1/5)*$F_{blend,max}$ (bbl/day)	$F^0_{i,2}$ = current CLRTO operation (bbl/day)	$F^0_{i,3}$ = same basis as $F_{i,BC}$ (bbl/day)
Reformate	1,400.0	5,695.6	3,000.0
LSR Naphtha	1,400.0	942.5	0.0
n-Butane	1,400.0	361.0	300.0
FCC Gas	1,400.0	0.0	3,700.0
Alkylate	1,400.0	0.0	0.0

The computational results show that this approach is computationally very efficient (convergence is obtained in mostly small CPU times compared to the 9-hour batch runs and requires up to three restarts, if any at all). The value of $MaxGap_{ell}$ obtained from Problem 3.6 was confirmed by applying the parameter settings obtained from the monitoring method (Table 3.11) to a CLRTO simulator. In this case, a gap of \$1,312.6/day is obtained after the system reaches steady operation, which is very close to the value of $MaxGap_{ell}$ (\$1,314.0/day). The difference is likely due to round-off errors in the parameters. For example, when using a value of reformate octane of 92.738 (instead of 92.74), a gap of \$1,313.6/day was found by solving Problem 3.6, illustrating the sensitivity of this system to small parameter changes.

Table 3.13. Computational Results for Problem 3.6

Starting Points	CPU sec	# func. eval	# restarts	Solution
$F^0_{i,BC} = F^0_{i,nom} = F^0_{i,1}$; $\lambda^0_{BC} = \lambda^0_{nom} = \mathbf{0}$	3.625	5,913	3	Good
$F^0_{i,BC} = F^0_{i,nom} = F^0_{i,1}$; $\lambda^0_{BC} = \lambda^0_{nom} = \lambda_{nom}$	25.766	123,374	1	Bad
$F^0_{i,BC} = F^0_{i,nom} = F^0_{i,2}$; $\lambda^0_{BC} = \lambda^0_{nom} = \mathbf{0}$	0.109	48	0	Bad
$F^0_{i,BC} = F^0_{i,nom} = F^0_{i,2}$; $\lambda^0_{BC} = \lambda^0_{nom} = \lambda_{nom}$	1.156	664	1	Good
$F^0_{i,BC} = F^0_{i,3}$; $F^0_{i,nom} = F^0_{i,2}$; $\lambda^0_{BC} = \lambda^0_{nom} = \mathbf{0}$	0.859	306	1	Good
$F^0_{i,BC} = F^0_{i,3}$; $F^0_{i,nom} = F^0_{i,2}$; $\lambda^0_{BC} = \lambda^0_{nom} = \lambda_{nom}$	0.031	37	0	Good

Another way to evaluate the results in Table 3.11 is to run Monte Carlo simulations on the system. The largest profit gap found in 8,768 Monte Carlo runs with the same ellipsoidal uncertainty region was \$1,053.6/day. This value is within 20% of the result from Problem 3.6 (\$1,314.0/day). The fact that even 8,768 runs were not able to find the largest value of the profit gap at the 95% confidence level shows the strength of the monitoring method developed in this section. The number of Monte Carlo runs (8,768) was deemed sufficient because there were no significant changes in the results from when approximately 5,000 runs were made.

In this case study, $MaxGap_{ell}$ (\$ 1,314.0/day) is much less conservative than $MaxGap_{int}$ (\$3,024.9/day), as expected because the box description of uncertainty encompasses a larger parameter region than the ellipsoid, as can be seen in Figure 3.4.

The solution of the $MaxGap_{ell}$ problem does not appear to be at the boundary in Figure 3.4 because this is a two-dimensional projection of the 10-dimensional object, and there is parameter variation in the remaining 8 dimensions of the ellipsoid. Actually, it is on the boundary of the 10-dimensional ellipsoid, since the ellipsoidal constraint is active at the solution.

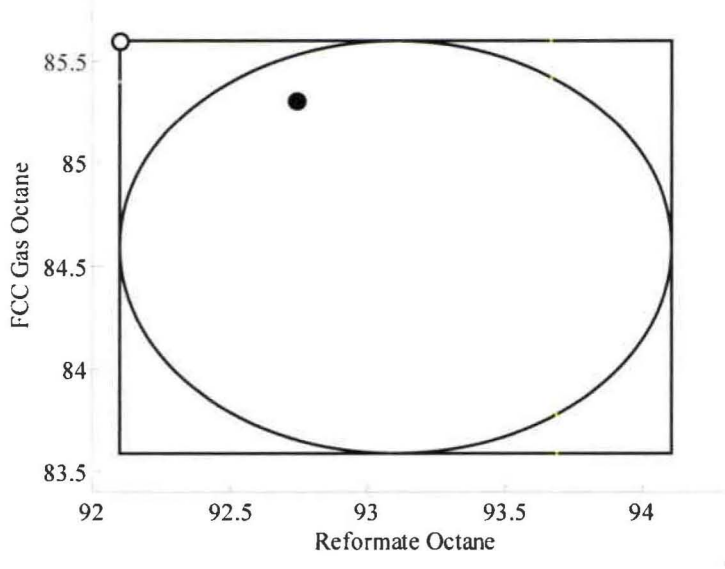

Figure 3.4. Interval Uncertainty versus Ellipsoidal Uncertainty Results (o - interval, ● - ellipsoidal)

3.4.2. Conclusions

The monitoring of closed-loop RTO systems using $MaxGap_{ell}$ as a criterion has the same advantages as the ones presented in Section 3.3.2 for $MaxGap_{int}$; namely, it is a one-step optimization problem that handles closed-loop systems and parametric sources of uncertainty appearing in all types of constraints. In addition, $MaxGap_{ell}$ uses a description of uncertainty that also enables the establishment of correlation among parameters, which exists in many applications in the process industries. Therefore, it is a more realistic monitoring criterion than $MaxGap_{int}$.

On the other hand, it suffers from some of the drawbacks mentioned in Section 3.3.2. The computation of $MaxGap_{ell}$ still requires a solution of a non-convex optimization problem, where a global solution can only be guaranteed by the use of a global solver. Also, for large-scale problems, the formulation may become computationally very expensive due to the increasing number of complementarity constraints.

Since $MaxGap_{ell}$ is still a conservative estimate of the potential economic loss due to parametric uncertainty, Sections 3.5 and 3.6 introduce extensions for obtaining a better estimate of potential profit loss to be used for monitoring CLRTO.

3.5. Method Based on the Expected Value of the Largest Profit Gap

In order to obtain an improved estimate of the largest profit gap, its expected value is calculated over a range of confidence levels. It is important to note that this approach considers the *distribution* of the parameters instead of only considering parameter ranges or bounds of an ellipsoidal region. For illustration purposes, a bivariate normal distribution of two random variables, X and Y, is presented in Figure 3.5.

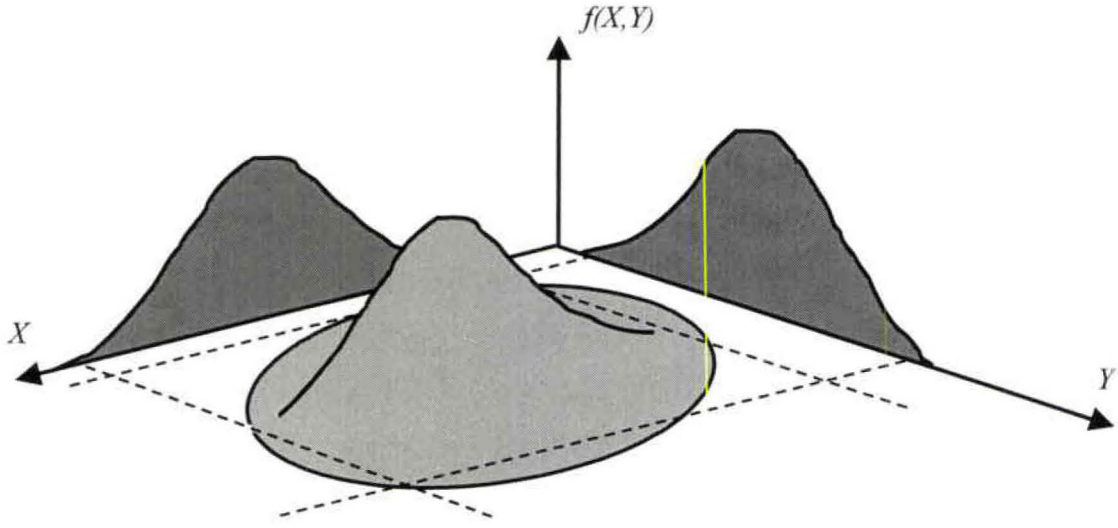

Figure 3.5. Joint Probability Density of Normally Distributed Random Variables X and Y, with Respective Marginal Distributions

The method in Section 3.4 calculates the Largest Profit Gap for a fixed confidence level. The expected value of a function Z that depends on X and Y is calculated by integrating over the entire surface in Figure 3.5; for example, for two variables, the integration is given in the following (Montgomery and Runger, 1994).

$$\mathrm{E}(Z) = \int_{-\infty}^{\infty}\int_{-\infty}^{\infty} Z(x,y) f_{X,Y}(x,y)\,dx\,dy \qquad (3.3)$$

In equation (3.3), $f_{x,y}(x,y)$ is the joint probability density function. For discrete random variables, the summation operator replaces the integrals:

$$\mathrm{E}(Z) = \sum_{x}\sum_{y} Z(x,y) f_{X,Y}(x,y) \qquad (3.4)$$

In order to approximate the expectation operator, the probability distribution was discretized at a number of different confidence levels, and the expected value of the largest profit gap was calculated according to equation (3.4). When there are n random variables, this equation becomes

$$E(Z) = \sum_{x_1} \cdots \sum_{x_n} Z(x_1,...,x_n) f_{X_1 \ldots X_n}(x_1,...,x_n) \qquad (3.5)$$

Equation (3.5) provides a method for evaluating the expected value of a function. If Z = Profit Gap, each sample would entail the solution of two convex optimization problems: one for the CLRTO model with no mismatch, and another for a CLRTO system with model mismatch. The difference between the objective function of these two optimization problems is defined as the Profit Gap. However, this approach may require a very large number of samples depending on the number of uncertain parameters.

When considering $Z = MaxGap_{ell}$, the bilevel Problem 3.6 is solved for a few different levels of significance. This approach requires few evaluations of Problem 3.6. Even though a nonconvex optimization problem has to be solved at each evaluation, this approach was selected because it scales well as the number of parameters increases. The method is developed in detail and applied in subsequent sections.

3.5.1. Determination of Smallest Confidence Level that Yields $MaxGap_{ell} \geq T$

The first step is to determine the confidence level below which the $MaxGap_{ell}$ is zero. At very small confidence levels, the uncertain parameters lie in a very small region around the nominal parameters. Therefore, up to a given confidence level, the largest profit gap may be zero for the linear programming CLRTO problem being considered. If the value of the largest confidence level that yields a zero largest profit gap is determined, fewer discretization points are needed for a good approximation of the expected value of

the largest profit gap. The formulation to determine the largest confidence level that still yields a maximum profit gap of zero is stated in Problem 3.7.

Problem 3.7 :

$$\min_{Pr_{BC},\, Pr_{nom,CL},\, \varepsilon^j,\, Q_i^j} \quad C_{Gapmin}$$

subject to

$$Pr_{nom,CL} = \max_{F_{i,nom}} \sum_{i=1}^{n} (value - cost_i) F_{i,nom}$$

s.t.

$$\sum_{i=1}^{n} F_{i,nom} (Q_{i,nom}^j + \varepsilon^j) \geq Q_{blend,min}^j \sum_{i=1}^{n} F_{i,nom}$$

$$\sum_{i=1}^{n} F_{i,nom} (Q_{i,nom}^j + \varepsilon^j) \leq Q_{blend,max}^j \sum_{i=1}^{n} F_{i,nom}$$

$$F_{blend,\min} \leq \sum_{i=1}^{n} F_{i,nom} \leq F_{blend,\max}$$

$$F_{i,\min} \leq F_{i,nom} \leq F_{i,\max}$$

$$\varepsilon^j \sum_{i=1}^{n} F_{i,nom} = \sum_{i=1}^{n} F_{i,nom} \left(Q_i^j - Q_{i,nom}^j\right)$$

} Nominal CLRTO for any plant realization Q_i^j

$$Pr_{BC} = \max_{F_{i,BC}} \sum_{i=1}^{n} (value - cost_i) F_{i,BC}$$

s.t.

$$\sum_{i=1}^{n} F_{i,BC} . Q_i^j \geq Q_{blend,min}^j \sum_{i=1}^{n} F_{i,BC}$$

$$\sum_{i=1}^{n} F_{i,BC} . Q_i^j \leq Q_{blend,max}^j \sum_{i=1}^{n} F_{i,BC}$$

$$F_{blend,\min} \leq \sum_{i=1}^{n} F_{i,BC} \leq F_{blend,\max}$$

$$F_{i,\min} \leq F_{i,BC} \leq F_{i,\max}$$

} Best result for CLRTO for any plant realization Q_i^j

$$(Q - Q_{nom})^T \mathbf{V}^{-1}(Q)(Q - Q_{nom}) = C_{Gap\min}$$

} Ellipsoidal uncertainty bounds

$$Pr_{BC} - Pr_{nom,CL} \geq Gap_{\min}$$

} Profit gap must be greater than Gap_{min}.

Table 3.14. Solution of Problem 3.7 for Different Values of Gap_{min}

Gap_{min} ($/day)	C_{Gapmin}	$\alpha(\chi^2, 10\ dof)$
0	0.07959	0.0
500	3.459	0.0315
1314.0	18.3106	0.9501

The case study considered was the same as the one in Section 3.4.1. From the results in Table 3.14, since the largest α that yields Gap_{min} = \$0/day was zero, and even very small confidence levels of 3.15% yielded a significant value of the largest profit gap (\$500/day), the approximation of the integral was made starting at zero confidence level.

The next step is to formulate a series of problems that can be used to approximate the expected value. To calculate the expected value of profit, three approximations to the integral were used: backward difference equation (3.6), forward difference equation (3.7) and trapezoidal approximation equation (3.8), which are illustrated in Figure 3.6.

$$\mathrm{E}(MaxGap_{ell})_{BW} = \sum_{k=1}^{nc}(\alpha_k - \alpha_{k-1})MaxGap_{ell}(\alpha_k) \qquad (3.6)$$

$$\mathrm{E}(MaxGap_{ell,})_{FW} = \sum_{k=1}^{nc}(\alpha_{k+1} - \alpha_k)MaxGap_{ell}(\alpha_k) \qquad (3.7)$$

$$\mathrm{E}(MaxGap_{ell})_{TR} = \sum_{k=1}^{nc}\frac{(\alpha_k - \alpha_{k-1})}{2}[MaxGap_{ell}(\alpha_{k-1}) + MaxGap_{ell}(\alpha_k)] \qquad (3.8)$$

$MaxGap_{ell}$ in equations (3.6) to (3.8) is obtained by solving Problem 3.6. The backward difference provides an upper bound to the estimate of the area below the curve. The forward difference provides a lower bound to this estimate, and the trapezoidal approximation is the average of the two previous estimates, as illustrated in Figure 3.6.

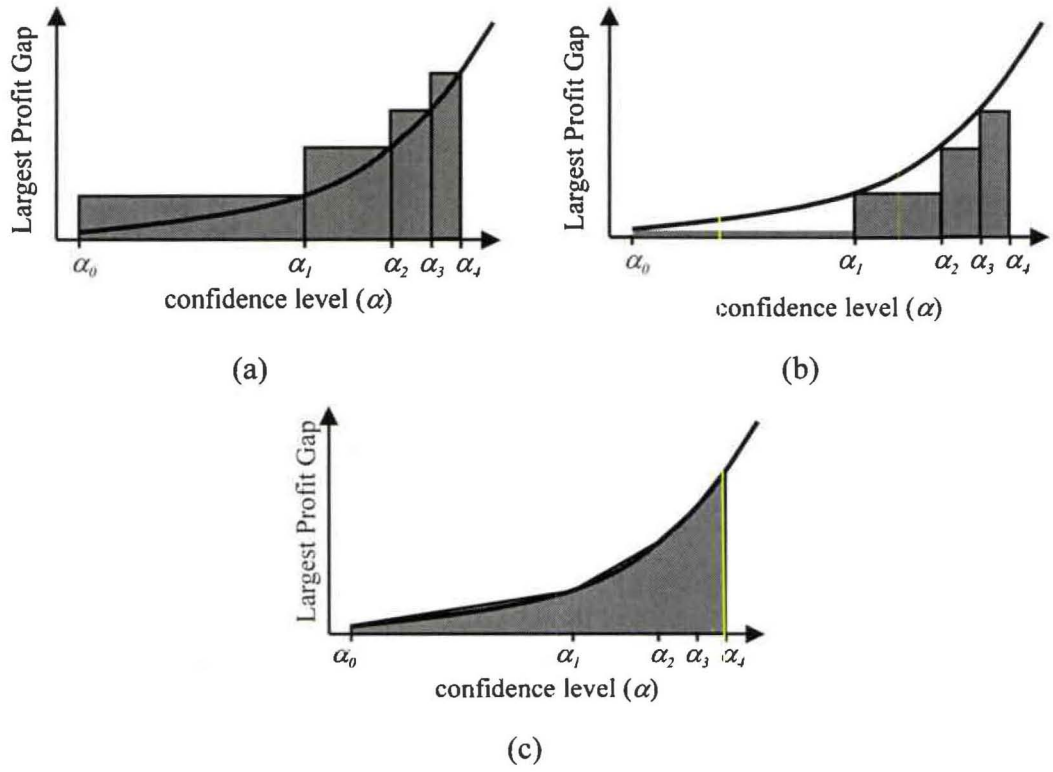

Figure 3.6. Integration using (a) backward difference, (b) forward difference and (c) trapezoidal approximation

The importance of using the three approximation approaches simultaneously is to assess the error in the estimate. If the three areas are similar, the number (and location) of approximation points is deemed appropriate. If the results differ above a user-defined threshold, more points can be added to the discretization, in the region where the values of the areas differ by unacceptable amounts.

Because it is likely to be the closest approximation to this curve, the trapezoidal approach is taken as the best estimate of the expected profit gap for comparing with the other approaches.

Table 3.15. Results for the Approximation of the Integral

	$\alpha \leq 0.50$	$\alpha \geq 0.50$ $\alpha \leq 0.75$	$\alpha \geq 0.75$ $\alpha \leq 0.90$	$\alpha \geq 0.90$ $\alpha \leq 0.95$	$\alpha \geq 0.95$ $\alpha \leq 0.99$	$\alpha \geq 0.99$	$E(MaxGap_{ell})$ ($ / day)
BW	447.2	264.7	182.4	65.7	60.2	-	1,020.3
FW	-	223.6	158.8	60.8	52.6	15.0	510.9
TR	223.6	244.2	170.6	63.2	56.4	-	758.0

3.5.2. Case Study

The same case study as in Section 3.4.1 was considered. Table 3.15 shows the three different approximations of the expected values for each confidence level interval, and the final expected value of the largest profit gap $E(MaxGap_{ell})$. Details on the computational experience can be found in Appendix C.

From Table 3.15, at least one additional point should be added between $\alpha = 0.0$ and $\alpha = 0.50$ due to the large difference between the areas for the three approximations. If another point is added at $\alpha = 0.25$, the results in Table 3.16 are obtained. After the addition of another discretization point of the confidence region, the difference between the expected largest profit gap calculated by the three methods decreased significantly. The results in Table 3.16 were confirmed by running 8,768 Monte Carlo simulations. The expected largest profit gap using trapezoidal approximation from the simulated data was $685.7/day, which is roughly $140/day less than $E(MaxGap_{ell})_{TR}$ and $10/day less than $E(MaxGap_{ell})_{FW}$. Even though $E(MaxGap_{ell})_{FW}$ is a lower bound for the integral, it is based on calculating the *largest* Profit Gap. It is important to point out that although over 8,000 Monte Carlo runs were performed, a larger number of realizations might increase the

Table 3.16. Results for the Refined Approximation of the Integral

	$\alpha \leq 0.25$	$\alpha \geq 0.25$ $\alpha \leq 0.50$	$\alpha \geq 0.50$ $\alpha \leq 0.75$	$\alpha \geq 0.75$ $\alpha \leq 0.90$	$\alpha \geq 0.90$ $\alpha \leq 0.95$	$\alpha \geq 0.95$ $\alpha \leq 0.99$	$\alpha \geq 0.99$	$E(MaxGap_{ell})$ ($ / day)
BW	185.2	223.6	264.7	182.4	65.7	60.2	-	981.9
FW	-	185.2	223.6	158.8	60.8	52.6	15.0	696.1
TR	92.6	204.4	244.2	170.6	63.2	56.4	-	831.5

value of the expected largest profit gap coming from simulated data, since local optimal points may have been found during the Monte Carlo simulations. Also, the discretization of the parameter region may have been too coarse. If more accuracy in the estimate were required, another point could be added between $\alpha = 0.0$ and $\alpha = 0.25$. However, since the inconsistencies were considered small, further computation was not justified.

As anticipated, the integration of $MaxGap_{ell}$ over several confidence levels provides a smaller estimate of the economic impact of parametric uncertainty on the objective function ($831.5/day) than does $MaxGap_{ell}$ ($ 1,314.0/day) or $MaxGap_{int}$ ($3,024.9/day) for the same system. However, this evaluation requires the solution of several non-convex optimization problems. In this case, obtaining $E(MaxGap_{ell})_{TR}$ required 7 times more computational time than the obtaining $MaxGap_{ell}$. Therefore, there is a trade-off between the improved representation of the monitoring goal and its computational demands.

The expected value of the *largest* profit gap $E(MaxGap_{ell})_{TR}$ is a more accurate criterion for determining the potential profit loss in the closed-loop system due to parametric mismatch, but it is still conservative (an overestimate) when compared to the expected value of the profit gap. Section 3.6 presents a method for determining upper- and lower-bounds on the expected value of the profit gap.

3.6. Method Based on the Expected Value of the Profit Gap

In most applications of monitoring uncertain plant operations, the expected value of the profit gap (E(*Gap*)), the difference between the best and worst profits for CLRTO over the uncertainty range of the parameters is the best estimate of the effect of parameter uncertainty on the objective function. Calculating the expected value of a function usually requires computationally expensive methods such as function integration or sampling from the parameter space. In this section, a method is presented that reduces the size of the parameter space based on bounds of the objective function in a subspace. The result is a reduction in the computational burden of the calculations.

The approach taken here is similar to the previous section, in that equation (3.5) is applied to estimate the expected value, and the function "Z" is the $MaxGap_{ell}$ (Problem 3.6). In this section, we take advantage of the insight that the $MaxGap_{ell}$ depends strongly on "direction", i.e., the worst case $MaxGap_{ell}$ in a ellipse will usually be much worse (larger) than the average Gap in the ellipse. Therefore, the regions in this section are divided by confidence level and "direction"; here, angles are used to define the direction. In addition, since we seek the expected value of the Gap (profit loss), and not the $MaxGap_{ell}$, we evaluate the expected values of both the maximum and the minimum profit gaps in each region.

A case study with only two uncertain parameters is considered so that a graphical interpretation can be presented. The parameter values for this case study can be seen in Tables A.1 to A.3. The only uncertain parameters in this case are Reformate octane and LSR Naphtha octane, each with a variance of 0.167 octane^2. In a two-dimensional multivariate distribution, this variance allows for maximum variations of ±1.0 octane in each parameter.

The method divides the parameter space into several regions and determines the expected largest profit gap (E($MaxGap_{ell}$) from Section 3.5) in each region. If the expected largest gap in a region is small (near zero), there is no reason to sub-divide the region further, since the Gap in the region is also very small.

If the expected largest gap is significant, the value of the expected *smallest* profit gap is also evaluated: in order to obtain a lower bound of E(*Gap*) in a parameter region, the profit gap in the objective function of Problem 3.6 was *minimized* for that region. This objective function will be denoted as $MinGap_{ell}$. As in the calculation of the upper bound of E(*Gap*) (E($MaxGap_{ell}$)), the lower bound of E(*Gap*) was calculated by using the forward difference approximation to obtain the expected smallest profit gap (E($MinGap_{ell}$)) over large regions of the parameter space.

When the values of the expected largest and smallest profit gaps in a region are sufficiently close, an estimate of the Gap has been determined, and there is no reason to sub-divide the region further. If the difference is large, the region can be sub-divided

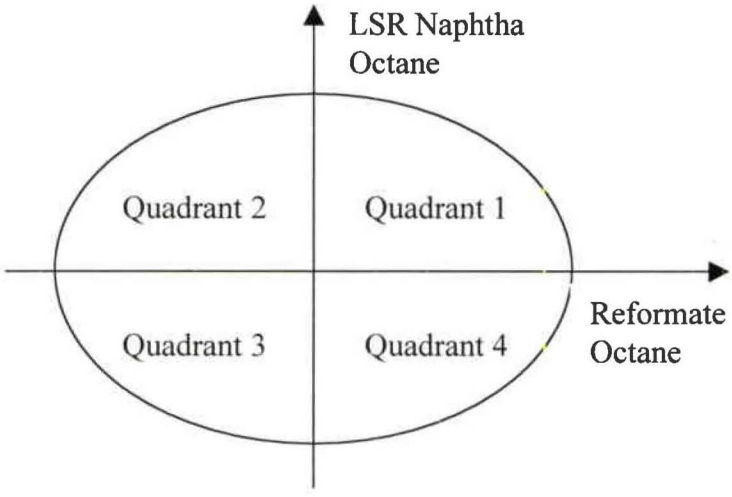

Figure 3.7. First Division of Parameter Space

until the difference in the expected profit gaps is sufficiently close. When all regions have been evaluated, the total expected value is the sum of the profit gaps for each region weighted by its probability.

In the two-dimensional case study, this method was initially applied to each of the four quadrants, as shown in Figure 3.7. As a first step, the calculations were performed without any concern for direction with 6 confidence levels: 25%, 50%, 75%, 90%, 95% and 99%.. The value for the upper bound of E(*Gap*), $E(MaxGap_{ell})_{BW}$ was \$275.8/day. The value of $E(MinGap_{ell})_{FW}$ (lower bound of E(*Gap*)) for the entire parameter region was \$0.0/day. This is too large a difference, so the method proceeded by subdivisions according to direction within each confidence region.

After dividing the parameter space in four quadrants shown in Figure 3.7, the upper and lower bounds of E(*Gap*) became \$131.3/day and \$3.7/day, respectively (Table 3.17). Since the difference between the bounds was still considered too large, further divisions were warranted. Since Quadrants 1 and 4 had \$0.0/day values for $E(MaxGap_{ell})_{BW}$ (upper bound), they did not need to be further evaluated, thus reducing the computational requirements substantially. The values in Quadrants 2 and 3 were significantly different and were subdivided in 45° halves. From Table 3.18 to Table 3.20,

Table 3.17. First division of parameter space

	$E(MaxGap_{ell})_{BW}$ ($/day)	$E(MinGap_{ell})_{FW}$ ($/day)
Quadrant 1	0.0	0.0
Quadrant 2	249.5	0.0
Quadrant 3	275.8	14.6
Quadrant 4	0.0	0.0
Bounds on E(*Gap*)	131.3	3.7

Table 3.18. Second division of parameter space

	$E(MaxGap_{ell})_{BW}$ ($/day)	$E(MinGap_{ell})_{FW}$ ($/day)
Quadrant 1	0.0	0.0
Quadrant 2 (90°-135°)	59.9	0.0
Quadrant 2 (135°-180°)	249.5	14.4
Quadrant 3 (180°-225°)	275.8	86.4
Quadrant 3 (225°-270°)	250.1	14.6
Quadrant 4	0.0	0.0
Bounds on E(*Gap*)	104.4	14.4

Table 3.19. Third division of parameter space

	$E(MaxGap_{ell})_{BW}$ ($/day)	$E(MinGap_{ell})_{FW}$ ($/day)
Quadrant 1	0.0	0.0
Quadrant 2 (90°-112.5°)	0.0	0.0
Quadrant 2 (112.5°-135°)	59.9	0.0
Quadrant 2 (135°-157.5°)	173.9	14.4
Quadrant 2 (157.5°-180°)	249.5	56.8
Quadrant 3 (180°-202.5°)	275.8	86.4
Quadrant 3 (202.5°-225°)	275.8	86.6
Quadrant 3 (225°-247.5°)	250.1	57.0
Quadrant 3 (247.5°-270°)	174.5	14.6
Quadrant 4	0.0	0.0
Bounds on E(*Gap*)	91.2	19.7

the angles are considered to originate on the intersection between Qadrant 1 and Quadrant 4, and to increase counter-clockwise. After the second subdivision of the parameter space, E(*Gap*) was determined to be between \$14.4/day and \$104.4/day (Table 3.18). Even though E($MaxGap_{ell}$)$_{BW}$ in sub-quadrant 2, from 90° to 135° was fairly small (\$59.9/day), it was further subdivided because it was adjacent to a large parameter region (Quadrant 1), which had a \$0.0/day E($MaxGap_{ell}$)$_{BW}$.

As can be seen in Table 3.19, the third subdivision of Quadrant 2 showed that 25% of the area in Quadrant 2 (90°-112.5°) yielded a \$0.0/day E($MaxGap_{ell}$)$_{BW}$, which leads to a less conservative estimate of E(*Gap*). After the third subdivision of the parameter space, E(*Gap*) was determined to be between \$19.7/day and \$91.2/day. Only the regions of the parameter space that yielded a E($MaxGap_{ell}$)$_{BW}$ larger than \$200.0/day were then further subdivided.

Table 3.20. Fourth division of parameter space

	E($MaxGap_{ell}$)$_{BW}$ (\$/day)	E($MinGap_{ell}$)$_{FW}$ (\$/day)
Quadrant 1	0.0	0.0
Quadrant 2 (90°-112.5°)	0.0	0.0
Quadrant 2 (112.5°-135°)	59.9	0.0
Quadrant 2 (135°-157.5°)	173.9	14.4
Quadrant 2 (157.5°-168.8°)	218.8	56.8
Quadrant 2 (168.8°-180°)	249.5	73.8
Quadrant 3 (180°-191.3°)	269.1	86.4
Quadrant 3 (191.3°-202.5°)	275.8	94.1
Quadrant 3 (202.5°-213.8°)	275.8	86.4
Quadrant 3 (213.8°-225°)	269.4	86.6
Quadrant 3 (225°-236.3°)	250.1	74.0
Quadrant 3 (236.3°-247.5°)	218.1	57.0
Quadrant 3 (247.5°-270°)	174.5	14.6
Quadrant 4	0.0	0.0
Bounds on E(*Gap*)	88.8	21.0

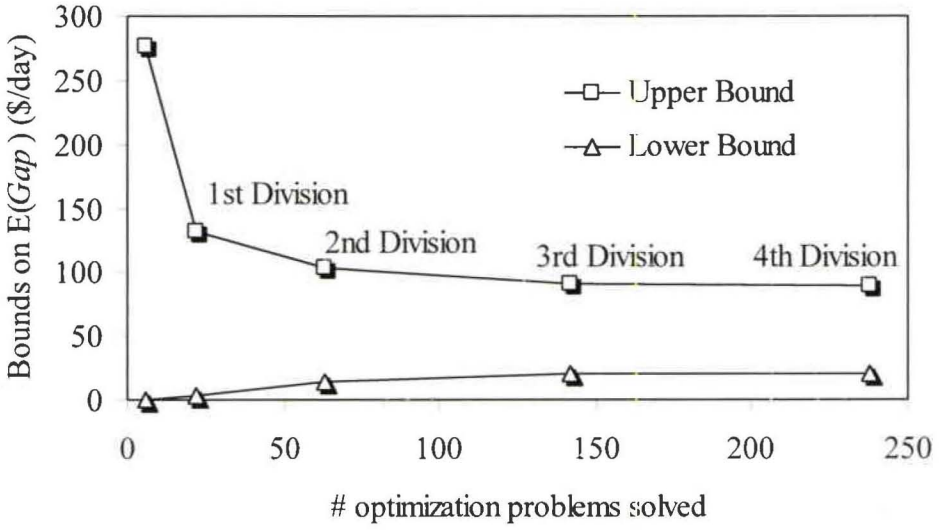

Figure 3.8. Estimation of Upper and Lower Bounds of E(*Gap*)

The fourth subdivision of the parameter space can be seen in Table 3.20, and resulted in E(*Gap*) bounds of \$21.0/day and \$88.8/day. Since the additional subdivision did not change the upper and lower bound estimation significantly, and since the bounds are only \$67.8/day apart, no further subdivisions of the parameter space were made.

Figure 3.8 shows the estimation of upper and lower bounds of E(*Gap*) with the number of required solutions of Problem 3.6 ($MaxGap_{ell}$). Between the 3rd and 4th divisions of the parameter space, the rate of change of the bounds was very small, being another indication that the procedure could be interrupted. In order to verify the results, 1,103 Monte Carlo simulations were performed on this system, resulting in an estimated E(*Gap*) of \$27.2/day, which lies within the estimated upper and lower bounds.

For higher-dimensional systems, regions of the parameter space should be divided by hyper-planes, and the procedure of estimating bounds for E(*Gap*) should be applied to the areas divided by these hyper-planes. Depending on the problem structure, this could be computationally more efficient than sampling the parameter space to determine the expected value of the profit gap, since large areas of the parameter space could potentially be eliminated. This is especially true for large-scale systems in which large

parameter regions yield very small profit gaps. Furthermore, since upper and lower bounds are calculated, the procedure of estimating E(*Gap*) only needs to be applied until the bounds are close enough to each other.

3.7. Relationship to Decision Analysis Theory

The methods in this chapter deal with monitoring optimization systems under uncertainty, and thus, they are related to problems of decision-making under uncertainty. Therefore, they have similarities to some of the technology developed in the Operations Research (OR) field. The most relevant topics in OR that are related to this chapter are (Maximum) Regret and Expected Value of Perfect Information

Regret is defined as the deviation of the objective function at any given point from the best possible one (Averbakh, 2000). Typically, OR methods determine the Regret by solving the problem for samples of uncertain parameters from the allowable space. This method can be appropriate when the uncertainty contains a small number of discrete variables, such as options for a process technology (e.g., distillation, membrane, no recovery). However, sampling can impose a substantial computational burden when the region of uncertain parameters is large. By using the approach in this thesis, the maximum Regret is evaluated by solving one problem, which can be more computationally efficient and is essential for the experimental design method introduced in Chapter 4.

The Expected Value of Perfect Information (EVPI) is the difference between the results of the decision made with perfect information and the decision made with original information (Winston, 1994). This problem is typically solved by Monte Carlo simulations, scenario enumerations or decision trees in literature, which scale poorly for large-dimensional systems. Section 3.6 presented a method for determining bounds on the value of the EVPI, which corresponds to the expected value of the profit gap.

3.8. Conclusions

Model-based optimization of plant operations is susceptible to mismatch between the model used for optimization and the true plant. This chapter has presented methods for estimating the effect of model mismatch on optimization performance, where performance is the deviation from the maximum achievable profit. The methods monitor the performance without interfering with the operation of the process, i.e., no experiments are required.

The mismatch is characterized by a range of parameter values in a linear programming optimization model. Depending upon the method used, the monitoring method determines one of the following metrics.

- The maximum achievable profit, including the most favourable parameters that could exist in the plant
- Whether the current optimal corner point is the only possible optimal corner point within the parameter uncertainty (assured optimality)
- The maximum profit loss due to model mismatch (Maximum Regret)
- The expected value of the maximum profit loss due to model mismatch
- Bounds on the expected value of the profit loss (EVPI)

Each subsequent method provides more information and better monitoring; however, the computational demands increase as well. Importantly, the method that evaluates the maximum profit loss due to mismatch requires the solution to a single optimization problem. This method is integrated into the experimental design for process improvement in the next chapter.

The key application addressed is closed-loop, linear real-time optimization, which has found wide application to blending over that last 20 years. Therefore, a new formulation that represents the behaviour of the closed-loop system has been developed. In contrast, many applications of optimization in operations optimization are referred to

as "open-loop", indicating that no feedback information is used in subsequent optimization executions. In reality, many of these applications include some form on periodic model correction based on measurements; therefore, many applications referred to as "open-loop" are really "closed-loop" with a slow period on the feedback. This situation is demonstrated, for instance, by the existence of reactive scheduling problems (Herroelen and Leus, 2005). The results in this chapter can be applied to both automated CLRTO and "manual" optimization with model corrections introduced by the engineer, as long as the linear programming model contains only continuous variables (not discrete) and the feedback is applied consistently as modelled.

Nevertheless, the methods in this chapter can also be applied to truly open-loop decisions with little modification. Some extensions to open-loop systems are presented in Appendix E with applications to previously published case studies.

The formulations in this chapter required the solution of optimality conditions as constraints in an "outer" optimization problem. The method builds on recent advances in optimization methods and software, using the IPOPT-C solver for the non-convex problems involving complementarity constraints. Even with this software, several restarts and selection of the best of several local solutions were required to achieve reliable monitoring results.

The case studies in the chapter are representative of the on-line gasoline and fuel oil blending in industry, as well as other industries such as cement production. However, these are not necessarily large-scale problems, and further investigation is required to establish the limits of application of the method. In terms of the complementarity constraints that arise in the formulation, IPOPT has been reported to handle up to 1,748 complementarity constraints so far (Raghunathan and Biegler, 2003). Certainly, further work is required to refine the method developed for the expected value of the profit loss.

When monitoring indicates a significant potential profit loss, the engineer would like to understand the likely cause(s) and take actions to improve process operations. These topics are addressed in the next chapter.

Chapter 4

RTO Performance Enhancement and Diagnostics

4.1. RTO Performance Enhancement

In Chapter 3, methods were developed that monitor closed-loop RTO performance. If the optimizer performance is deemed unacceptable, i.e., the largest profit gap is considered excessive, uncertainty in key model parameters needs to be reduced. This chapter introduces methods for diagnosing and improving optimization performance.

There are several ways to obtain a more accurate process model. In some processes, parameters may be physically measurable, so sensors can be installed in order to obtain an accurate estimate of their true values. In gasoline-blending processes, for instance, octane number and Reid vapour pressure (RVP) are potentially measurable parameters. Sensors, however, can be very expensive. The cost of a single near infrared (NIR) sensor that can measure different properties for one component stream costs in the order of US$300,000, without considering maintenance costs (Measurementation Inc., 2004). An alternative to measuring parameters is to rely on a more accurate process model than the one used in the RTO. However, if not available, such a model may be very expensive to develop. In the blending application, the linear model would have been developed by local linearization of a more accurate nonlinear model, if one existed.

Finally, model parameters can be re-estimated based on existing process measurements available during plant operation. Since typical variation in the plant is limited, significant improvement in parameter accuracy will usually require designed experiments in the plant. The experimental approach to model improvement is selected for model improvement.

Two different approaches to experimental design were developed in this work. One approach requires the number of optimal bases to be no more than one given the parametric uncertainty while minimizing cost. The second approach maximizes the profit during the remaining batch duration by improving the performance monitoring metric (reducing the largest profit gap) while also performing low-cost experiments. The latter approach was solved using two different optimization methods: model-based methods and direct search methods using Derivative-Free Optimization (DFO).

All of the experimental design formulations proposed in this chapter have a flexible constraint structure that can be tailored to the specific plant situation. For example, the user may choose constraints on product quality, component and blended product flowrates, and changes in flowrates between contiguous steady states, among others.

The parameter-updating strategy embedded in the experimental design formulations is Bayesian Estimation, which allows for the direct incorporation of estimates of the uncertainty in the model parameters based on prior information, which includes previous experiments. The inclusion of prior information prevents unnecessarily large experiments in the plant. As a safeguard against underestimating prior parameter variance, a larger variance than assumed by plant personnel can be used (Box and Tiao, 1973). The effect of different prior variances on the intercepts of the equations is discussed in Chapter 5. More details on Bayesian parameter estimation can be found in Appendix B.

As discussed in Chapter 2, conventional experimental design methods reduce the size of the parameter confidence region. The formulations in Sections 4.1.1 and 4.1.2 are focused on improving the performance of the CLRTO system. These new designs reduce

parametric uncertainty in the constraints that most influence the potential loss in profit. Another contribution is the fact that the cost of experimentation is considered, building on the work of Yip and Marlin (2001).

In the following section, the model enhancement based on corner point information is presented, followed by the method based on the largest profit gap.

4.1.1. Performance Enhancement Based on Corner Point Information

As mentioned in Chapter 3, if there is only one possible corner point in a linear closed-loop RTO system with parametric uncertainty between the plant and optimizer, that corner point corresponds to the true plant optimum (Forbes and Marlin, 1994). Therefore, the first approach to designing experiments to improve CLRTO performance requires that the final parameter uncertainty lie within the parameter region that yields a single corner point. In this formulation, the experiments are performed to achieve this goal at the lowest possible cost to plant operation. The experiments for the gasoline-blending problem are determined by solving the following bilevel mathematical program.

Problem 4.1:

$$\min_{F_{ki}} \sum_{k=1}^{nexp} \sum_{i=1}^{n} \mu_i \left(F_{i,k} - F_{i,\min} \right)$$

subject to

$$\begin{cases}
\sum_{i=1}^{n} F_{i,exp,k} \left(Q^j_{i,nom} + \varepsilon^j_{exp} \right) \geq Q^j_{blend,min} \sum_{i=1}^{n} F_{i,exp,k} \\
\sum_{i=1}^{n} F_{i,exp,k} \left(Q^j_{i,nom} + \varepsilon^j_{exp} \right) \leq Q^j_{blend,max} \sum_{i=1}^{n} F_{i,exp,k} & k = 1 \,..\, nexp \\
F_{i,min} \leq F_{i,exp,k} \leq F_{i,max,} & j = oct,\ RVP \\
F_{blend,min} \leq \sum_{i=1}^{n} F_{i,exp,k} \leq F_{blend,max} \\
V(Q) = \left(V(Q)|_{t-1} + X^T_{exp} V(z)^{-1} X_{exp} \right)^{-1} \\
\min_i \delta \geq 0. \\
\delta = \min_{\lambda, Q^j_i} \lambda_i \\
\quad s.t. \begin{cases} \nabla_F Pr|_F - \boldsymbol{\lambda}^T \nabla_F g_A|_F = \mathbf{0} \\ Q^j_{i,nom} - 1.96\sqrt{V(Q)} \leq Q^j_{i,nom} \leq Q^j_{i,nom} + 1.96\sqrt{V(Q)} \end{cases} , \forall\ i, j
\end{cases}$$

Guarantees unique optimum basis using quality bounds after experimentation

The solution of the "inner problem" ensures that only one optimal corner point is possible for all realizations of the uncertain parameters *after the experiments*. Therefore, an estimate of the variance is required. As mentioned in the introduction of this chapter, the parameter-updating strategy of choice was Bayesian Estimation, which allows for the incorporation of estimates of the uncertainty in the model parameters based on prior information. The prior information will be plant experience for the first experiment in a batch and will combine experience and experimentation for later iterates. In this way, the estimate of the variance-covariance matrix of the parameters $V(Q)$ will rely on prior knowledge of $V(Q)|_{t-1}$ (equation (B.3) in Appendix B).

Even though this problem presents discontinuous derivatives, the Sequential Quadratic Programming (SQP) method in *fmincon* was able to find locally optimal solutions. The good performance is likely due to two factors. First, the (multiple) starting

points used were reasonably close to the optimum (Biegler and Grossmann, 2004). Second, for these problems, sudden changes in the directionality of decision variables should not occur with the discontinuity due to the need to reduce uncertainty in key component properties by using the same key component flowrates.

In Problem 4.1, the parameters ε_{exp}^{j} correspond to the bias values in the CLRTO before running the experiment. The parameters μ_i in the objective function correspond to the marginal costs (Lagrange multipliers) of each component flow at the current RTO run. These costs will be zero for variables between their bounds (basic variables). In the gasoline-blending process, the product quality specifications are for the total, integrated product. Therefore, changes to the basic flows that are not at their bounds can be compensated after the experiment to have no net effect on the product qualities or total flows used to produce the blend. Changes to any component flow that is at its upper or lower bound results in a cost because the integrated flow will deviate from the predicted best value due to the experiment. The objective function of Problem 4.1 shows costs on flows at their lower bounds ($F_{i,min}$). In the case of flows at their upper bounds, the objective function should be $\mu_i.(F_{i,max} - F_{i,k})$.

Since the experimental design is formulated as a mathematical program, many options exist in the definition of the constraints in the experimental design to satisfy specific problem requirements. For the experimental design defined in Problem 4.1, the flows of components and final product and the blended qualities can vary within their bounds. Since the blended gasoline product is stored in a large tank before being shipped to customers, no requirement exits for strict control of instantaneous product qualities during the experiment (Diaz and Barsamian, 1996; Sakr et al., 1988). Because of this, the experimental design formulation in Problem 4.1 only requires feasibility of the nominal model during the experiment. Other strategies for experimental designs, such as restricting changes in the flow rates from the current operation or introducing chance constraints (Ben-Tal and Nemirovski, 1998) that would require the uncertain model to be

Table 4.1. Description of Case for Approach Based on Corner Points

	$Q_{i,nom}^{oct}$ (octane)	$Q_{i,nom}^{RVP}$ (psi)	$V(Q_{i,nom}^{oct})$ (octane^2)	$V(Q_{i,nom}^{RVP})$ (psi^2)	$Q_{i,true}^{oct}$ (octane)	$Q_{i,true}^{RVP}$ (psi)	$cost_i$ ($/bbl)
Reformate	92.33	2.6	0.0256	1e-8	92.3	2.6	34.2
LSR Naphtha	63.90	10.9	0.664	1e-8	64.0	10.9	26.5
n-Butane	92.5	138.8	1e-8	1e-8	92.5	138.8	10.3
FCC Gas	84.6	6.4	1e-8	1e-8	84.6	6.4	31.8
Alkylate	96.6	6.7	1e-8	1e-8	96.6	6.7	34.4

(Variances are before an experiment)

feasible during experimentation could be easily incorporated at the cost of introducing nonlinear, conic constraints.

An additional variable in the design is the *nexp* number of experiments. When considering multiple experiments, the process constraints in Problem 4.1 have to be repeated for each experiment. Also, the new experiments are included in matrix X_{exp} and affect Problem 4.1 through *V(Q)* (See (B.3) in Appendix B). To demonstrate the experimental design method, a case study involving uncertain Reformate and LSR Naphtha octane numbers is presented. All other component properties were assumed to have very small uncertainties, as can be seen in Table 4.1. During the experiment, Q_{blend}^{oct} was required to be above or equal to 80.0 octane and Q_{blend}^{RVP}, below or equal to 10.8 psi. These bounds were included to prevent large deviations in product quality from occuring in the product tank that is not perfectly mixed.

The steady-state CLRTO was operating with the flowrates F_i seen in the left-most column in Table 4.2 with a profit of $10,257/day. After a single experiment $F_{i,exp}$, parameter uncertainty was reduced so that only one corner point was possible, and with the updated parameters obtained from the experiment, the CLRTO system converged to a different corner point, that had a profit of $10,680/day. Its flowrates can be seen in the right-most column of Table 4.2. Note that the objective function for the experimental design (i.e., the cost of the experiment) was 0.0, since only basic variables of the original basis were changed during the experiments.

Table 4.2. Results – CLRTO Flowrates in Experimental Design Based on Corner Points

	F_i CLRTO before experiments (bbl/day)	$F_{i,exp}$ (bbl/day)	F_i CLRTO after experiment (bbl/day)	$V(Q^{oct}_{i,nom})$ after experiment (octane^2)
Reformate	5696.0	5620.7	3212.7	0.0176
LSR Naphtha	942.0	1421.3	0.0	0.330
n-Butane	362.0	293.0	324.4	1e-8
FCC Gas	0.0	0.0	3463.0	1e-8
Alkylate	0.0	0.0	0.0	1e-8

Computational Experience:
CPU seconds ~ 1,500

Additional scenarios are discussed in Zyngier and Marlin (2003). Generally, as the number of experiments is increased, the deviation from the nominal flow rates for each experiment decreases. Each individual experiment may be smaller since the multiple experiments can provide the equivalent information as a single, large experiment. Also, in some cases, a single experiment would not be able to generate enough information for the simultaneous update of several parameters, so that the design problem would be infeasible. Naturally, the time for experimentation will increase as the number of experiments increases.

The approach developed in this section reduces the uncertainty in the coefficients of the linear programming problem to levels where only one corner point is possible, thus guaranteeing that the "true" plant optimum has been achieved. However, in systems where corner points adjacent to the optimum have similar profits, this approach will likely be too expensive; i.e., many experiments might be required in exchange for potentially small (even negligible) economic benefits. Since the experimental design strategies presented in the following sections are improved approaches that take into account the difference in profit between corner points, the additional case studies in Zyngier and Marlin (2003) are not shown in detail.

4.1.2. Performance Enhancement Based on Largest Profit Gap

Since the method in Section 4.1.1 will cause excessive experimentation in some cases, a different experimental design strategy was developed that considers the potential improvement in the system measured by the objective function (profit). This is done by applying a CLRTO performance metric developed in Chapter 3. Since the cost of model uncertainty becomes a sub-problem in the experimental design, a metric that can be obtained from a single optimization is embedded in the experimental design formulation.

The performance metric chosen for use in the experimental design was the largest profit gap with ellipsoidal description of parameter uncertainty ($MaxGap_{ell}$). It is a better representation of the monitoring goal than the metric with interval description of uncertainty ($MaxGap_{int}$) since it allows for the incorporation of correlation among parameters, while being computationally more tractable than expected value approximations that require enumeration of several segments. In the gasoline-blending process, correlation among component properties may occur due to disturbances in upstream operation. Some of these disturbances are imperfect separation in distillation columns (resulting in correlated octane and RVP properties, for example), or different feed properties and operations of upstream reactors, which also affects component properties in a correlated manner.

Problem 4.2:

$$\min_{F_{exp}} t_1^*[\, MaxGap_{ell}\,] - t_2^*[\, Pr_{exp}\,]$$

Subject to

$$Pr_{exp} = \sum_{i=1}^{n} (value - cost_i) F_{i,\exp}$$

$$Q^j_{blend,min} \sum_{i=1}^{n} F_{i,exp} \le \sum_{i=1}^{n} F_{i,exp} \left(Q^j_{i,nom} + \varepsilon^j_{exp}\right) \le Q^j_{blend\,max} \sum_{i=1}^{n} F_{i,exp} \qquad j = oct,\ RVP$$

$$F_{blend,\min} \le \sum_{i=1}^{n} F_{i,\exp} \le F_{blend,\max}$$

$$F_{i,\min} \le F_{i,\exp} \le F_{i,\max}$$

$$V(Q) = \left(V(Q)\,|_{t-1} + X^T_{\exp} V(z)^{-1} X_{\exp}\right)^{-1}$$

$MaxGap_{ell}$ ← details in Problem 3.6

The formulation of the experimental design based on the largest profit gap is given in Problem 4.2. The objective function is a time-weighted average of the performance metric and the cost of the experiment: the weighting factors t_1 and t_2 correspond to the batch time remaining after the experiment and the time to run an experiment, respectively. Therefore profit is being maximized over the remaining batch duration.

The formulation in Problem 4.2 is a three-level optimization problem, since Problem 3.6 consists of a bilevel programming problem. In this work, two different ways of solving this problem have been evaluated. The first one consists of replacing the $MaxGap_{ell}$ problem by its optimality conditions, and solving Problem 4.2 as a one-level optimization problem using a gradient-based, interior point method. The second approach considers Problem 3.6 to be a black-box function. The inner problem ($MaxGap_{ell}$) is solved as a bilevel problem using methods explained in Chapter 3, with the uncertainty V(Q) value calculated after the experiment, and the "outer" optimization problem is solved using a direct-search optimization method. The selection of a direct search method

for the outer problem is based on the discontinuities in derivatives that occur as the active set changes.

The first approach to solving Problem 4.2 is to replace Problem 3.6 by its KKT conditions and solve the overall problem with IPOPT-C (Raghunathan and Biegler, 2003). Details about IPOPT-C can be found in Appendix D. Since Problem 4.2 is ill-conditioned due to the change in corner points (where different Lagrange multipliers and slack variables reach values of zero) and highly nonlinear due to the complementarity constraints and the embedded Bayesian parameter estimation, its solution benefits from "good" starting points. In this work, a "good" starting point is considered to be any point that leads the optimization problem to a local minimizer, with delays due to computation times that do not result in significant economic loss in the system. This will be discussed in Section 4.1.2.2.

A drawback to the first approach to solving Problem 4.2 is that, since the substitution of the innermost optimization problem with its KKT conditions introduces nonlinearities in the system, the next optimization level is not guaranteed to achieve a local optimum of the problem unless the second-order optimality conditions of the innermost problem (Problem 3.6) are included in the formulation. This approach, however, causes the problem to be computationally intractable. Another option is to not include the second-order optimality conditions within the optimization problem, but to verify if they are satisfied at the solution of the problem (Clark and Westerberg, 1990). If they are not satisfied, the problem should be re-solved from another starting point. Alternatively, the solution could be perturbed to verify optimality (Forbes *et al.*, 1994).

Since these are all computationally intensive alternatives, a direct search method known as Derivative-Free Optimization (DFO) (Conn *et al.*, 1997) was also applied to Problem 4.2. This method is based on approximating the objective function by a (simpler) surrogate model within a trust region, and then optimizing the surrogate model to obtain an improved point. Then, the size of the trust region is increased or decreased, according to a new point being a better or worse objective function value than the current point, until the convergence tolerances are met.

It is well known in the literature that the traditional direct-search Nelder-Mead simplex method can have poor convergence properties (Wright, 1996). Preliminary studies were performed in this work that confirmed that DFO converged faster than Nelder-Mead for all cases. More details about the DFO algorithm can be found in Appendix D. DFO, however, cannot handle constraints directly. These have to be replaced in the objective function as penalty terms. The reformulation of Problem 4.2 so that DFO can be applied is seen in Problem 4.3.

Problem 4.3:

$$\min_{F_{exp}} \; t_1^*[\, MaxGap_{ell}\,] - t_2^*[\, Pr_{exp}\,] + \text{sum(penalty terms)}$$

$MaxGap_{ell}$ is determined by the solution of Problem 3.6, and the profit during experiment is defined in the first constraint of Problem 4.2. In order to increase the chances of finding "good" local optima for $MaxGap_{ell}$ during DFO implementation, at each DFO iteration, Problem 3.6 was solved for two different starting points (different sets of Lagrange multipliers), with several restarts. Of course, the formulation and restart procedures increased computation times for this approach.

The penalty term for each constraint was defined as: 10^3*(l_1-norm of constraint violation). The following constraints were considered during the design of experiments:

$$Q^j_{blend,min}\sum_{i=1}^{n} F_{i,exp} \le \sum_{i=1}^{n} F_{i,exp}\left(Q^j_{i,nom} + \varepsilon^j_{exp}\right) \le Q^j_{blend,max}\sum_{i=1}^{n} F_{i,exp} \qquad j = oct,\ RVP \qquad (4.1)$$

$$F_{blend,\min} \le \sum_{i=1}^{n} F_{i,\exp} \le F_{blend,\max} \qquad (4.2)$$

$$F_{i,\min} \le F_{i,\exp} \le F_{i,\max} \qquad (4.3)$$

Before each function evaluation, the parameter variances were re-estimated according to the following equation, derived from Bayesian parameter estimation (for details, see Appendix B).

$$V(Q) = \left(V(Q)|_{t-1} + X_{\exp}^{T} V(z)^{-1} X_{\exp}\right)^{-1} \quad (4.4)$$

4.1.2.1. Case Study Description

Next, we illustrate the methods proposed in Section 4.1.2 through a case study. The description of the case study before experimentation can be seen in Table 4.3. Note that the "true" values are not used in the calculations for the experimental design.

The monitoring results yield the following: $MaxGap_{ell}$ = \$1,456.8/day, where Pr_{BC} = \$8,895.9/day and $Pr_{nom,CL}$=\$7,439.1/ day.

4.1.2.2. Solution Using Optimality Conditions

The first solution strategy is the substitution of the inner $MaxGap_{ell}$ problem with its optimality conditions. Naturally, this approach benefits from good starting points. A method for obtaining a good starting point (for convergence) for Problem 4.2 is outlined as follows. First, Problem 4.2 with ellipsoidal uncertainty is modified (*Modified Problem 4.2*) so that the flowrates during the experiment are not taken into account in the overall profit, and that they are not used to update the model parameters. This implies that the cost of experimentation is not taken into account in the objective function, and that the parameter variances are fixed.

Table 4.3. Description of Case Study

	$Q_{i,nom}^{oct}$ (octane)	$Q_{i,nom}^{RVP}$ (psi)	$V(Q_{i,nom}^{oct})$ (octane^2)	$V(Q_{i,nom}^{RVP})$ (psi^2)	$Q_{i,true}^{oct}$ (octane)	$Q_{i,true}^{RVP}$ (psi)	$cost_i$ (\$/bbl)
Reformate	91.90	2.60	0.0546	0.0546	92.3	2.7	34.2
LSR Naphtha	63.89	11.01	0.0524	0.0524	64.0	10.9	26.5
n-Butane	92.40	137.90	0.0546	0.0546	92.5	138.0	10.3
FCC Gas	84.90	6.50	0.0546	0.0546	85.3	6.4	31.8
Alkylate	97.08	6.62	0.0373	0.0370	97.0	6.7	34.4

Modified Problem 4.2:

- Change objective function of Problem 4.2 to: Maximize ($Pr_{BC} - Pr_{nom,CL}$): the experiment is not considered in the overall profit
- Solve the problem with this new objective function and fixed parameter variances (the flowrates during experiment are not used to update the model parameters)

The following variable values were used as starting points to the Modified Problem 4.2:

- $F_{i,BC}$, $F_{i,nom}$ and λ, from solution of $MaxGap_{ell}$ problem
- $F_{i,exp}$ = [1,400.0 1,400.0 1,400.0 1,400.0 1,400.0]
- Remaining Lagrange multipliers = 1.0. These variables correspond to the additional multipliers created by the replacement of the inner (bilevel) problem with its optimality conditions.

The solution of the Modified Problem 4.2 seen in Table 4.4 is then used as a starting point for Problem 4.2. The results can be seen in Table 4.5.

Table 4.4. Results of Modified Problem 4.2

	$F_{i,BC}$ (bbl/day)	$F_{i,nom}$ (bbl/day)	$F_{i,exp}$ (bbl/day)
Reformate	0.0	0.0	2877.3
LSR Naphtha	1,860.8	71.0	1,119.1
n-Butane	177.3	214.2	372.0
FCC Gas	0.0	4,500.0	2,634.0
Alkylate	4,961.9	2,214.7	2,997.5
Pr_{exp} = \$11,230.1/day*($F_{blCLRTO}/F_{blexp}$) =			\$7,861.1/day

Computational Experience:

CPU seconds	: 2.0
# function evaluations	: 124
# restarts	: 0

Table 4.5. Solution of Problem 4.2 for Method using Optimality Conditions

	Q_i^{oct} (octane)	Q_i^{RVP} (psi)	$F_{i,BC}$ (bbl/day)	$F_{i,nom}$ (bbl/day)	$F_{i,exp}$ (bbl/day)
Reformate	91.90	2.60	0.0	0.0	2,857.3
LSR Naphtha	64.15	10.81	1,858.4	71.4	1,114.1
n-Butane	92.40	137.90	175.2	214.3	369.0
FCC Gas	84.29	6.96	0.0	4,500.0	2,631.7
Alkylate	97.47	6.31	4,966.4	2,214.4	3,027.9

Pr_{exp} = \$11,107.9.0/day*($F_{bl,CLRTO}/F_{bl,exp}$) = \$7,775.5/day.

Computational Experience:

CPU seconds	: 56.3
# function evaluations	: 42,010
# restarts	: 3

After this experiment, the predicted $MaxGap_{ell}$ = \$1,476.3/day. Since the total blend flowrate during the experiment was allowed to vary (and in this case was different from the flowate during normal operation), a "normalized" profit during experiment (Pr_{exp}) was calculated. This was done in order to compare Pr_{exp} to the current CLRTO profit.

In this case, the predicted value of $MaxGap_{ell}$ after experimentation is slightly larger than its original value, which is not an expected result because the cost of the experiment should be offset by the reduction in $MaxGap_{ell}$. This result is likely due to the fact that the second order conditions were not included in the optimization problem when substituting Problem 3.6 with its KKT conditions. This experiment will be further discussed in the next section.

4.1.2.3. Solution Using a Direct Search Method

The second solution strategy is to use DFO to solve the problem in Table 4.3. The parameter values and initial starting point used in the case study are given in Table 4.6. The solution is given in Table 4.7. The predicted $MaxGap_{ell}$ after experiment is \$1,357.7/day, which is smaller than the original $MaxGap_{ell}$ of \$1,456.8/day, as expected.

Table 4.6. Parameter Values Used in Problem 4.3

	$Q^j_{blend,min}$	$Q^j_{blend,max}$
Octane (octane)	80.0	100.0
RVP (psi)	4.5	10.8
	$F_{blend,min}$ (bbl/day)	$F_{blend,max}$ (bbl/day)
	5,500.0	10,000.0

The normalized profit during experiment (Pr_{exp}) was equal to [\$1,917.0/day *($F_{bl,CLRTO}/F_{bl,exp}$)=] \$2,349.0/day.

Even though the number of function evaluations was much smaller than in the model-based method in Section 4.1.2.2, each function evaluation when using DFO is more expensive. This is because, in this case, each function evaluation involves the solution of the $MaxGap_{ell}$ problem in Chapter 3 from a few different starting points in order to increase the chances of finding a "good" local optimum. Thus, the CPU time was much larger for the direct-search method.

Table 4.7. Solution of Problem 4.3

	$F_{i,exp}$ (bbl/day)
Reformate	1,707.7
LSR Naphtha	690.2
n-Butane	21.9
FCC Gas	1,382.0
Alkylate	1,910.8

Pr_{exp} = \$1,917.5/day*($F_{bl,CLRTO}/F_{bl,exp}$) = \$2,349.6/day.

Starting point: $F_{i,exp}$ = [1,000.0 1,000.0 1,000.0 1,000.0 1,000.0]

Computational Experience:

CPU seconds : 1,839.6

function evaluations : 267

Table 4.8. Solution of Problem 4.3 – Different Starting Point

	$F_{i,exp}$ (bbl/day)
Reformate	2,855.9
LSR Naphtha	1,112.8
n-Butane	371.6
FCC Gas	2,632.1
Alkylate	3,027.6

Pr_{exp} = \$11,161.3/day*($F_{bl,CLRTO}/F_{bl,exp}$) = \$7,812.9/day.

Starting point from Table 4.5: $F_{i,exp}$ = [2,857.3 1,114.1 369.0 2,631.7 3,027.9]

Computational Experience:
CPU seconds : 589.7
function evaluations : 170

The predicted $MaxGap_{ell}$ after the experiment in Table 4.8 was \$ 1,415.7/ day, which is smaller than the original $MaxGap_{ell}$, as expected. The normalized profit during the experiment (Pr_{exp}) was [\$11,161.0/day *($F_{bl,CLRTO}/F_{bl,exp}$)=] \$7,812.7/day.

When using the starting point for $F_{i,exp}$ from Table 4.5, the computational effort of the direct-search method decreased significantly in comparison with the starting point of all flowrates equal to 1,000 bbl/day (seen in Table 4.7). Also, since the "black-box" function of the method based on DFO is a bilevel optimization problem with a linear inner problem (with no second-order optimality conditions), it is guaranteed that a local optimum is found for Problem 3.6, if one exists.

The profit during experimentation (Pr_{exp}) was much higher when using the results of the model-based method as a starting point for DFO. It is worth mentioning that the experiment in Table 4.8 was very similar to the starting point obtained from the model-based method, indicating that the optimization variable values in Table 4.5 were already very close to a local optimum.

There are a few options in designing experiments. One possibility is to calculate *nexp* experiments simultaneously. This allows for the incorporation of constraints on integrated rather than instantaneous product qualities, thus permitting instantaneous

infeasibility in the process and consequently a smaller number of experiments. However, this approach does not take into account the information that is being generated by each experiment before all *nexp* experiments are completed. Also, calculating *nexp* experiments increases the size of the experimental design problem thus increasing the computational demands.

Another option is to adopt a receding horizon strategy in designing the experiments. In this approach, an initial *nexp* experiments are designed, and only the first one is implemented. Then, using parameter values updated from the first experiment, (*nexp-1*) experiments are designed, and only the first one is implemented. The procedure continues until the $nexp^{th}$ experiment is implemented. This approach is likely to provide the best experimental designs, since the time horizon of the blending batch is taken into account and recently updated parameters are used in the design of each experiment. However, the computational burden of this method is very high, since several large experimental design problems must be solved.

Finally, each experiment can be designed individually, and its results can be implemented in the plant before calculating the subsequent experiment. This avoids the design of a large number of experiments simultaneously, thus easing the computational burden during each of the calculations for designing the experiments. Also, this approach uses updated parameter information in each design of experiment, and allows for the interruption of experimentation as soon as the stopping criterion (size of $MaxGap_{ell}$) is met. For its computational advantages, the sequential calculation of individual experiments was the chosen approach in this work.

During the experiments, the RTO system is turned off; i.e., no new feedback information is being used by the model. This could result in quality violations if process disturbances were to occur while experiments were being run. Either of the following modifications ensures that feedback information would be considered during the experimental design step: (1) Alternate experimentation with CLRTO runs. Therefore, one experiment would be implemented, followed by a single CLRTO run, followed by an experiment, and so on. (2) Update the bias parameter before each experiment, without

having a CLRTO run between experiments. The latter approach would be preferable because it would lead to a shorter model enhancement stage of a system.

The next section presents a new method for diagnosing CLRTO performance. This is a good tool for understanding the effect of specific parameter changes on the objective function value.

4.2. RTO Performance Diagnostics

Screening the importance of model parameters for a particular problem is very useful. With the performance monitoring strategies in Chapter 3, it is possible to determine the parameter values in the plant that result in the largest difference in profit during closed-loop operation. In the solution of the monitoring problem with interval uncertainty in Chapter 3, all parameters that influence the objective function are equal to their upper or lower bounds, so there is no insight as to which is the most relevant parameter. At best, the user obtains information about the directionality of the problem. In the case of monitoring CLRTO performance given ellipsoidal uncertainty, the most influential parameters are singled out, since they are taken to the bound of the (multi-dimensional) ellipsoid, while the remaining parameters do not deviate much from their nominal values. In this case, the monitoring approach may indicate which parameters are the most important ones for a particular case, but there is no insight as to a ranking of their importance with respect to the objective function value.

Knowledge of the parameters whose uncertainty affects CLRTO profit can be used to select measurements for the system; i.e., detect which process variables should have their samples analyzed at a laboratory or determine which on-stream analyzers should be installed. The diagnostics can also be used to guide laboratory experiments for model improvement, in that it indicates the importance of each parameter. Also, LP model structure improvements such as disjunctive modelling, separable programming, base-delta, etc., can be more easily made if there is information on parameter relevance to the optimization problem (Williams, 1999). The diagnostics formulation in Problem 4.4 finds the smallest trace of the parameter variance-covariance matrix that yields a profit

gap of at least the threshold value T. Thus, the diagnostic finds the smallest parameter uncertainty that yields a specified profit gap.

Problem 4.4:

$$\min_{Pr_{BC}, Pr_{nom,CL}, \varepsilon^j, Q_i^j, V_{ii}(Q)} \quad Tr(\mathbf{V}(Q))$$

subject to

$$Pr_{nom,CL} = \max_{F_{i,nom}} \sum_{i=1}^{n} (value - cost_i) F_{i,nom}$$

s.t.

$$\sum_{i=1}^{n} F_{i,nom} (Q_{i,nom}^j + \varepsilon^j) \geq Q_{blend,min}^j \sum_{i=1}^{n} F_{i,nom}$$

$$\sum_{i=1}^{n} F_{i,nom} (Q_{i,nom}^j + \varepsilon^j) \leq Q_{blend,max}^j \sum_{i=1}^{n} F_{i,nom}$$

$$F_{blend,\min} \leq \sum_{i=1}^{n} F_{i,nom} \leq F_{blend,\max}$$

$$F_{i,\min} \leq F_{i,nom} \leq F_{i,\max}$$

$$\varepsilon^j \sum_{i=1}^{n} F_{i,nom} = \sum_{i=1}^{n} F_{i,nom} \left(Q_i^j - Q_{i,nom}^j\right)$$

} Nominal CLRTO for any plant realization Q_i^j

$$Pr_{BC} = \max_{F_{i,BC}} \sum_{i=1}^{n} (value - cost_i) F_{i,BC}$$

s.t.

$$\sum_{i=1}^{n} F_{i,BC} \cdot Q_i^j \geq Q_{blend,min}^j \sum_{i=1}^{n} F_{i,BC}$$

$$\sum_{i=1}^{n} F_{i,BC} \cdot Q_i^j \leq Q_{blend,max}^j \sum_{i=1}^{n} F_{i,BC}$$

$$F_{blend,\min} \leq \sum_{i=1}^{n} F_{i,BC} \leq F_{blend,\max}$$

$$F_{i,\min} \leq F_{i,BC} \leq F_{i,\max}$$

} Best result for CLRTO for any plant realization Q_i^j

$$(Q - Q_{nom})^T \mathbf{V}^{-1}(Q)(Q - Q_{nom}) \leq \chi^2_{\alpha,dof}$$ } Ellipsoidal bounds

$$V_{ii,\min}(Q) \leq V_{ii}(Q) \leq V_{ii,\max}(Q)$$ } Bounds on variances

$$Pr_{BC} - Pr_{nom,CL} \geq T$$ } Profit gap threshold

This problem is solved for various values of T, and as T is reduced, a smaller number of (more important) parameters must have non-zero variances (be uncertain) so that the specified profit gap (T) is achieved. Therefore, the parameters whose variances

are last reduced as T is decreased are deemed to be the most relevant to the optimization problem. The smallest trace when $T = 0$ \$/day is also zero, since all variances must be non-negative.

In the case studies considered in the following section, all the off-diagonal elements of $\mathbf{V}(Q)$ are equal to zero (i.e., there is no correlation among parameters). In cases in which there is correlation among parameters, the off-diagonal (covariance) terms can be explicitly set as a function of the diagonal terms (variances), with fixed correlation. For example, if correlation exists between the first and second parameters, the off-diagonal terms of $\mathbf{V}(Q)$ can be expressed as $V_{12} = V_{21}$ = correlation* V_{11}* V_{22}.

It is important to note that this method does not assume a constant active set for the diagnostics. In the following section, this diagnostic method is applied to the gasoline-blending case study in Section 4.1.2.1.

4.2.1. Case Study

Given the parameter values in Table 4.3, the user may be interested in gaining insight into which are the most important parameters, and in which order. Therefore, the diagnostic method in Problem 4.4 was used. The results are shown in Figure 4.1.

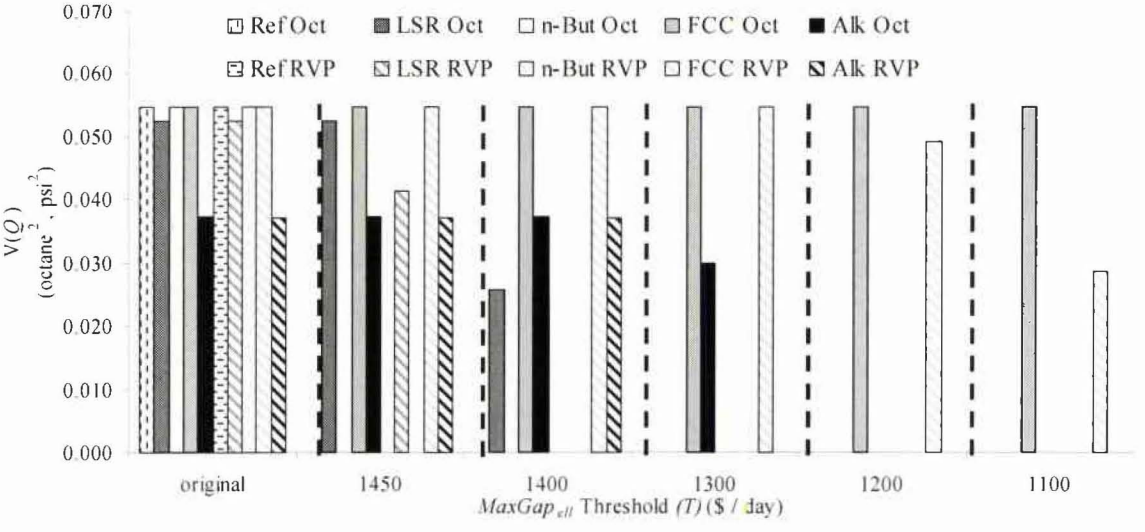

Figure 4.1. CLRTO Performance Diagnostics Results

The original variances from Table 4.3 (that yield a $MaxGap_{ell}$ of \$1,456.8/ day) are seen in the far left of the graph, under "original". This is the situation when the monitoring has been completed and no improvement through experimentation has been performed. When the value of the threshold T is reduced to \$1,450/day, Reformate octane and RVP, and n-Butane octane and RVP parameters have their variances reduced to zero in the solution of Problem 4.4. Therefore, for this case study, they are the least important parameters. For a value of T of \$1,400/day, the variance of LSR Naphtha RVP is reduced to zero and the variance of LSR Naphtha octane is decreased from its original value. This indicates that the uncertainty in LSR Naphtha RVP has a smaller effect on the objective function than LSR Naphtha octane, which in turn has a smaller effect than the remaining parameters.

The same analysis applies to the subsequent values of T. As T is assigned a value of \$1,100/day, the variance of FCC gasoline RVP starts to decrease, while the variance of FCC gasoline octane still retains its original value. This indicates that, for this case study, FCC gasoline octane is the parameter whose uncertainty has the largest effect on the objective function, followed by FCC gasoline RVP, Alkylate octane, Alkylate RVP, LSR Naphtha octane, and so on. As long as T is greater than zero, at least one parameter (in this case, FCC gasoline octane) will have a nonzero variance in order to achieve a positive value of profit gap.

The results in Figure 4.1 depend on the uncertainty scenario in the plant. For example, if before the diagnostics, laboratory experiments had been run on FCC gasoline thereby dramatically reducing the variances on its properties, these parameters (FCC gasoline octane and RVP) would not be considered the most important by the diagnostic method. In addition, the variances would have to be scaled by the nominal measurement values (or its expected range of variation), which was not necessary in this example because of the similarity in the scaling factors.

The most likely application of this diagnostic method is in improving measurements available for the CLRTO. The parameters most frequently isolated as the most important in the system would be chosen for evaluation, with the final selection of

measurements based on an economic analysis. In the case study, the FCC RVP and octane have been identified as the most important parameters.

4.3. Relationship to Decision Analysis Theory

As discussed in Chapter 3, the experimental design approaches in this chapter have similarities to Operations Research technology. Section 3.7 discussed the similarities between the monitoring approaches developed in this thesis and Regret and EVPI problems. The monitoring approaches provide the answer to the questions of what are the minimum- and maximum regrets (or expected value of the regret) under the current parametric uncertainty and which parameter scenarios lead to these regret values.

By using the experimental design strategies in Section 4.1, it is then possible to answer the questions "What is the lowest cost experiment(s) that reduces the regret to zero?" (Section 4.1.1) and "What is the economically optimal policy of experimentation and production to the end of the production run?" (Section 4.1.2). A parallel can be drawn between the experimental design approaches in this chapter and the Expected Value of Sample Information (EVSI), which is defined as the value of information from testing or sampling the system (Winston, 1994). When the costs for obtaining information and values for improved information are easily determined, the existing enumeration methods for EVSI are appropriate. However, in this work, the cost of experiment and possible economic improvement depend upon the values of the decision variables (the flows during the experiments) so that existing solution methods are not applicable. The approach in Section 4.1 provides a solution to the more challenging scenario, in which the expected value of improvement is replaced with (1) the maximum profit loss after experimentation and (2) the nominal profit during the experiment.

4.4. Conclusions

Key issues in the Statistics and Operation Research fields (Robinson, 2005) were addressed in this chapter; namely, screening the model parameters in order to determine their importance and designing profit-based experiments in order to reduce the uncertainty in key parameters.

The two novel approaches to experimental design based on corner point information and based on profit achieve improvement of the CLRTO system performance rather than information (reduction of the size of the parameter confidence region). The approaches provide technology that complements CLRTO monitoring in Chapter 3, in that a monitoring criterion is embedded into the experimental design formulation. Also, the experiments would not be initiated unless the monitoring indicated the possibility for significant improvement.

Two methods were evaluated to solve the experimental design formulation based on the largest profit gap (Problem 3.6). One was based on substituting the inner optimization problem in Problem 4.2 with its optimality conditions, while the other was based on a direct-search method, which approached the inner optimization problem in Problem 4.2 as an expensive, black-box function.

The first method resulted in a nonlinear optimization problem with 177 decision variables (which includes Lagrange multipliers), 289 constraints and 91 complementarity constraints, resulting in (289 + 91) 380 constraints. The solution of this formulation in the case study shown took approximately 1 CPU minute. However, the solution found is only a stationary point of the inner problem and has to be further tested for local optimality by probing the parameter space, or by evaluating the second-order derivatives at the solution. Results in the case study indicated that a valid solution is not reliably achieved.

The second method based on direct-search optimization consisted of only n decision variables, where n is the number of manipulated variables during the experiment, which was equal to five in the case study shown in this chapter. The constraints during the experiment were replaced by penalty functions in the objective

function. At each direct-search step, however, the inner "black-box" function evaluation corresponded to solving the $MaxGap_{ell}$ formulation in Problem 3.6, with 117 decision variables, 75 constraints and 30 complementarity constraints, resulting in (75 + 30) 115 constraints. As reported in Chapter 3, each solution of Problem 3.6 took about 2.0 CPU seconds, and the design of the experiment took approximately 10.0 CPU minutes with a penalty-free starting point.

Since the direct-search method solves the bilevel optimization Problem 3.6 as an inner problem, the equation-oriented approach to designing experiments was simplified to a bilevel optimization problem. This strategy also requires fewer function evaluations than the experimental design strategy based on optimality conditions. However, because of the relatively high computational requirement of each function evaluation (Problem 3.6), computation times of designing experiments based on DFO are higher. Nevertheless, the case study results using a direct-search method produced better results.

A new diagnostics method was also developed in order to rank parameter importance with respect to their effect on the objective function. This approach is not limited to a single active set and it does not require pre-selection of key variables. It could be used to simplify computational demands in the design of experiments by reducing the number of parameters included in its formulation. Alternatively, it can serve as a guide to improving the CLRTO system via laboratory measurements, on-stream sensors, or improved models.

All experimental design strategies and diagnostics were successfully implemented in a gasoline-blending case study. In Chapter 5, the monitoring methods from Chapter 3 and the diagnostics and enhancement methods from Chapter 4 are integrated into an overall scheme for application to an online closed-loop RTO system.

Chapter 5

Sequential Procedure for Implementation

In Chapter 3, methods were presented for monitoring the performance of CLRTO systems under parameter uncertainty. These methods may serve as an independent tool for detecting the degradation of the systems. Once a performance issue has been found in an RTO system, steps should be taken in order to eliminate it. Therefore, new experimental design and diagnostic strategies were developed and presented in Chapter 4.

A systematic integration of the previously presented monitoring, diagnosing and enhancing methods into a sequential procedure for closed-loop RTO systems is presented in this chapter. The goals of the sequential procedure are to achieve the following:

- To base the performance on the CLRTO objective, which is profit;
- Reduce the likelihood that a sensor failure or unexpected model mismatch will lead to poor monitoring performance;
- Interfere with the normal process operation as little as possible;
- Utilize all available information about the current situation (e.g., economics, bounds, *a priori* uncertainty estimates, etc.);
- Use formulations that are computationally tractable within the time available in typical industrial processes. For gasoline blending, computations ranged from a few seconds to 20 minutes, while the total batch time is approximately 10 hours.

The sequential procedure consists of the following five steps. First, the plant data is checked for consistency with the model structure and the uncertainty description. Second, performance monitoring is performed to provide information about the performance status of the CLRTO system. If monitoring indicates the potential for

significant improvement, the procedure proceeds to the third step. In the third step, plant operating data from the current blend is used to provide better estimates of the plant for use in the CLRTO model. If monitoring indicates that opportunity exists for further performance improvement after step three, the procedure proceeds to the fourth step, where designed experiments are introduced in the plant. This step is repeated until the best tradeoff between experimentation and model uncertainty is achieved. The fifth and final step involves implementing the final operating conditions. Note that the first two steps are performed prior to every CLRTO execution and that the first three steps require no perturbation in process operation.

In the following sections, details are given on each of the steps in the sequential procedure for CLRTO performance monitoring and enhancement. Three case studies are presented, The first two demonstrate the importance of the thorough method, since they start from the same initial condition and yet conclude at very different operations: clearly, heuristics would not suffice for these cases. A third case study emphasizes the importance of the experimental design. Since all steps in the sequential procedure, except for data checking, have already been presented in previous chapters, we proceed directly to the case studies.

5.1. Definition of Case Studies 1 and 2

In order to demonstrate the full potential of the sequential procedure, the two case studies in Table 5.1 and Table 5.2 are considered. All parameters representing the physics and chemistry of the true plant and of the CLRTO model are the same for both cases. In addition, the initial parameter uncertainties are the same, namely 0.0546 octane number^2 or psi^2, which, in a 10-degree-of-freedom multivariate normal distribution corresponds to a maximum variation of ±1.0 (octane number or psi) in a single parameter. The only differences between the case studies are the component costs, which vary by a maximum of 2.1%. Cost variation of this (or much greater) magnitude could occur due to, for example, fluctuations in the prices of crude oil, purchased intermediate material (e.g., FCC gasoline) or short-term plant inventory.

Table 5.1. Description of Case Study 1

	$Q_{i,nom}^{oct}$ (octane)	$Q_{i,nom}^{RVP}$ (psi)	$Q_{i,true}^{oct}$ (octane)	$Q_{i,true}^{RVP}$ (psi)	$cost_i$ ($/bbl)	F_i (bbl/day)
Reformate	91.9	2.6	92.3	2.7	34.0	0.0
LSR Naphtha	63.9	11.0	64.0	10.9	26.0	1,781.0
n-Butane	92.4	137.9	92.5	138.0	10.3	161.6
FCC Gas	84.9	6.5	85.3	6.4	32.5	0.0
Alkylate	97.1	6.6	97.0	6.7	34.5	5,057.4
Current Profit ($/day)						8,549.5

Table 5.2. Description of Case Study 2

	$Q_{i,nom}^{oct}$ (octane)	$Q_{i,nom}^{RVP}$ (psi)	$Q_{i,true}^{oct}$ (octane)	$Q_{i,true}^{RVP}$ (psi)	$cost_i$ ($/bbl)	F_i (bbl/day)
Reformate	91.9	2.6	92.3	2.7	34.2	0.0
LSR Naphtha	63.9	11.0	64.0	10.9	26.5	1,781.0
n-Butane	92.4	137.9	92.5	138.0	10.3	161.6
FCC Gas	84.9	6.5	85.3	6.4	31.8	0.0
Alkylate	97.1	6.6	97.0	6.7	34.4	5,057.4
Current Profit ($/day)						8,164.7

The last column in Table 5.1 and Table 5.2 represents the steady-state flowrates achieved under CLRTO prior to beginning the monitoring process, which are the same for both cases; therefore, these two cases would appear to be essentially the same to operating personnel.

5.2. Data Rectification

This first step in the sequential procedure is executed at every CLRTO execution after the flowrates have reached the values at which they can be accurately measured by the flow sensors. In this step, real-time measurements are checked for gross errors and model inconsistencies. If these inconsistencies exceed the expected random variation, performance monitoring is interrupted, and a warning is provided to plant personnel. The

situation should then be analyzed and corrected by the personnel before optimization proceeds. Typical causes for gross errors could be sensor failures (gross errors in the measurements) or improper connection of component tanks to pipes and meters (gross errors in the model structure). In addition, a component quality could differ a great deal from typical values because of unusual variation in plant operation or because the component has been purchased from an outside supplier. The personnel will troubleshoot the problem and restore the CLRTO to closed-loop operation when the data and model agree within the typical range of mismatch, at which point monitoring can resume.

The method for data rectification has not been explained in previous sections, and therefore, is introduced here. The model is used to predict some variables that are also measured; therefore, opportunity exists to compare the predictions with measurements. In traditional gross error detection methods, rigorous mass and energy balances provide the basis for evaluating the consistency of redundant measurements (Crowe, 1996). Data rectification, on the other hand, can be applied using not only the fundamental balance equations, but also component quality predictions for octane and RVP (Johnston and Kramer, 1995). Note that this step doesn't include new technology, but it is included to provide some assurance that the uncertainty bounds are valid for subsequent steps.

The total mass balance and the balances for octane and RVP are given in the following equations.

$$\sum_{i=i}^{n} F_{i,nom} - F_{blend,nom} = 0 \qquad (5.1)$$

$$\sum_{i=i}^{n} \frac{F_{i,nom} Q^{j}_{i,nom}}{F_{blend,nom}} - Q^{j}_{blend,nom} = 0 \qquad j = Octane, RVP \qquad (5.2)$$

All flowrates and the blended product qualities (Q^{j}_{blend}) are measured in real time but the component qualities ($Q^{j}_{i,nom}$) are not measured. Substituting the measurements and nominal values for the flowrates and component qualities in equations (5.1) and (5.2) will not result in a zero right-hand side because of variation in component qualities, as shown in the following equations.

$$\sum_{i=i}^{n} F_{i,meas} - F_{blend,meas} = \varphi_1 \qquad (5.3)$$

$$\sum_{i=i}^{n} \frac{F_{i,meas} Q^j_{i,nom}}{F_{blend,meas}} - Q^j_{blend,meas} = \varphi_k \qquad k = 2,3 \qquad (5.4)$$

The second and third elements of the variance-covariance matrix $V(\varphi)$ of the error vector $\varphi = [\varphi_1 \ \varphi_2 \ \varphi_3]^T$ are calculated by linearizing equations (5.4) around the nominal point used in the model equations (Narasimhan and Mah, 1989). This method assumes zero mean, independent, normally distributed measurement errors in the flows and in the blend octane and RVP properties.

$$V(\varphi_k) = \sum_i \left(\frac{F_{i,nom}}{F_{blend,nom}} \right)^2 V(Q_i^{j,plant}) + \sum_i \left(\frac{Q^j_{i,nom}}{F_{blend,nom}} \right)^2 V(F_i^{plant}) + \qquad (5.5)$$

$$+ \sum_i \left(\frac{F_{i,nom} Q^j_{i,nom}}{F^2_{blend,nom}} \right)^2 V(F^{plant}_{blend}) + V(Q^{j,plant}_{blend}) \qquad k = 2, 3$$

The first element of the variance-covariance matrix $V(\varphi)$ is calculated as follows.

$$V(\varphi_1) = \sum_i V(F_{i,meas}) + V(F_{blend,meas}) \qquad (5.6)$$

If a "perfect" model with "perfect" measurements were used, the value of the residual vector φ would be zero. Assuming zero-mean, independent, normally distributed noise in the errors, the magnitude of φ can be evaluated with respect to the expected range of error by comparing the value M from the following equation against the χ^2 statistic.

$$\varphi^T V^{-1}(\varphi)\varphi = M \qquad (5.7)$$

From equation (5.7), if $M \leq \chi^2_{DOF,\alpha}$ the model mismatch is deemed within the expected range, the monitoring procedure continues; if $M \geq \chi^2_{DOF,\alpha}$, a warning message should be sent to operating personnel, who can identify and correct the gross error by re-calibrating instruments, re-sampling purchased material to obtain correct composition information, etc. Three degrees-of-freedom (DOF) were used in this study because φ is 3-dimensional (one material balance and two component balances). In all calculations, the confidence level is $\alpha = 0.95$.

The data rectification step requires information on the uncertainty in the model parameters, as well as the measurement uncertainty. The variances of all octane and RVP model parameters $V(Q_i^{j,plant})$ would be based on historical plant data, and for this case study were taken to be 0.0546 (octane number^2 or psi^2, respectively). According to ASTM standards, the accuracies required for the final blend octane and RVP measurements are ±0.2 octane and ±0.15 psi, respectively (ASTM D-323; ASTM D-2699; ASTM D-2700). Interpreting these bounds as 95% confidence intervals, the variances of octane and RVP measurements used in this work were 0.01 octane^2 and 0.0056 psi^2, respectively.

Turbine flowmeters are sometimes used in gasoline-blending processes (Mudt, 2005). Their principle of operation is that the speed of rotation of a turbine within the meter is proportional to the volumetric flowrate through the pipe. This type of flowmeter has a typical accuracy of ±0.5% of the actual (flow)rate (*AR*) over a 10:1 flow range (Omega, 2005); that is, this accuracy is valid for flowrates from 10-100% of the largest flowrate.

Table 5.3. Variance of Flowrate Measurements (Accuracy = ±0.5% *AR*)

	AR	0.5%**AR*	V(F_i)
Reformate	0.0	0.0	1e-8
LSR Naphtha	1,781.0	8.9	19.8
n-Butane	161.6	0.8	0.2
FCC Gas	0.0	0.0	1e-8
Alkylate	5,057.4	25.3	159.9
Blend	7,000.0	35.0	306.3

The current CLRTO flowrates were used to estimate turbine meter accuracy. In Table 5.3, the variance was calculated assuming the variation in flowrates corresponds to two standard deviations.

Since the only difference between the case studies lies in economics, the data rectification step is the same for both Case 1 and Case 2. A Monte Carlo study was performed in order to identify the rate of false alarms in this system; i.e., when M is larger than the chi-square statistic (Table 5.4). In order to mimic the real plant more closely, the sampled flowrates were not allowed to have negative values.

In practice, false alarms are expected to happen. If the value of M in equation (5.7) is slightly above the chi-square statistic, thus indicating that the model is inconsistent with the data, the data rectification check should be repeated at several additional CLRTO executions to reduce false alarms. Since the likelihood that three adjacent measurements will be above the 95% confidence limits under normal operation is very small (0.05*0.05*0.05 = 0.0125%), if the third consecutive data point still indicates inconsistencies, the sequential procedure should be interrupted in order to perform offline troubleshooting. In order to proceed with the case studies, it will be assumed that the model has been deemed consistent with the data.

Table 5.4. Data Rectification - 5,000 Monte Carlo Runs

	$\chi^2_{3,0.95}$
Number of false alarms	214 (4.3%)

5.3. Monitoring RTO Performance

After verifying that plant measurements are consistent with the model and parameter uncertainty descriptions, the potential cost of uncertainty to the CLRTO is determined. In Chapter 3, five different methods were presented to determine the effect of uncertainty on the objective function. Here, the method based on the largest profit gap, considering ellipsoidal uncertainty ($MaxGap_{ell}$, Section 3.4) is used due to the good trade-off between the quality of the description of the monitoring goal and the computational burden of the method.

The performance monitoring can begin when the CLRTO has reached steady state. When applying Problem 3.6 to Case Study 1, a $MaxGap_{ell}$ of \$2,205 4/day was found, where Pr_{BC} = \$9,810.3/ day and $Pr_{nom,CL}$ = \$7,604.9/ day. The results can be seen in Table 5.5.

Table 5.5. Monitoring Results (Problem 3.6) - Case Study 1

	Q_i^{oct} (octane)	Q_i^{RVP} (psi)	$F_{i,BC}$ (bbl/day)	$F_{i,nom}$ (bbl/day)
Reformate	92.47	2.16	5,648.7	0.0
LSR Naphtha	63.82	11.06	969.2	1,702.8
n-Butane	92.42	137.88	382.1	150.1
FCC Gas	84.90	6.50	0.0	0.0
Alkylate	96.56	7.01	0.0	5,147.2

Table 5.6. Monitoring Results (Problem 3.6) - Case Study 2

	Q_i^{oct} (octane)	Q_i^{RVP} (psi)	$F_{i,BC}$ (bbl/day)	$F_{i,nom}$ (bbl/day)
Reformate	91.90	2.60	0.0	0.0
LSR Naphtha	63.69	11.17	194.4	1,734.3
n-Butane	92.41	137.89	235.0	154.0
FCC Gas	85.55	5.97	4,500.0	0.0
Alkylate	96.80	6.84	2,070.7	5,111.6

For Case Study 2, Problem 3.6 resulted in a $MaxGap_{ell}$ of \$1,484.9/day, where Pr_{BC} = \$9,098.2/ day and $Pr_{nom,CL}$ = \$7,613.3/ day. The results can be seen in Table 5.6.

Since the potential profit losses ($MaxGap_{ell}$) for both case studies are unacceptably large, enhancement actions are taken in order to improve the estimates of the model parameters.

5.4. Updating RTO Model Parameters using Available Data

Section 5.3 indicates that economic improvement might be possible. Therefore, RTO model parameters are re-estimated in order to reduce their uncertainty. Recent historical data offers some additional information at essentially no cost. CLRTO systems change plant operation as a response to process disturbances (including model mismatch); therefore, data in the current batch is likely to provide an opportunity for parameter estimation. Note that this "transient" data is actually a series of steady states as the CLRTO approaches its final steady-state operation.

The Bayesian approach to parameter estimation presented in Appendix B is employed to update the model parameters due to the use of prior knowledge about parameter values and variances. We note that the estimation using recent data without perturbations might often not improve the estimates, i.e., reduce the confidence intervals, sufficiently to achieve the desired small monitoring metric $MaxGap_{ell}$. The variation in the transient CLRTO data used in this section is a result of achieving the predicted optimum operation. This variation might not change the key flowrates by large enough magnitudes to improve the estimates of the component qualities. However, since this data

Table 5.7. Transient CLRTO flowrates

	F_i (bbl/day) RTO run 1	F_i (bbl/day) RTO run 2	F_i (bbl/day) RTO run 3
Reformate	0	0.0	0.0
LSR Naphtha	1,790.0	1,781.1	1,781.0
n-Butane	163.9	161.6	161.6
FCC Gas	0.0	0.0	0.0
Alkylate	5,046.0	5,057.3	5,057.4

provides valid process information and is free of cost to operation and since the parameter updating method is very fast, it is suggested that the updating step using available closed-loop data be performed in case the model improvement is sufficient.

Results from using equations (B.2) and (B.3) to update model parameters using the available closed-loop data from Table 5.7 can be seen in Table 5.8. In these case studies, the intercepts in the model equations were assumed known and equal to zero (a case with uncertain intercepts will be shown later in this chapter). The transient CLRTO flowrates are the same for both Case Studies 1 and 2, since model and plant parameters are initially the same.

After the parameters were updated using the closed-loop data in Table 5.7, the CLRTO system in Case Studies 1 and 2 converged to different optimal bases (Table 5.9), with profits of \$9,118.1/day and \$8,678.5/day, respectively. This corresponds to an improvement of \$568.6/day (Case Study 1) and \$513.8/day (Case Study 2) in comparison with the initial basis seen in the last column of Table 5.1.

Table 5.8. Parameter Update with Available Data

	$Q_{i,nom}^{oct}$ (octane)	$Q_{i,nom}^{RVP}$ (psi)	$V(Q_{i,nom}^{oct})$ (octane^2)	$V(Q_{i,nom}^{RVP})$ (psi^2)
Reformate	91.90	2.60	0.0546	0.0546
LSR Naphtha	63.88	11.02	0.0491	0.0489
n-Butane	92.40	137.90	0.0546	0.0546
FCC Gas	84.90	6.50	0.0546	0.0546
Alkylate	97.05	6.66	0.0107	0.0088

Table 5.9. New optimal CLRTO bases

	F_i (bbl/day) Case Study 1	F_i (bbl/day) Case Study 2
Reformate	5695.6	0
LSR Naphtha	942.5	177.1
n-Butane	361.9	223.2
FCC Gas	0.0	4500
Alkylate	0.0	2099.7
Profit (\$/day)	9118.1	8678.5

$MaxGap_{ell}$ (Problem 3.6) was calculated again after the parameter update in order to determine if further model enhancement was necessary. For Case Study 1, $MaxGap_{ell}$ was equal to \$1,785.6/day (with Pr_{BC} = \$ 8,837.5/day and $Pr_{nom,CL}$ = \$7,051.9/day), while for Case Study 2, a $MaxGap_{ell}$ of \$1,304.3/day was obtained (where Pr_{BC} = \$8,474.0/day and $Pr_{nom,CL}$ = \$7,169.7/day). Since $MaxGap_{ell}$ was still deemed large for both cases, additional model improvement was required, and cost-efficient experiments were designed.

5.5. RTO Performance Enhancement

Since the monitoring metric after the parameter update using normal operating data was still large in Section 5.4, experimentation was deemed necessary in order to improve CLRTO performance in both case studies. The experimental design calculations were performed using Derivative-Free Optimization (Appendix D), since it is a more reliable method for the proposed experimental design formulation than model-based methods. The following constraints were included in the design using the data in Table 5.10; they were implemented as penalty functions in the design calculations in the outer problem.

$$Q^j_{blend,min}\sum_{i=1}^{n}F_{i,exp} \le \sum_{i=1}^{n}F_{i,exp}\left(Q^j_{i,nom}+\varepsilon^j_{exp}\right) \le Q^j_{blend,max}\sum_{i=1}^{n}F_{i,exp} \qquad j = oct,\ RVP \qquad (5.8)$$

$$F_{blend,\min} \le \sum_{i=1}^{n}F_{i,\exp} \le F_{blend,\max} \qquad (5.9)$$

$$F_{i,\min} \le F_{i,\exp} \le F_{i,\max} \qquad (5.10)$$

Table 5.10. Parameter Values Used in Case Studies 1 and 2

	$Q^j_{blend,min}$	$Q^j_{blend,max}$
Octane (octane)	88.5	100.0
RVP (psi)	4.5	10.8
	$F_{blend,min}$ (bbl/day)	$F_{blend,max}$ (bbl/day)
	6,999.0	7,000.0

The experiments were calculated sequentially, as discussed in Chapter 4. After each experiment and parameter update, $MaxGap_{ell}$ was calculated in order to check the improvement in performance due to experimentation. If the performance was deemed satisfactory (i.e., if the largest profit gap was below a user-defined threshold), no additional experiments were designed. The results for the design of experiments are discussed separately for each case study in Sections 5.5.1 and 5.5.2. In Section 5.5.3, a case study with uncertain intercepts is presented.

5.5.1. Case Study 1

The trend plot of the flowrates for Case Study 1 during the entire sequential procedure for RTO performance monitoring and enhancement is given in Figure 5.1. Table 5.11 presents the seven experiments calculated for this case study. After experiment 7, the CLRTO system performance was deemed satisfactory since $MaxGap_{ell}$ was small ($82.1/day).

The total cost of experimentation was calculated as the marginal costs associated with variables (flowrates) at their lower- or upper bounds, times the deviation of the

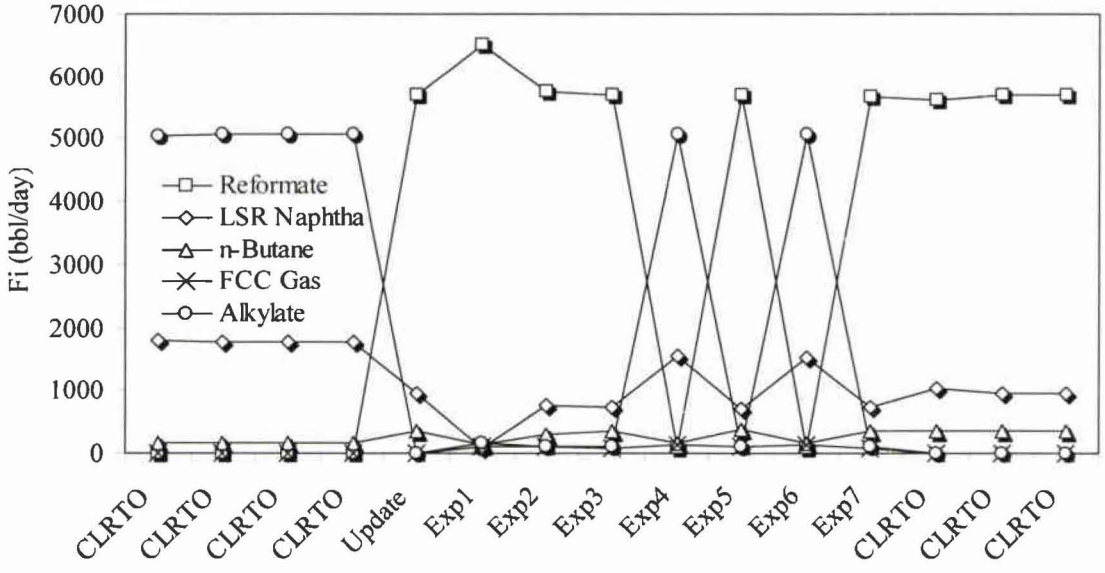

Figure 5.1. Results for Case Study 1

Table 5.11. Experiments for Case Study 1

	$F_{i,exp1}$ (bbl/day)	$F_{i,exp2}$ (bbl/day)	$F_{i,exp3}$ (bbl/day)	$F_{i,exp4}$ (bbl/day)	$F_{i,exp5}$ (bbl/day)	$F_{i,exp6}$ (bbl/day)	$F_{i,exp7}$ (bbl/day)
Reformate	6,498.0	5,736.0	5,705.8	84.7	5,690.6	95.0	5,677.1
LSR Naphtha	92.3	755.2	734.8	1,545.2	705.8	1,518.9	744.0
n-Butane	137.6	300.1	354.5	172.2	369.1	160.2	367.2
FCC Gas	118.4	103.9	91.5	123.3	113.5	149.8	90.9
Alkylate	153.6	104.6	113.3	5,074.3	121.0	5,076.2	120.7
$MaxGap_{ell}$ ($/day)	494.5	365.0	308.2	216.3	173.8	117.2	82.1
Reduction of initial $MaxGap_{ell}$	78%	83%	86%	90%	92%	95%	96%

variables from those bounds, as defined in Problem 4.1. The cost was also multiplied by the ratio between the duration of the experiment (15 minutes) and total batch time (9 hours) as in Problem 4.2. The total cost of experimentation in Figure 5.1 was $7.0. This value is very small because the original system has nearly alternative solutions (i.e., its marginal costs are close to zero). In a real plant, however, there would be additional resistance to changing plant operation, especially due to the transients involving pump startups and shutdowns. This could be avoided by adding constraints in the design of experiments to keep flowrates within bounds defined by operations personnel.

The parameter variances after the update with available CLRTO data and their variances after the 7th experiment are shown in Table 5.12. Note that the experiments focused on reducing the variances mainly of Reformate octane and RVP, and of Alkylate octane and RVP. These parameters were determined automatically by the experimental design problem, without input from the user. By analyzing the results in Table 5.12 together with Figure 5.1, it is clear that the key decision in this case study is whether Reformate or Alkylate should be added to the blend. Note that both contribute high octane to the product, but are costly.

If the diagnosis procedure presented in Chapter 4 were used in this system after the parameter update with CLRTO data (Table 5.8), it would be possible to determine the parameter importance in this system before any experiments were run. Figure 5.2 shows

Table 5.12. Diagnosis and Experimental Design Results (Case Study 1)

Ordering According to Diagnosis	After Update		After 7th Exp	
	$V(Q_{i,nom}^{oct})$ (octane^2)	$V(Q_{i,nom}^{RVP})$ (psi^2)	$V(Q_{i,nom}^{oct})$ (octane^2)	$V(Q_{i,nom}^{RVP})$ (psi^2)
Reformate	0.0546	0.0546	0.0029	0.0016
Alkylate	0.0107	0.0088	0.0055	0.0039
LSR Naphtha	0.0491	0.0489	0.0334	0.0276
n-Butane	0.0546	0.0546	0.0524	0.0510
FCC Gas	0.0546	0.0546	0.0543	0.0540

that the single most important parameter in this case study is Reformate Octane, followed by Alkylate Octane, Reformate RVP and Alkylate RVP. This matches the results obtained in Table 5.12, since the experiments reduced the variances of the most important parameters more than the variances of the remaining parameters.

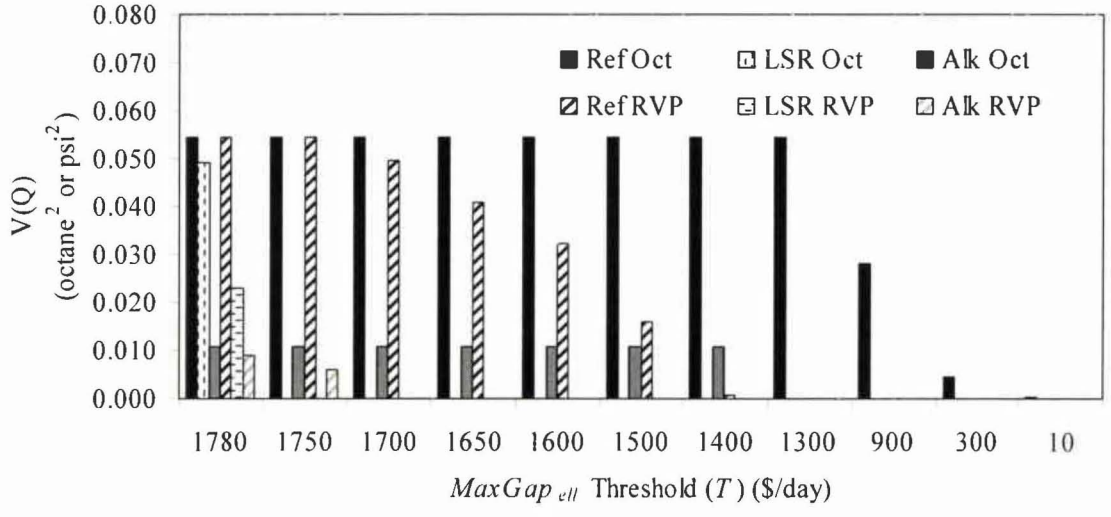

Figure 5.2. Diagnosing Case Study 1

5.5.2. Case Study 2

The same procedure was applied to Case Study 2. The flowrates for the entire sequential procedure can be seen in Figure 5.3, and the flowrates during experimentation are in Table 5.13. The total cost of experimentation was \$28.5. After experiment 10, the CLRTO system performance was deemed satisfactory since $MaxGap_{ell}$ was small (\$103.2/day).

The reason why $MaxGap_{ell}$ increased slightly after Experiment 5 was because initially there was significant mismatch in Reformate octane. Since Experiment 5 improved the estimate in this parameter substantially, the largest profit gap was calculated with smaller parameter variances, but around a different nominal model.

In this case, $MaxGap_{ell}$ around the new nominal model was larger than around the original nominal model. With a few additional experiments as shown in these results, the performance metric was reduced to acceptable levels.

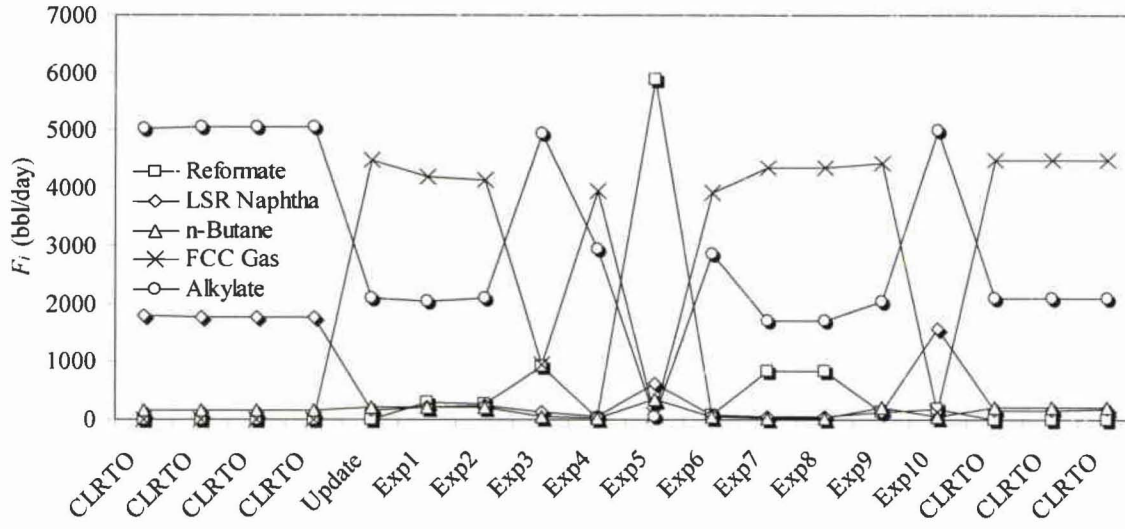

Figure 5.3. Results for Case Study 2

Table 5.13. Experiments for Case Study 2

	$F_{i,exp1}$ (bbl/day)	$F_{i,exp2}$ (bbl/day)	$F_{i,exp3}$ (bbl/day)	$F_{i,exp4}$ (bbl/day)	$F_{i,exp5}$ (bbl/day)	$F_{i,exp6}$ (bbl/day)	$F_{i,exp7}$ (bbl/day)	$F_{i,exp8}$ (bbl/day)	$F_{i,exp9}$ (bbl/day)	$F_{i,exp10}$ (bbl/day)
Reformate	305.2	279.6	915.8	27.4	5,882.7	90.2	835.0	838.4	131.1	179.7
LSR Naphtha	218.6	244.5	136.2	48.6	638.9	81.7	58.3	57.8	148.7	1,590.9
n-Butane	229.9	224.5	53.4	40.5	361.8	42.5	32.6	27.2	227.3	65.5
FCC Gas	4,205.1	4,151.1	949.9	3,941.2	73.8	3,917.3	4,370.4	4,371.5	4,447.0	140.6
Alkylate	2,040.1	2,099.5	4,944.7	2,942.2	42.9	2,868.3	1,703.6	1,705.1	2,045.5	5,023.3
$MaxGap_{ell}$ ($/day)	540.7	371.3	335.3	277.4	283.3	245.5	204.4	173.4	156.8	103.2
Reduction of initial $MaxGap_{ell}$	64%	75%	77%	81%	81%	83%	86%	88%	89%	93%

The results from Case Studies 1 and 2 show that the sequential procedure is able to determine the sources of uncertainty in the RTO model and reduce the variances in the key model parameters through focused experiments. Even though the two case studies had exactly the *same initial optimal basis* (same flowrates) and used the same RTO model on the same true plant, different economics resulted in different requirements for model enhancement in each case. This difference was recognized by the sequential procedure, and Case Studies 1 and 2 converged to *different optimal bases for Cases 1 and 2* (Table 5.9)!

5.5.3. Case Study 1B: Intercept in Parameter Estimation

In the previous studies, the product quality model intercepts have been assumed to be exactly zero. For example, in the quality equations (B.1) shown in Appendix B, a linear blending model with intercepts θ_0^j equal to zero is assumed for octane and RVP properties in the component streams. The use of uncertain model intercepts can play a significant role in Bayesian parameter estimation.

Many refineries use a linear model without intercept for calculating blended gasoline octane (Zahed et al., 1993), since it only needs a small amount of data and produces simpler correlations between component properties (Müller, 1992). Since it is

known that octane does not blend linearly (Singh et al., 2000), model mismatch must be handled by this linear model.

Reid vapour pressure blends linearly on a molar basis. When blending on a volumetric basis as done in (B.1), practitioners often use the Chevron RVP blending index (Gary and Handwerk, 1984). Even though the index allows vapour pressure to blend in an approximately linear fashion without intercept, it does not provide a perfect correlation. Therefore, there may also be some residual nonlinearity in the linear blending model for this property.

The intercepts in equation (B.1) can account for some of the linearization error incurred by approximating the nonlinear process model by a linear model one. The proper choice of whether to include intercepts in the model depends on plant experience: one should evaluate the effect of linearization for the range of operating conditions in the plant. This evaluation could be performed using laboratory blending data or by implementing the real-time monitoring and diagnosis system with an intercept and observing if the intercept is significantly different from zero.

The prior variances of the intercepts in equation (B.1) play a significant role in the parameter estimation: the larger these variances are, the smaller the effect of new data points on the estimated octane and RVP coefficients. However, too small a prior variance on the intercepts is equivalent to not using intercepts at all in the formulation.

In order to illustrate the effect of uncertainty in the intercept, Case Study 1 was repeated using the same prior variance in the intercepts as in the estimated parameters. Since there were 12 degrees of freedom in this system (10 octane and RVP properties and 2 intercepts), all variances were assumed to be 0.0476 (octane^2 or psi^2) so that the individual parameter variations did not exceed ±1.0 (octane^2 or psi^2) at the 95% confidence level. The results can be seen in Table 5.14.

Table 5.14. Experiments for Case Study 1 with Uncertain Intercepts

	$F_{i,exp1}$ (bbl/day)	$F_{i,exp2}$ (bbl/day)	$F_{i,exp3}$ (bbl/day)	$F_{i,exp4}$ (bbl/day)	$F_{i,exp5}$ (bbl/day)	$F_{i,exp6}$ (bbl/day)	$F_{i,exp7}$ (bbl/day)
Reformate	5,725.6	191.5	5,684.8	551.6	5,700.7	5,705.1	5,686.2
LSR Naphtha	722.4	1,583.1	742.4	1,045.7	719.7	709.3	752.5
n-Butane	310.8	151.8	363.4	140.5	350.5	282.1	337.9
FCC Gas	106.3	66.5	105.3	179.3	122.9	184.7	105.9
Alkylate	134.9	5,007.1	104.1	5,082.6	106.1	118.2	117.5
$MaxGap_{ell}$ ($/day)	1,378.6	1,096.2	814.2	629.6	477.2	398.0	357.1
Reduction of initial $MaxGap_{ell}$	37%	50%	63%	71%	78%	82%	84%

The initial monitoring step yielded the same metric value as shown previously ($MaxGap_{ell}$ = $2,205.4/day). After the update with closed-loop data, $MaxGap_{ell}$ had a value of $2,123.6/day (with Pr_{BC} = $ 9,288.8 /day and $Pr_{nom,CL}$ = $7,165.1/day). Since $MaxGap_{ell}$ was still large ($2,123.6/day), experiments were designed. In this case, because of the uncertain intercepts in the quality balance equations, the reduction of the initial profit gap wasn't as substantial as in the case with no intercepts, as expected. In fact, after Experiment 7, the reduction of the initial $MaxGap_{ell}$ was of 84%, instead of the 96% obtained in the case with the known, zero intercepts.

By applying the diagnostics method from Chapter 4 on this system, it is evident from Figure 5.4 that the most important parameter is Reformate octane, followed by Alkylate octane, Reformate RVP and Alkylate RVP. It is assumed that if a sensor is placed to measure a given component quality, the quality's uncertainty is considered to be reduced to zero. The effect of installing sensors in this system after the 7th experiment can be seen in Table 5.15.

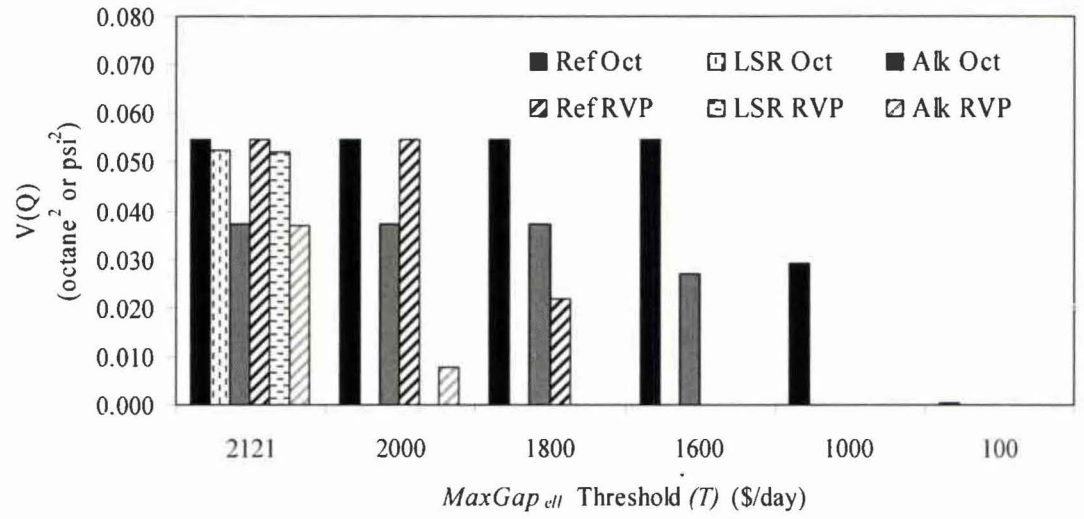

Figure 5.4. Diagnosing Case Study 1 with Uncertain Intercepts

The evaluation of whether sensors should be installed or not is problem-dependent. For example in this case study, sensors may be useful if the system remains very sensitive to information on Reformate and Alkylate properties, i.e., if the $MaxGap_{ell}$ remains large after several experiments. Based on an analysis of substantial amount of historical data, if this situation occurs frequently, onstream analyzers could be appropriate. If this situation occurs only infrequently, offline lab samples may be more appropriate for these key component qualities.

Table 5.15. Effect of sensors

Sensor Location	$MaxGap_{ell}$ ($/day)
No sensors	357.1
$Q_{ref}^{oct,plant}$	260.6
$Q_{ref}^{oct,plant}$, $Q_{alk}^{oct,plant}$	0.5

The cost of installing a Near Infra-Red (NIR) analyzer, which is capable of measuring several component qualities including octane and RVP, is roughly $300,000 (Measurementation, Inc., 2004). In order to decide how many sensors should be installed, if any at all, one should note that $MaxGap_{ell}$ corresponds to a conservative estimate of the profit gap: a more realistic estimate could be obtained by using the more refined approaches in Chapter 3 (the expected value of $MaxGap_{ell}$, or ideally, the expected value of the profit gap). Also, maintenance and installation costs of the sensors should be taken into consideration before making the decision to purchase the sensor. The decision would be based on an economic analysis using standard time-value of money measures, e.g., net present value (NPV).

5.6. Two-Parameter Case Study 3

In the case studies shown in the previous sections, the use of closed-loop RTO data was sufficient for the system to attain the correct basis, and the experiments were performed in order to achieve a small enough largest profit gap. This means that for these cases, the experiments did not increase profit; they increased the probability that the highest profit had been achieved. However, this does not occur in all situations. As an example, we present a case study with two uncertain parameters, defined in Table 5.16.

Table 5.16. Description of Two-Parameter Case Study

	$Q_{i,nom}^{oct}$ (octane)	$Q_{i,nom}^{RVP}$ (psi)	$Q_{i,true}^{oct}$ (octane)	$Q_{i,true}^{RVP}$ (psi)	$cost_i$ ($/bbl)	F_i (bbl/day)
Reformate	91.9	2.6	92.3	2.7	34.2	0.0
LSR Naphtha	64.0	11.0	64.0	10.9	26.5	1796.3
n-Butane	92.5	137.9	92.5	138.0	10.3	161.1
FCC Gas	84.8	6.5	85.3	6.4	31.8	0.0
Alkylate	97.0	6.6	97.0	6.7	34.4	5042.5
Current Profit ($/day)						8,274.1

The variances of Reformate octane and FCC Gas octane parameters were assumed to be 0.1280 octane^2, which, in a 3-degree-of-freedom multivariate normal distribution (2 octane parameters and one intercept for the blended octane equation) corresponds to a maximum variation of ±1.0 octane in each parameter.

When monitoring the performance of the system, a value of $897.7/day was found for $MaxGap_{ell}$, where Pr_{BC} = $ 9,123.0/ day and $Pr_{nom,CL}$ = $ 8,225.3/ day. Since this value is considered too high, transient RTO data without experimentation (Table 5.17) was used to update model parameters.

Since the initial transient data contained no information on the component streams with uncertain parameters, the largest profit gap $MaxGap_{ell}$ remained the same ($897.7/day) after model updating using the initial data. Two designed experiments were required to reduce the profit gap to an acceptable level, as shown in Table 5.18.

Table 5.17. Transient RTO runs

	F_i (bbl/day) RTO run 1	F_i (bbl/day) RTO run 2
Reformate	0	0.0
LSR Naphtha	1,796.4	1,796.3
n-Butane	161.1	161.1
FCC Gas	0.0	0.0
Alkylate	5,042.5	5,042.5

Table 5.18. Experiments for Two-Parameter Case Study

	$F_{i,exp1}$ (bbl/day)	$F_{i,exp2}$ (bbl/day)
Reformate	55.8	27.4
LSR Naphtha	9.3	60.0
n-Butane	19.5	61.3
FCC Gas	3,974.9	3,953.5
Alkylate	2,940.5	2,897.8
$MaxGap_{ell}$ ($/day)	213.9	53.1
Reduction of initial $MaxGap_{ell}$	76%	94%

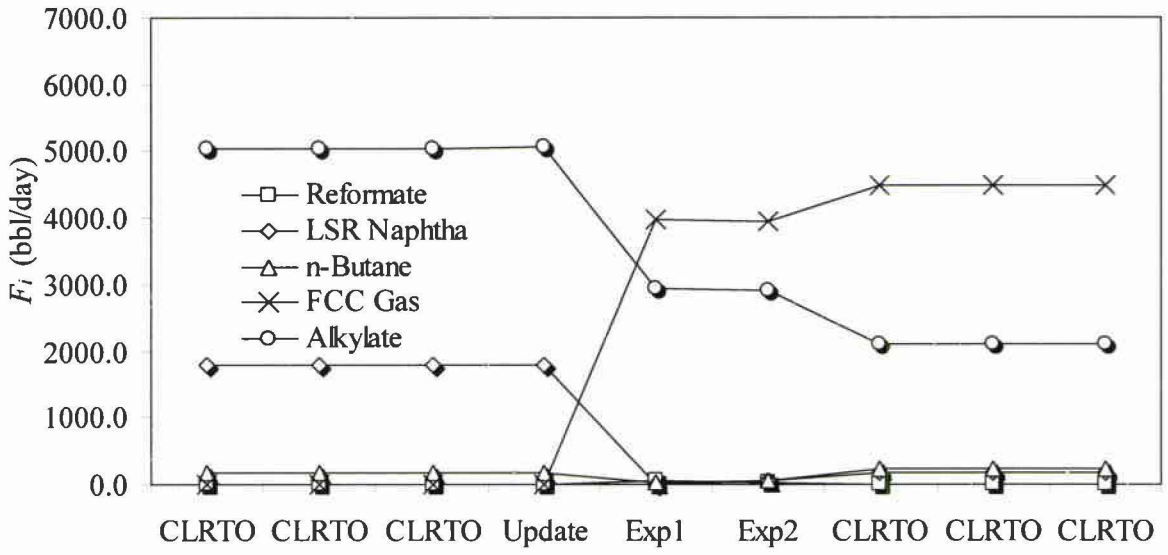

Figure 5.5. Results for Two-Parameter Case Study

The profile of the flowrates during the sequential procedure for this case study can be seen in Figure 5.5. In this example, the total cost of experimentation was $1.0.

Note that the optimal basis of this system after the update with initial CLRTO data remained was the same as the initial basis. After the second experiment, the CLRTO system performance was deemed satisfactory since $MaxGap_{ell}$ was small ($53.1/day). After experimentation, the system converged to a new optimal basis, with a profit of $8,626.6/day. This represented an improvement of ($8,626.6/day – $8,274.1/day =) $352.5/day to plant operation.

5.7. Conclusions

In this chapter, the new methods presented in previous chapters were integrated into a sequential procedure for monitoring, diagnosing and improving the performance of linear CLRTO systems. The sequential nature of this procedure allows for its interruption as soon as CLRTO performance is deemed satisfactory.

The monitoring method does not interfere with the closed-loop RTO. It checks data for validity before performance monitoring is performed, and it evaluates the

potential profit loss in the system based on prior information about model uncertainty. From the results in Chapter 3, $MaxGap_{ell}$ was the monitoring metric that possessed the best trade-off between quality of representation of monitoring goal and computational expense; therefore, it was the chosen metric for the sequential procedure. The monitoring strategy allows for the incorporation of correlation among parameters and handles all types of constraints (equality and inequality) directly in closed- or open-loop systems. It can also handle uncertainty in any coefficient of the original CLRTO problem.

Experimentation is only performed when uncertainty (based on prior information) and current batch data do not provide sufficient model accuracy to reduce the monitoring metric ($MaxGap_{ell}$) to acceptable levels. Derivative-Free Optimization is used to solve the experimental design formulation due to its greater reliability in comparison to the optimality-based methods. The experiments are designed to maximize the overall profit during the process batch and to have a very flexible constraint structure. The experimental design can be tailored to plant requirements by defining additional constraints, such as limitations to the changes in variables from their current values or on final product quality. This is desired since blended gasoline is usually stored in large tanks with no agitation, so stratification of material could occur.

The sequential procedure provides a clear record of the key parameters whose uncertainty might influence profit tracking. The diagnosis method presented in Chapter 4 can effectively rank parameters in terms of importance with respect to the objective function of the original problem without assuming a constant LP basis. This information could be used to simplify the design of experiments by determining variables that should have improved estimates, or for determining process sensor location.

The case studies in this chapter have demonstrated the efficacy of the sequential method for CLRTO performance monitoring, diagnosing and enhancement. The experimentation and diagnosing reduced the uncertainty as predicted and resulted in the closed-loop RTO system converging to the true plant optimum in all cases.

Chapter 6

Conclusions and Future Work

Real-time optimization systems use an updated model in order to track optimum operation in a plant. In all commercial real-time optimization systems with feedback only some of the model parameters are updated at every CLRTO execution. Therefore, some process parameters such as component properties, prices and costs are not known exactly, but instead, within some uncertainty region. The CLRTO system determines the operating conditions in the system by optimizing the uncertain model. As a result, there is generally no guarantee that the optimum of the true plant has been achieved and no straightforward manner for estimating the deviation from the true plant optimum.

This thesis focuses on determining the cost of the uncertainty in closed-loop LP problems under limited feedback. Methods were developed for diagnosing the optimization system by calculating measures of the profit loss due to parameter uncertainty and by identifying parameters that affect the objective function the most. In addition, novel formulations were developed for designing profit-based experiments to update model parameters when their uncertainty needs to be reduced. None of these methods assumes knowledge about the true values of unmeasured process variables in the plant. The only assumptions are that their uncertainty ranges (or in some cases, distributions) are known and that there is no significant structural mismatch between model and plant.

In the following sections, some conclusions and contributions of this work are presented in more detail.

6.1. Conclusions

6.1.1. Problem Definition

This thesis addressed monitoring, diagnosis and improvement of the performance of a class of closed-loop optimization systems. The key assumptions and characteristics of the models considered in this research are stated in the following paragraphs.

- Linear Programming: The systems in this work can be adequately modeled using linear programming, including linearization of properties and quality-flow constraints in the gasoline-blending process. All variables are continuous between their bounds, and no significant structural mismatch exists.
- Closed-loop optimization: The optimization is performed periodically after the model has been updated using selected measurements of output variables. In this study, only the steady state behaviour of the system is monitored. The transient to the steady state is not evaluated because the material is mixed prior to being shipped to the customers, and therefore deviations from specifications are moderated by mixing and deviations in the mean can be can be corrected by modifying the target of qualities at the mixing point.
- *Measurements*: Measurements for use in the real-time system are assumed to be limited.
- *Uncertain feedback parameters*: The plant parameters are not known exactly, and some may not be observable using commonly available data. At least some of the uncertain parameters are multiplied with variables in the LP model.
- *Correlated parameters*: The uncertain parameters may be correlated due to the chemistry and physics of the upstream processes.
- *Limited interference*: The monitoring and enhancement system developed in this thesis introduces as little change as possible to the process operation, so as to reduce modifications of product qualities, production rate and economic performance.

- *Real-time implementation*: Uncertainty, input variable bounds, output constraint limits, and economic coefficients define a scenario, and the scenario can change from day to day. Therefore, the system should be implemented in real time.

The research addresses the performance of the closed-loop real-time optimization. Therefore, methods were developed to determine how close a real-time optimizer is to the best possible closed-loop operation for a given plant realization. For a closed-loop system, this metric represents the effect of uncertainty on the system for a single plant realization. For open-loop systems, however, this metric represents the effect of disturbances such as the properties of the blending components, which have a strong effect on profit. This topic is further discussed in Appendix E.

Linear CLRTO with limited feedback is applied to relevant industrial problems, such as blending of components into a final product. Examples of such blending problems are present in the cement industry, coal industry and in refinery operations, such as the blending of crude oil, diesel and gasoline. In the gasoline-blending process, it is common to have a bias model updating strategy, which can lead to the wrong corner point if the mismatch between plant and model parameters is too large. Because of its economic relevance, this process was used in several case studies throughout the thesis. Other types of problems to which the technology in this work is applicable are:

- The steady-state LP in every MPC controller (at least 4,000 installed worldwide). The monitoring and diagnosis is directly applicable, while the experimentation would require modification: in this case, the experimentation process would be dynamic, where the experimental design would perturb the dynamic system to obtain improved estimates for the steady-state gains. Depending on the goals of the design (improved estimates of steady-state gains, dynamic performance), the experimental design would be substantially different, requiring design of the input forcing (magnitude, frequency content, etc.), consideration of constraints in the dynamic variables during the experiment, and model building diagnostics (Box and Jenkins, 1970).

- Any production planning problem that can be re-solved periodically using updates from recent measurements. This could be a daily re-optimization performed "off-line", which would emulate the CLRTO implementation.

6.1.2. Monitoring CLRTO Performance

In most processes, the condition of the true plant relative to its optimum cannot be determined by measurements. There may be too few measurements available to update all of the uncertain parameters, or, in the gasoline blending process, some flows may not be in the current optimal basis (*i.e.*, their flows may be zero), and therefore do not have any effect on the output measurements.

The CLRTO performance measure was based on the value of the objective function, *i.e.*, profit, in the gasoline case study. Variability of the optimization variables (flows in the blending problem) was not considered important in terms of performance. The methods in this research could be applied to optimization including other terms in the objective function, which would be a form of goal programming.

In order to assess CLRTO performance, an *a priori* estimate of parameter uncertainty from previous batches is used. The performance metrics developed in this work estimate the deviation of current operation from the true plant optimum due to uncertainty in the RTO model parameters. The first metric developed was the largest profit gap (*MaxGap*), calculated with interval or ellipsoidal uncertainty description of the parameters. This metric corresponds to the Maximum Regret in Decision Analysis theory. In this work, *MaxGap* is calculated in a single computation, and therefore does not require the enumeration of scenarios, as is the case in traditional Decision Analysis literature. This metric can be very relevant in some problems (other than gasoline blending) in which the worst case involves a very undesirable incident, such as bankruptcy of a company, failure of a building, explosion of a process, etc. *MaxGap* defines an upper bound on the loss due to imperfect modeling of the plant. Due to its computational tractability, it can also be embedded in the experimental design formulation, where sampling would not have been computationally tractable.

If more accuracy is required in assessing performance, an improved monitoring metric was developed that incorporates information about the parameter distribution, i.e., the expected value of the largest profit gap, E(*MaxGap*). It is a less conservative, but computationally more intensive method than *MaxGap*. It is still of manageable computational complexity for monitoring purposes. For this metric, a method was developed for approximating the integral needed for calculating the expected value of a function based on parameter confidence level information.

The most meaningful monitoring metric for CLRTO systems is the expected value of the profit gap, E(*Gap*), which corresponds to the Expected Value of Perfect Information (EVPI) in Decision Analysis literature. It is a very expensive metric to calculate even for monitoring-only applications, and it does not scale well with the number of uncertain parameters. A method for eliminating large parameter regions was developed that can potentially reduce the computational burden of calculating this metric. In this work, the E(*Gap*) metric was only applied to a two-dimensional problem; therefore more studies are needed in order to develop efficient strategies for larger-scale systems.

Main Contributions:

- Modeling CLRTO systems to identify performance loss due to uncertain parameters. Because of its goals, modeling required a novel formulation, different from the one required for (open-loop) evaluation of best- and worst-case optimization of systems due to process disturbances;
- Definition of useful measures of CLRTO performance;
- Formulating and solving three novel real-time monitoring metrics;
- All performance metrics can handle parameter uncertainty (and most of them, correlation) in any parameter of the closed-loop system. The uncertain parameters can be in equality or inequality constraints.

6.1.3. Diagnosing CLRTO Performance

The purpose of diagnosing the performance of a CLRTO system is to rank parameters for importance with respect to their effect on the objective function. If used in real-time applications, it can direct unscheduled laboratory analyses, while in offline applications, diagnosing can aid in model improvement and sensor location. Therefore, diagnosing complements the monitoring problem in that monitoring determines the effect of parameter uncertainty in the system, while diagnosing identifies the key parameters responsible for such an effect.

The diagnostic method developed in this thesis determines parameter importance at different values of the profit gap metric. As distinguished from conventional sensitivity analysis literature, it is not limited by the assumption of a constant active set. The CLRTO diagnosing formulation is a bilevel optimization problem that was solved with an interior-point solver, IPOPT-C.

The calculations for the diagnosis procedure are much simpler than the ones for experimental design. Therefore, it is expected that the diagnosis will find application as a method for evaluating optimization systems, even when the complete sequential procedure for CLRTO monitoring and enhancement has not been implemented.

Main Contribution:

- Formulation and solution of a CLRTO performance diagnostics method that identifies key parameters at various levels of profit loss due to CLRTO parameter uncertainty.

6.1.4. CLRTO Model Improvement

Whenever CLRTO performance is deemed unsatisfactory, experimental design can be used in order to improve it. This new formulation provides a profit-based objective, rather than an information-based objective as in conventional optimal design of experiments. The objective of the experimental design formulation is to improve the total

profit in the operation from the beginning of the experiment until the end of the batch. The profit during experimentation was also considered.

The experimental design formulation considers the effect of parameter variance on profit and provides flexibility in the experiments by incorporating constraints to manipulated and dependent variables. More than one experiment may be required to achieve acceptable CLRTO performance.

The experimental design is geared towards optimizing the overall profit of the system, and it can be applied to small- to mid-sized problems. Since the performance metric was an inner problem for the experimental design calculations, the largest profit gap (*MaxGap*) was the metric of choice because it can be solved in a single optimization problem.

The cost of experimenting is based on whether the manipulated variables involved are basic or non-basic. Since batch processes are considered, the effects on the product composition on changes in basic variables that are not at their bounds can be compensated for ("blended out") after the experiment has been performed, and thus are considered to have zero cost to operation. The same does not apply to variables at their lower or upper bounds. Since the effect of experimentation will be felt at the final product tank, modifying these values has a cost that is associated with their marginal values.

Main Contribution:

- Formulation and solution of the profit-based experimental design problem. The challenging three-level optimization was solved by two methods, with the Derivative-Free Optimization (DFO) method being more reliable in the case studies.

6.1.5. Real-Time Method for Monitoring and Enhancing RTO Performance

This thesis presented a systematic way of applying the monitoring and enhancement methods to existing CLRTO systems. The first data rectification step

employs existing technology to check that the key assumptions about the uncertainty magnitudes are valid for the operating region. Then, the performance monitoring and enhancement techniques developed in this work are applied until satisfactory performance is achieved. The diagnostics methodology can be used for offline evaluation of the process improvements.

Main Contribution:

- A stage-wise procedure that employs the simplest computations and least intrusive procedures possible at the earlier stages of the CLRTO executions in a process.

6.1.6. Monitoring Open-Loop Optimization

The methods developed for monitoring the performance of closed-loop systems in this work can be extended in a straightforward manner to open-loop LP problems. In this case, the monitoring methods determine the best- and worst-case performance of the optimization of a system with no feedback or recourse. These cases may correspond to the best and worst effect of process disturbances in a plant, for example. There was a preliminary application to a nonlinear optimization problem, but further study is required.

Main Contribution:

- Formulation and solution of monitoring open-loop linear optimization problems with uncertain parameters in the objective function, equality and inequality constraints. Stochastic correlation among parameters in also handled.

6.1.7. Limitations of the Methods

While the developments in the thesis have opened new avenues in the area of closed-loop optimization under uncertainty, they are not without limitations. The formulations for monitoring, diagnosing and designing experiments are nonlinear, nonconvex optimization problems, so there is no guarantee of global optimality.

There may be computational issues with larger-scale problems due to the rising number of complementarity constraints if there are additional inequality constraints in the original optimization problem, and/or due to the increasing number of uncertain parameters. Complementarity constraints are particularly challenging because singularities occur at each active set change.

The solvability of the problem is somewhat dependent on the solver being used. IPOPT-C has been reported to solve up to 1,748 complementarity constraints so far. Its success is partly based on softening the complementarity constraints, as discussed in Appendix D. With future developments in solver technology and in computational power, application of methods in this thesis may broaden.

6.2. Future Work

This thesis presents new approaches for monitoring, diagnosing and enhancing CLRTO performance. Several new research topics were addressed, such as monitoring the performance of closed-loop systems, profit-based design of experiments and the diagnosis of optimization systems (Robinson, 2005). Therefore, many potential research topics stem from this work.

- *Larger LP Problems*: The CLRTO performance monitoring, diagnosing and enhancement methods can be applied to other relevant larger-scale (20+ manipulated variables) LP problems. Even though a small open-loop NLP case study was presented in this thesis, a general methodology to handle nonlinear CLRTO systems is also needed.
- *Mixed-Integer Problems with Uncertainty*: It would be beneficial to extend the methods to mixed-integer linear programming problems, such as the ones encountered in the scheduling and planning problems.
- *Performance Monitoring*: Besides profit, other CLRTO performance metrics exist, such as frequent switching between two corner points, as occurs in some

Model-Predictive Controllers. The inclusion of these metrics in the monitoring approaches should be assessed.

- *Diagnosing*: The formulation in this thesis minimizes the trace of the variance-covariance matrix in order to achieve a user-specified profit gap threshold value. Another possible formulation for the diagnosis problem is to minimize the number of parameters that need to be updated so that the largest profit gap is below a maximum acceptable value, which becomes a mixed-integer problem.
- *Design of Experiments*:
  - The experimental design strategy could be altered in order to reduce its computational burden. First, the system can be diagnosed in order to determine the key parameters responsible for a user-specified profit gap threshold. Then, experimentation could be performed only on the subset of parameters identified by the diagnosis, thus reducing the computational burden of designing experiments. Also, similarly to the extension for diagnosing, the experimental design formulation could directly include the number of parameters being re-estimated in its objective function, which should be minimized. This would give the problem a mixed-integer formulation.
  - The design of experiments in this thesis has the maximization of profit during the experiment as part of the objective function. This leads the optimizer to increase the flowrates of profitable components during the experiment as much as possible, instead of reducing the flowrates of components that lead to experimental costs. In future work, the cost of experimentation could be considered explicitly in the objective function, which would possibly lead to a reduction in the production rate during the experiments, if production rate were left unconstrained. A reduction in production rate would lead to reduced costs of experimentation, although sensor accuracy might be (negatively) affected.

- *Improved CLRTO Design*: An interesting extension of this work is to determine which values of the nominal CLRTO model parameters would make the performance of the closed-loop system least sensitive to uncertainty in the plant. The methods developed in this thesis may also be applied to plant design problems, in which sensors could be systematically placed in order to improve the performance of the CLRTO system, balancing the capital/operating cost vs. improvements.
- *Structural Mismatch*: The effects of likely structural mismatch should be investigated. One approach would be to pose multiple, disjunctive LP models with different structures for a single model in the system. Then, the linear combination of these models would provide a relaxation yielding a convex model (for an LP) which would provide an upper bound on system profit. How tight (useful) the bound is would need to be evaluated.

Nomenclature

a	payoff
A	left-hand side parameters
AR	actual rate
b	right-hand side parameters
BW	backward difference approximation
c	objective function coefficients
C	concentration
C_{Gapmin}	largest confidence level that yields a profit gap of Gap_{min}
$cost$	cost of components available for blending
D	set of decisions
DOF	degrees of freedom
$EVPI$	expected value of perfect information
$EVSI$	expected value of sample information
f	objective function
F	flowrate
$\boldsymbol{F}$	vector of flowrates
FS	full scale
FW	forward difference approximation
g	inequality constraints
Gap_{min}	minimum profit gap
h	equality constraints
$\#ineq$	number of inequality constraints
J	objective function
k	reaction rate

L	Lagrangean
MAP	maximum achievable profit
$Maxgap$	largest profit gap
$Mingap$	smallest profit gap
n	number of components available for blending
Nc	number of constraints
p	probability of constraint satisfaction
	probability of each realization of the uncertain variables
Pr	profit
Q	properties of components available for blending
	surrogate function
r	regret
T	profit gap threshold
TR	trapezoidal approximation
U	variance-covariance matrix of model parameters
V	volume
$value$	value of gasoline
x	optimization variables
	molar fraction
X	input variables
Y	interpolation set
z	output variables

Greek letters

α	confidence level
	recycle ratio of components A and B
β	updated bias parameter
	recycle ratio of components X and Y
δ	smallest Lagrange multiplier

Δ	change in value
	trust region radius
ε	bias
ϕ	basis in the space of quadratic polynomials
Φ	coefficient matrix of surrogate model
φ	error vector
λ	Lagrange multipliers
μ	barrier parameter
σ	standard deviation
θ	parameters

Subscripts

0	initial value
a	set of active constraints
	component A
A	active inequality constraints
a0	initial value for component A
Alk	alkylate
AP	approach for calculating expected profit gap
b	component B
BC	best-case scenario
blend	variables that refer to blended gasoline product
But	n-Butane
BW	backward difference approximation
CL	closed-loop
conf	confidence level (%)
dof	degrees of freedom
ell	ellipsoidal uncertainty description

eq	equality constraints
exp	experiment
FCC	FCC Gasoline
FW	forward difference approximation
i	index for components available for blending
	index for decisions
I	inactive inequality constraints
in	inequality constraints
int	interval uncertainty description
j	index for realizations of uncertain variables
LSR	Light-Straight Run Naphtha
meas	measured
min	lower bound
max	upper bound
nc	number of confidence levels
nom	nominal
OL	open-loop
P	number of uncertain parameters
r	component R
Ref	Reformate
t	RTO execution time
TR	trapezoidal approximation
true	true value in the plant
WC	worst-case scenario
x	component X
y	component Y

Superscripts

0	initial value

j	set of component properties (octane number, RVP)
plant	plant
oct	octane
RVP	Reid vapour pressure

Operators

E(.)	expected value
Tr(.)	trace of a matrix
V(.)	variance-covariance matrix
∇	gradient

Bibliography

ABB (2006). Industrial^{IT}: Solutions for the Cement Industry. http://library.abb.com/GLOBAL/SCOT/SCOT244.NSF/VerityDisplay/10EC4CAF7CF0A99AC1256FFE003442F6/$File/Dispatch_Automation_3BHT_490_264_lr.pdf (25 March 2006)

Arwikar, K., Gildea, E., and Nikeus, L.-A. (2002). Integrating and Optimizing Blending Operations at Preem's Gothenburg Refinery. *NPRA Computer Conference*. CC-02-155, Austin, TX.

AspenTech (2006) Aspen Blend Brochure. www.aspentech.com/brochures/Aspen_Blend.pdf (25 March 2006)

ASTM D-323. Standard Test Method for Vapor Pressure of Petroleum Products (Reid Method). ASTM International.

ASTM D-2699. Standard Test Method for Research Octane Number of Spark-Ignition Engine Fuel. ASTM International.

ASTM D-2700. Standard Test Method for Motor Octane Number of Spark-Ignition Engine Fuel. ASTM International.

Averbakh, I. (2000) Minmax Regret Solutions for Minimax Optimization Problems with Uncertainty. *Operations Research Letters,* 27: 57-65.

Bay, T., Ross, C., Andrews, J., and Gilliland, J. (1969). Dynamic Control of the Cement Process with a Digital Computer System. *Progress in Direct Digital Control*, ISA, Pittsburg, 117-126.

Ben-Tal, A. and Nemirovski, A. (1998) Robust Convex Optimization. *Mathematics of Operations Research,* 23 (4): 769-805.

Ben-Tal, A. and Nemirovski, A. (2000) Robust Solutions of Linear Programming Problems Contaminated with Uncertain Data. *Mathematical Programming,* 88: 411-424.

Biegler, L.T. and Grossmann, I.E. (2004) Retrospective on Optimization. *Computers and Chemical Engineering,* 28: 1169-1192 .

Birchfield, G.S. (2002). Advanced Process Control, Optimization and Information Technology in the Hydrocarbon Processing Industries - The Past, Present and Future. Aspentech publication. http://www.aspentech.com/publication_files/ Advanced_Process_Control.pdf (25 Mar. 2006)

Box, G.E.P. and Draper, N.R. (1969). *Evolutionary operation. A statistical method for process improvement.* NY: John Wiley & Sons, Ltd.

Box, G.E.P. and Jenkins, G.M. (1970). *Time Series Analysis: Forecasting and Control.* San Francisco: Holden-Day.

Box, G.E.P. and Tiao, G.C. (1973). *Bayesian Inference in Statistical Analysis.* Reading:Addison-Wesley.

Brooke, A., Kendrick, D. and Meeraus, A. (1996). *GAMS: A User's Guide.* San Francisco, CA: GAMS Development Corp.

Charnes, A. and Cooper, W.W. (1963) Deterministic Equivalents for Optimizing and Satisficing under Chance Constraints. *Operations Research,* 11 (1): 18-39.

Chin, A. (2006) *Private communication.*

Chinneck, J.W. and Ramadan, K. (2000). Linear Programming with Interval Coefficients. *Journal of the Operational Research Society,* 51: 209-220.

Clark, P.A., and Westerberg, A.W. (1990). Bilevel Programming for Steady-State Chemical Process Design - I. Fundamentals and Algorithms. *Computers and Chemical Engineering*, 14 (1): 87-97.

Conn, A.R., Scheinberg, K., and Toint, Ph.L. (1996). On the Convergence of Derivative-Free Methods for Unconstrained Optimization. *Invited presentation at the Powellfest*, Report 96/10, Cambridge.

Conn, A.R., Scheinberg, K., and Toint, Ph.L. (1997). Recent Progress in Unconstrained Nonlinear Optimization without Derivatives. *Mathematical Programming*, 79: 397-414.

Crowe, C.M. (1996). Data Reconciliation - Progress and Challenges. *Journal of Process Control*, 6 (2/3): 89-98 .

CTA (2006). Center for Transportation Analysis website. http://www-cta.ornl.gov/data/tedb24/Spreadsheets/Table10_03.xls (8 Feb. 2006)

Dennis, J.E., Jr. and Torczon, V. (1991) Direct Search Methods on Parallel Machines. *SIAM Journal on Optimization*, 1: 448:474.

Diaz, A., Barsamian, J.A. (1996) Meet Changing Fuel Requirements with Online Blend Optimization. *Hydrocarbon Processing,* 71-76 .

Draper, N. and Smith, H. (1998) *Applied Regression Analysis.* 3rd edition. NY: John Wiley & Sons, Ltd.

Drezner, Z. (2001). The Maximum Possible EVPI. *INFORMS Transactions on Education*, 1(3): 117-118.

Fan, E. (2002). Global Optimization of the Lennard-Jones Atomic Clusters. M.Sc. Thesis, Department of Computing and Software, McMaster University.

Forbes, J.F. and Marlin, T.E. (1994). Model Accuracy for Economic Optimizing Controllers: The Bias Update Case. *Industrial & Engineering Chemistry Research*, 33: 1919-1929.

Forbes, J.F., Marlin, T.E., and MacGregor, J.F. (1994). Model Adequacy Requirements for Optimizing Plant Operations. *Computers and Chemical Engineering*, 18 (6): 497-510.

Foxboro (2006). Invensys's Blend Optimization and Supervisory System – BOSS. http://www.foxboro.com/us/eng/products/ automationsystems/ MRA/MRAProdBlending.htm (11 Mar. 2006).

Fraleigh, L.M. (1999) *Optimal Sensor Selection and Parameter Estimation for Real-Time Optimization*. M.Sc. Thesis, Department of Chemical & Materials Engineering, Univ. of Alberta.

Gary, J.H., Handwerk, G.E. (1984) *Petroleum Refining - Technology and Economics*. NY: Marcel Dekker, Inc.

Grossmann, I.E. and Sargent, R.W.H. (1978). Optimum design of chemical plants with uncertain parameters. *AIChE Journal*, 24 (6): 1021-1028.

Han, S.P. (1977). A Globally Convergent Method for Nonlinear Programming. *Journal of Optimization Theory and Applications*, 22 (3): 297-309.

Healy, W.C., Jr., Maassen, C.W. and Peterson, R.T. (1959) A New Approach to Blending Octanes, *API Refining Division Midyear Meeting*, 39 (III): 132-192

Herroelen, W.S. and Leus, R., (2005). Project Scheduling under Uncertainty, Survey and Research Potentials. *European Journal of Operational Research,* 165 (2): 289-306.

Honeywell (2006). OpenBPC (Open Blend Property Control). http:// hpsweb.honeywell.com/Cultures/en-US/Products/ OperationsApplications/ BlendingMovementAutomation/ OpenBPC/ default.htm (11 Mar. 2006).

Hughes, W.R. (1995). Valuing Information in Decision Making Under Uncertainty. *Australian Journal of Management*, 20 (1): 105-114.

Ierapetritou, M.G., Pistikopoulos, E.N., and Floudas, C.A. (1996) Operational Planning Under Uncertainty. *Computers and Chemical Engineering*, 20 (12): 1499-1516.

INFORMS (2006) "Mathematical Programming Glossary", http://glossary.computing.society.informs.org/index.php? (22 July 2006)

Johnston, L.P.M., and Kramer, M.A. (1995). Maximum Likelihood Data Rectification: Steady-State Systems. *AIChE Journal*, 41 (11): 2415-2426.

Keeler, S.E. and Reilly, P.M. (1992). The Design of Experiments When There Are Errors in All the Variables. *Canadian Journal of Chemical Engineering,* 70: 774-779.

Kelly, J.D. (2006) *Private communication.*

Kothare, M.V.; Balakrishnan, V., and Morari, M. (1996) Robust Constrained Model Predictive Control using Linear Matrix Inequalities. *Automatica,* 32 (10): 1361-1379.

Liao, Y.-F., Wu, C.-H., and Ma, X.-Q. (2005). New Hybrid Optimization Model for Power Coal Blending. *Proceedings of the 4th International Conference on Machine Learning and Cybernetics,* 4023-4027, Guangzhou.

Lin, X., Janak, S.L., and Floudas, C.A. (2004) A New Robust Optimization Approach for Scheduling under Uncertainty. *Computers and Chemical Engineering*, 28: 1069-1085.

Long, DA (1981). Iron Ore Quality Control. – II. *Engineering and Mining Journal*, 182 (12): 56-67.

Mathworks (1999) *Optimization Toolbox Documentation.* The Mathworks, Inc., Natick, MA, USA.

Measurementation Inc. (2004). FTNIR Application Note. http:// www.measurementation.com/products/pdf/nr800/Heavy%20Oil.PDF. (25 Mar. 2006).

Montgomery,D. C. and Runger,G. C. (1994). *Applied Statistics and Probability for Engineers*. NY: John Wiley & Sons, Ltd.

Mudt, D. (2005) *Private communication.*

Müller, A. (1992). New method produces accurate octane blending values. *Oil & Gas Journal,* 23 (3): 80-90.

Narasimhan, S., and Mah, R.S.H. (1989). Treatment of General Steady State Process Models in Gross Error Identification. *Computers and Chemical Engineering*, 13 (7): 851-853.

Nash, S.G. and Sofer, A. (1996). *Linear and Nonlinear Programming.* NY: Mc-Graw Hill.

Nocedal, J., Wächter, A., and Waltz, R.A. (2005). Adaptive Barrier Strategies for Nonlinear Interior Methods. *Research Report RC23563*, IBM T. J. Watson Research Center, Yorktown, USA.

Omega Engineering, Inc. website (2005). http://www.omega.com. (27 Apr. 2005).

PetroMetrix (2006) www.petrometrix.com/ gasoline.html (11 Feb. 2006).

Pinto, J.C. (2001) On the Costs of Parameter Uncertainties. Part 2: Impact of EVOP Procedures on the Optimization and Design of Experiments. *Canadian Journal of Chemical Engineering,* 79 (3): 412-421.

Qin, S.J. and Badgwell, T.A. (1997). An Overview of Model Predictive Control Technology. *Chemical Process Control,* 93: 232-256.

Qin, S.J. and Badgwell, T.A. (2003) A Survey of Industrial Model Predictive Control Technology. *Control Engineering Practice,* 11: 733-764.

Raghunathan, A.U., and Biegler, L.T. (2003) Mathematical Programs with Equilibrium Constraints (MPECs) in Process Engineering. *Computers and Chemical Engineering*, 27: 1381-1392.

Reilly, P.M. (1973). Linear Regression from a Bayesian Viewpoint. Lecture Notes.

Robertson, D.G. and Lee, J.H. (2002). On the Use of Constraints in Least Squares Estimation and Control. *Automatica,* 38: 1113-1123.

Robertson, D.G., Lee, J.H., and Rawlings, J.B. (1996). A Moving Horizon-Based Approach for Least-Squares Estimation. *AIChE Journal*, 42 (8): 2209-2224.

Robinson, S.M. (ed) (2005). *Statistics and Operations Research: Opportunities at the Interface*. NSF Award, DMS-0343462. Workshop on Opportunities at the Statistics-Operations Research Interface. Santa Fe, NM.

Rooney, W.C. and Biegler, L.T. (2001). Design for Model Parameter Uncertainty using Nonlinear Confidence Regions. *AIChE Journal,* 47(8): 1794-1804.

Rooney, W.C. and Biegler, L.T. (2003). Optimal Process Design with Model Parameter Uncertainty and Process Variability. *AIChE Journal,* 49(2): 438-449.

Rusin, M.H., Chung, H.S. and Marshall, J.F. (1981) A 'Transformation' Method for Calculating the Research and Motor Octane Numbers of Gasoline Blends. *Industrial Engineering Chemistry Fundamentals*, 20: 195-204.

Ryu, J.H., Dua, V., and Pistikopoulos, E.N. (2004). A Bilivel Programming Framework for Enterprise-Wide Process Networks under Uncertainty. *Computers and Chemical Engineering*, 28: 1121-1129.

Sahinidis, N.V. (2004). Optimization under Uncertainty: State-of-the-Art and Opportunities. *Computers and Chemical Engineering*, 28: 971-983.

Sasaki, S., Sugawara, H., Ishiguri, A., and Kubo, K. (1997). Blending Optimization System. *Yokogawa Technical Report English Edition,* 24.

Sakr, M.M.F., Bahgat, A., and Sakr, A.F. (1988). Computer-Based Raw Material Blending Optimization in a Cement Manufacturing Plant. *Control and Computers,* 16 (3): 75-78.

Sen, S. and Higle, J.L. (1999) An Introductory Tutorial on Stochastic Linear Programming Models. *Interfaces*, 29(2): 33-61.

Scheinberg, K. (2000). Derivative Free Optimization Method. *Lecture Notes.*

Shih, J.-S., and Frey, H.C. (1993). Coal Blending Optimization under Uncertainty. *Proceedings of the 10th Annual International Pittsburgh Coal Conference*, 1110-1115, Pittsburgh, PA.

Singh, A., Forbes, J.F., Vermeer, P. and Woo, S.S. (2000). Model-based real-time optimization of automotive gasoline blending operations, *Journal of Process Control*, 10(1): 43-58.

SPE (2006). Society of Petroleum Engineers website, http://www.spe.org/spe/jsp/basic/0,,1104_1732,00.html (19 Jan. 2006)

Snee, R.D. (1981). Developing blending models for gasoline and other mixtures. *Technometrics,* 23 (2): 119-130.

Symonds, G.H. (1955). *Linear Programming: The Solution of Refinery Problems.* NY: Standard Oil Company.

Szoke, R.W., and Kennedy, J.P. (1984) Optimizing Control of a Catalytic Reformer with Digital Instrumentation. *NPRA Computer Conference.* CC-84-117, 1-10, Cherry Hill, NJ.

Torczon, V. (1989). *Multi-Directional Search: A Direct Search Algorithm for Parallel Machines.* Ph.D. Thesis, Department of Mathematical Sciences, Rice University.

Oak Ridge National Laboratory (2004). Transportation Energy Data Book, 24th Edition. Center for Transportation Analysis, www-cta.ornl.gov/data/tedb24 (25 Mar. 2006)

Vermeer, P. J., Pedersen, C.C., Canney, W.M., & Ayala, J.S. (1996) Design and Integration Issues for Dynamic Blend Optimization. *NPRA Computer Conference*. CC-96-130, Atlanta, Georgia.

Vicente, L.N., and Calamai, P.H. (1994). Bilevel and Multilevel Programming: a Bibliography Review. *Journal of Global Optimization,* 6: 1-25.

Wächter, A. (2002). *An Interior Point Algorithm for Large-Scale Nonlinear Optimization with Applications in Process Engineering.* Ph.D. thesis, Department of Chemical Engineering, Carnegie Mellon University.

Wagler, R.M.. (2006) *Private communication.*

Warren, A.L. and Marlin, T.E. (2002). Constrained MPC under closed-loop uncertainty. *Proceedings of the 2004 American Control Conference,* 5: 4607-4612.

Winston, W.L. (1994). *Operations Research – Applications and Algorithms.* 3rd edition. California: Duxbury Press.

Williams, H.P. (1999). *Model Building in Mathematical Programming.* 4th Edition. England: John Wiley & Sons, Ltd.

Wittenmark, B. (2002). *Adaptive Dual Control.* In Unbehauen, H. (ed.): *Control Systems, Robotics and Automation.* Encyclopaedia of Life Support Systems, developed under the auspices of the UNESCO. Eolss Publishers, Oxford, UK.

Wright, M.H. (1996). Direct Search Methods: Once Scorned, Now Respectable. In D.F. Griffiths and G.A. Watson (eds.), *Numerical Analysis 1995*, 191-208, Addison-Wsley Longman, Harlow, UK.

Yip, W.S. and Marlin, T.E. (2001). Designing Plant Experiments for Real-Time Optimization Systems. *Control Engineering Practice*, 11 (8): 837-845.

Zahed, A.H., Mullah, S.A., and Bashir, M.D. (1993). Predict Octane Number for Gasoline Blends. *Hydrocarbon Processing*, 85-87.

Zhou G., Xiong, W., Zhang, S., Yao, Z., Zhang, W., and Wang, G. (2003). Investigation and technological optimisation of iron ore bedding and blending process. *Ironmaking & Steelmaking*, 30 (6): 461-466.

Zyngier, D., and Marlin, T.E. (2003). Monitoring, Diagnosing and Improving the Performance of Real-Time Optimization Systems. *8th International Symposium on Process Systems Engineering (PSE)*, 394-399.

Appendix A

Gasoline Blending Process

Blending is a very important process in, among others, petroleum processing, cement manufacturing and food processing. Because of its economic importance and relatively simple models, blending was one of the first applications of Closed-loop, Real-Time Optimization (CLRTO). As an example, CLRTO has been applied to commercial gasoline-blending processes since the 1960's (Birchfield, 2002). Gasoline blending was selected as the industrial example for this study because of the following reasons.

- The process can be modeled with reasonable accuracy using linear programming
- CLRTO has been applied to many gasoline blending processes
- The process has significant uncertainty in parameters that multiply variables, i.e., left-hand side coefficients in a linear program
- The process is economically important and has opportunity for further improvements via monitoring and diagnosis
- The process is representative of other CLRTO systems using an LP

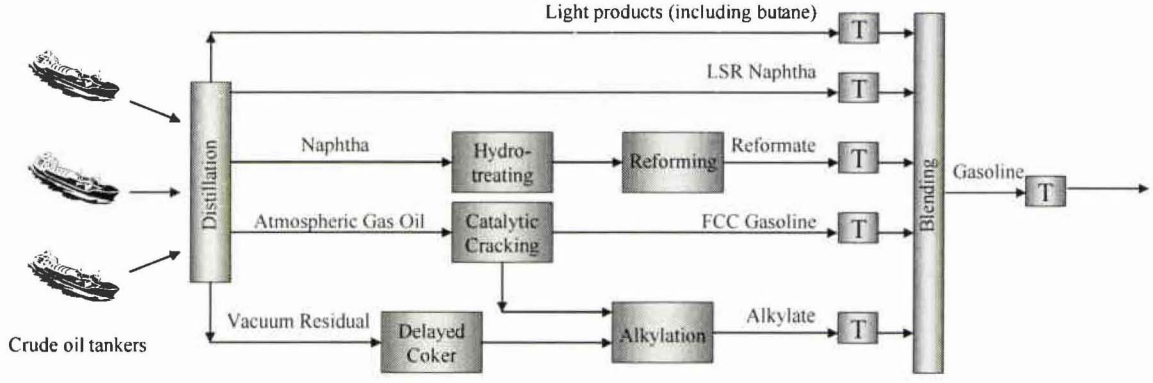

Figure A.1. Simplified Flowchart of an Oil Refinery (The tanks are indicated by a "T".)

A.1. Process Description

A simplified flowchart of a petroleum refinery is presented in Figure A.1, in which the five components for gasoline blending considered in this thesis are shown. The refinery makes many products, and only the gasoline is shown on the diagram. Some of the major process units are shown as blocks in the figure. Each block contains a very complex set of process equipment involving physical separation and in some cases, molecular modification by chemical reactions. The refinery operates continuously making material that is stored in the component tanks. The goal is to maintain constant qualities for materials going to component tanks, but this goal is not exactly achieved because of disturbances in crude composition and variability in process operating conditions. The potential for purchasing blending components from other companies also exists, and these import streams are not shown in Figure A.1. Gasoline product is made periodically by blending material from selected component tanks. The product is stored in a product tank after the blender and is shipped to a distribution point after the gasoline batch has been completed.

A typical gasoline blender may produce about 10,000 barrels of gasoline a day. At the price of $50/barrel, the revenues are at around $180 million a year. Even if only a very small improvement of 0.10% is made on this process, revenues will increase by roughly $180,000 a year, which is substantial. Because of its wide application and opportunity for high returns, gasoline blending was used as the case study in this work. However, the techniques developed here are applicable to many other LP-based closed-loop optimizations.

A.2. Modeling Assumptions

A batch gasoline-blending process is considered as the example process. The components Reformate, Light Straight Run (LSR) Naphtha, n-Butane, FCC Gasoline and Alkylate are blended to form the gasoline product. The properties of each component change due to variations in feed material and upstream process operation, but the

component properties do not change significantly during a batch because of the large component tanks. This blending process has very fast dynamics and reaches steady-state operation between CLRTO executions, which typically occur at every 15 minutes (Mudt, 2005). The gasoline batch process usually lasts anywhere from 8 to 16 hours. The resulting production of gasoline is stored in a product tank. Achieving instantaneous product quality specifications is not required: only the final outcome of the integrated blending batch in the product tank must satisfy the specifications. It is assumed that the mixing in the blend point is perfect by the use of static mixers (PetroMetrix, 2006), as well as that no change in specific gravity occurs during mixing (i.e., volume flows add linearly).

A typical gasoline-blending process has between 5 and 10 component streams (Arwikar *et al.*, 2002, Mudt, 2005), which are the variables adjusted for optimization. One key goal is the production rate, which is naturally the sum of the component flow rates. In addition, many product quality specifications must be satisfied, but only some product qualities are measured onstream, in real time, such as octane number and RVP (Zahed *et al.*, 1993, Arwikar *et al.*, 2002).

The two key component qualities measured onstream in this thesis were octane number and Reid vapour pressure (RVP). Octane numbers characterize the anti-knock properties of the fuel and can be calculated as the arithmetic mean between motor octane number (MON) and research octane number (RON). Anti-knock is the characteristic of a fuel to resist premature detonation when exposed to high pressures and temperatures in the combustion chamber of an engine. MON represents the engine anti-knock performance under severe operating conditions, while RON represents the engine anti-knock performance under mild conditions of operation (ASTM D-2699, ASTM D-2700). RVP is also a very important property of the fuel, since it affects engine startup and warmup, and the tendency to vapour lock under high operating temperatures or high altitudes (ASTM D-323). Vapour lock occurs whenever gas bubbles block the flow of fuel to the carburetor.

Gasoline blending is a (mildly) nonlinear process (Singh *et al.*, 2000). However, a linear model can be formulated when (1) blending indices compensate for some nonlinearities (Gary and Handwerk, 1984), (2), the component flow ratios remain within established limits where the blending indices provide acceptable accuracy and (3) models are formulated using flow-quality units (Williams, 1999). If the flow ratios vary significantly from a priori estimates, the linear model can be modified and the LP resolved, until sufficient accuracy is achieved; this would be a form of sequential LP (SLP). For the moderate changes typically made by an online optimizer, CLRTO blending is typically implemented as a linear program (Zahed *et al.*, 1993; Diaz and Barsamian, 1996; Vermeer *et al.*, 1996). The choice of linear programming is strongly affected by the need for a very reliable optimization calculation in the closed-loop optimization. Therefore, qualities are assumed to blend linearly in this thesis.

$$F_{blend}\left(Q^j_{blend}\right)_{max} \geq \sum_{i=1}^{n} F_i Q_i^j \qquad j = oct,\ RVP \qquad \text{(A.1a)}$$

$$F_{blend}\left(Q^j_{blend}\right)_{min} \leq \sum_{i=1}^{n} F_i Q_i^j \qquad \text{(A.1b)}$$

$$Q^j_{blend} \leq \left(Q^j_{blend}\right)_{\max} \qquad \text{(A.1c)}$$

$$Q^j_{blend} \geq \left(Q^j_{blend}\right)_{\min} \qquad \text{(A.1d)}$$

$$\text{where } F_{blend}\left(Q^j_{blend}\right) = \sum_{i=1}^{n} F_i Q_i^j \qquad \text{(A.1e)}$$

The flow-quality formulation of blending is seen in the set of equations (A.1) (Williams, 1999), where n is the number of components. The equality constraint in equation (A.1e) contains a nonlinear term because the flowrate and quality of the product are variables. However, the linear inequalities in equations (A.1a) and (A.1b) are equivalent and can be used to impose the same relationships as equations (A.1c) and (A.1d) in a linear program.

The Chevron blending index (Gary and Handwerk, 1994) is used to predict the RVP of blended products through a linear combination of the RVP blending indices (*RVPBI*) shown below.

$$RVPBI = RVP^{1.25} \tag{A.2}$$

$$F_{blend}\left(RVPBI_{blend}\right) = \sum_{i=1}^{n} RVPBI_i F_i \tag{A.3}$$

The gasoline-blending process has important uncertainty in the parameters, specifically the unmeasured component qualities, since the components are either purchased or come from upstream operations, which have variable operating conditions. In this thesis, the effects of changes in component qualities of streams entering the tanks are considered insignificant over the time when the monitoring and diagnosis are performed. This is a reasonable assumption, since components are stored in very large tanks, which are assumed to be well mixed. The effect of heels in the product tank is not considered explicitly; however, in practice it simply affects the targets for the specifications at the blending point before the product tank.

If most component properties were measured accurately and without fault, there would be much reduced need for a performance assessment of the CLRTO system. However, quality analyzers are quite expensive (roughly US$ 300,000 for each Near Infra-Red analyzer, which should be placed on each component stream) (Measurementation Inc., 2004). Therefore, component properties are only measured off-line very infrequently (once a week or even once a month) (Mudt, 2005; Kelly, 2006). Nevertheless, production from the plant flows into the component tanks continuously. Therefore, mismatch between model and plant parameters is likely, making this a very good case study for the methods developed in this work.

The available measurements are considered to be the final gasoline octane number and RVP properties and the flowrates for all streams. It is assumed that samples taken for onstream analysers are representative. The accuracy of the octane and RVP measurements are considered to be ±0.2 octane and ±0.15 psi, respectively, which

correspond to the legal requirements for spark-ignition engine fuels (ASTM D-323; ASTM D-2699; ASTM D-2700).

Turbine flowmeters are often used in gasoline-blending processes because of their better accuracy and wider range than standard orifice flow meters (Mudt, 2005). Their principle of operation is that the speed of rotation of a turbine within the meter is proportional to the volumetric flowrate through the pipe. This type of flowmeter has a typical accuracy of ±0.5% of the actual (flow)rate (*AR*) over a 10:1 flow range (Omega, 2005); that is, this accuracy is valid for flowrates from 10-100% of the largest flowrate.

A.3. Blending Model

The behaviour of the "true" gasoline blending model can be seen described by the following set of linear equations:

$$\sum_{i=1}^{n} F_{i,true} Q_i^{j,plant} \geq Q_{blend,min}^{j} \sum_{i=1}^{n} F_{i,true} \qquad j = oct,\ RVP \qquad (A.4)$$

$$\sum_{i=1}^{n} F_{i,true} Q_i^{j,plant} \leq Q_{blend,max}^{j} \sum_{i=1}^{n} F_{i,true} \qquad (A.5)$$

$$F_{blend,min} \leq \sum_{i=1}^{n} F_{i,true} \leq F_{blend,max} \qquad (A.6)$$

$$0 \leq F_{i,true} \leq F_{i,max} \qquad (A.7)$$

Therefore, the "true" plant optimum for this system would be to maximize the objective function (profit): $\sum_{i=1}^{n} (value - cost_i) F_{i,true}$ subject to the constraints (A.4) to (A.7).

A.4. Blending Model Uncertainty Description

For most of the case studies in the thesis, the octane and RVP properties of each of the five component streams were assumed uncertain, giving ten uncertain parameters. Two uncertainty descriptions were used, ellipsoidal and interval. The uncertainty was taken symmetrically around the nominal parameter values.

- For cases with interval description of uncertainty, bounds of ± 1.0 (octane or psi) were used. (Szoke and Kennedy. 1984, Mudt, 2005)
- For cases with ellipsoidal description of uncertainty, the largest variation possible at the 95% confidence level for any parameter in the ellipse was taken to be ±1.0 (octane or psi). Therefore, the uncorrelated variances of each of the ten parameters were calculated as $1/\chi^2_{0.95,10} = 0.0546$ (octane^2 or psi^2). Any different values for parameter uncertainty are defined in the chapters where the cases are presented.

In Chapters 3 through 5, several case studies are presented. Cases with two and ten uncertain parameters are shown, as well as examples with interval and ellipsoidal uncertainty description. The different results and computational experience are discussed as the case studies are presented.

Regardless of the octane and RVP specifications, the typical optimum lies at the maximum RVP and minimum octane. However, depending on the individual properties, different combinations of components could meet the specifications. Due to different component properties between blends, the results of specific case studies could change. This justifies the need for implementing optimization online, rather than simply analyzing the system once offline.

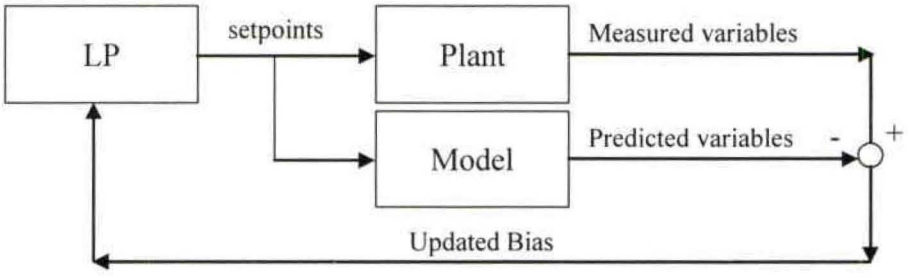

Figure A.2. MPC Structure

A.5. Model Predictive Control Structure

As mentioned in Chapter 1, the CLRTO systems considered in this work have a Model-Predictive Control (MPC) structure (Qin and Badgewell, 2003). This structure calculates manipulated variable moves based on an estimate of future plant behaviour for a finite time horizon. Only the calculated change in manipulated variable for the first time increment is implemented. The controller repeats its calculations periodically, implementing a rolling horizon controller. For the blending process, the plant (and model) dynamics are fast compared with the controller execution; therefore, the controller performs an optimization of a steady-state model.

At each execution period, some process variables are measured, and the measurements are compared with the respective model predictions (Figure A.2). The difference between the measured and predicted variable values is the prediction of future disturbances. It is called the "bias" when the future disturbances are assumed to equal the current disturbances and the bias for each measured output is added to the model equations for that predicted output.

In the gasoline-blending problem, the "Plant" is equivalent to the problem in Section A.3. The updated bias in Figure A.2 is calculated as:

$$\varepsilon^j \sum_{i=1}^{n} F_{i,nom} = \sum_{i=1}^{n} F_{i,nom} \left(Q_i^{j,plant} - Q_{i,nom}^{j} \right) \qquad j = oct,\ RVP \qquad (A.8)$$

Finally, the "LP" in this case corresponds to the following problem:

$$\max_{F_{i,nom}} \sum_{i=1}^{n} (value - cost_i) F_{i,nom} \qquad (A.9)$$

s.t.

$$\sum_{i=1}^{n} F_{i,nom} (Q_{i,nom}^{j} + \varepsilon^{j}) \geq Q_{blend,min}^{j} \sum_{i=1}^{n} F_{i,nom}$$

$$\sum_{i=1}^{n} F_{i,nom} (Q_{i,nom}^{j} + \varepsilon^{j}) \leq Q_{blend,max}^{j} \sum_{i=1}^{n} F_{i,nom}$$

$$F_{blend,\min} \leq \sum_{i=1}^{n} F_{i,nom} \leq F_{blend,\max}$$

$$0 \leq F_{i,nom} \leq F_{i,\max}$$

The flowrates $F_{i,nom}$ obtained from solving the LP in problem (A.9) are the setpoints that are sent to the controllers in the plant.

A.6. Nominal Parameter Values in Case Studies

The nominal values for the blending model and economics are presented in here. These are the values used in the CLRTO. The monitoring calculations use the uncertainty descriptions described in Section A.4. The true plant blending component qualities were taken to be different from the nominal, using either an interval or ellipsoidal range that has the nominal values as the midpoint. The uncertainty descriptions for each case are described with the cases in the body of the thesis.

The values for all model and plant parameters are shown in the following tables. Currency denoted by $ corresponds to US Dollars. Barrels are units often used in the oil industry, even in countries using SI units. One barrel (bbl) corresponds to approximately 0.159 m^3 or 159 liters (SPE, 2006).

Table A.1. Production Requirements

value	($/bbl)	33.0
$F_{blend,min}$	(bbl/day)	6,999.0
$F_{blend,max}$	(bbl/day)	7,000.0
$Q^{oct}_{blend,\min}$	(octane)	88.5
$Q^{oct}_{blend,\max}$	(octane)	100.0
$Q^{RVP}_{blend,\min}$	(psi)	4.5
$Q^{RVP}_{blend,\max}$	(psi)	10.8

Table A.2. Component Availability and Cost

Components	$F_{i,,min}$ (bbl/day)	$F_{i,,max}$ (bbl/day)	$cost_i$ ($/bbl)
Reformate	0.0	12,000.0	33.8
LSR Naphtha	0.0	6,500.0	26.0
N-Butane	0.0	3,000.0	10.3
FCC Gasoline	0.0	4,500.0	31.3
Alkylate	0.0	7,000.0	37.0

Table A.3. Plant Component Quality Data

Components	$Q^{oct}_{i,nom}$ (octane)	$Q^{RVP}_{i,nom}$ (psi)
Reformate	93.1	2.7
LSR Naphtha	64.3	10.9
N-Butane	92.5	138.0
FCC Gasoline	84.6	6.4
Alkylate	96.6	6.7

The values in Table A.1 and in Table A.2 were taken from Forbes and Marlin (1994). The gasoline production rate was bounded between 6,999-7000 bbl/day in order to achieve a practically constant gasoline production rate. All case studies led the system to the upper flowrate bound $F_{blend,max}$ because the objective of the CLRTO was to achieve the highest operation profit, which in the case studies considered in this work, corresponded to the highest gasoline production rate. The component qualities in Table A.3 were calculated based on the tables in Gary and Handwerk (1984).

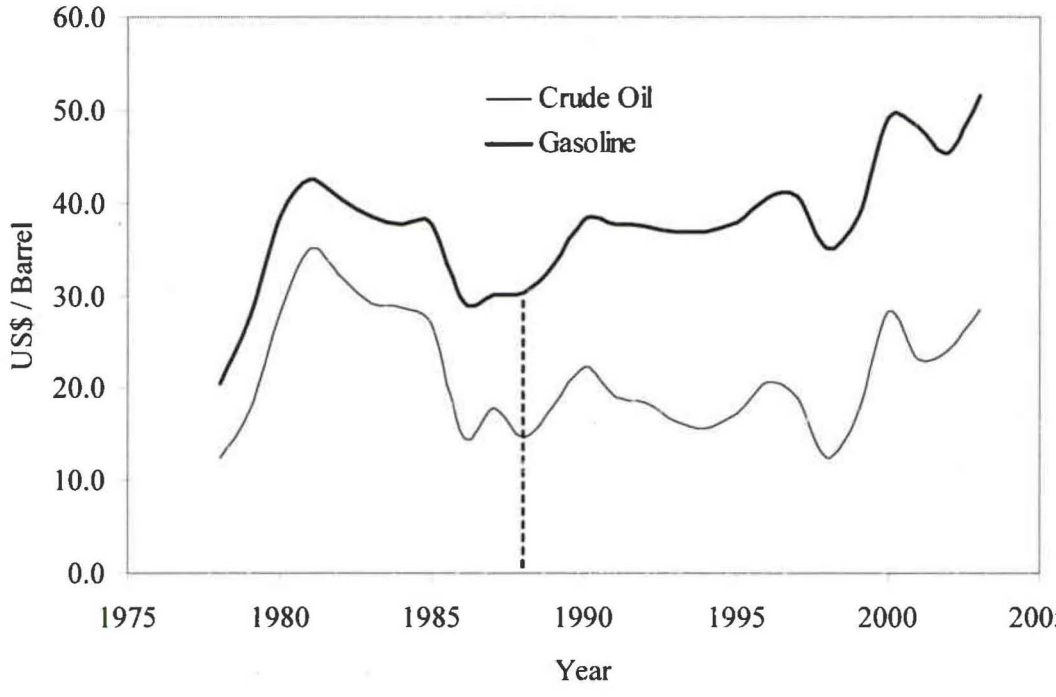

Figure A.3. Pricing of Crude Oil and Gasoline (CTA, 2006)

The price of petroleum crude oil and products is volatile (see Figure A.3). The case study provides consistent economics for 1988 when the crude price was $14.7/bbl. Therefore, the question arises regarding whether the case studies are characteristic of typical situations, or specific to a particular time. The prices of all components and gasoline are essentially proportional to the cost of crude oil. Therefore, volatility in pricing changes all cost coefficients by approximately the same factor, which would require multiplying the LP objective function by a constant (for example, doubling crude cost would incur in multiplying the objective function by 2). Consequently, the results for the case studies regarding multiple bases, importance of parameters and experimental designs would be unaffected by pricing volatility, since the economic effect of any improvement would be multiplied by the same constant as the objective function. However, other changes that affect only individual components or the gasoline price could change the results of case studies. This, along with frequently changing bounds on

component flow rates and model mismatch, justifies the need for implementing the performance evaluations online, rather than simply analyzing offline for one single time and scenario.

Appendix B
Bayesian Parameter Estimation

In traditional parameter estimation literature (Montgomery and Runger, 1994), it is assumed that there is enough data available in order to estimate parameters and their variances. At the beginning of a blending batch, however, even though there are often vast amounts of historical data from previous batches, the current batch does not usually contain enough data points to obtain good estimates of model parameters.

In the gasoline-blending case study, the parameters that need to be estimated are the octane and RVP properties of each component. The quality equations can be expressed as:

$$Q_{blend}^{j} = \theta_{o}^{j} + \sum_{i=1}^{nc} Q_{i,nom}^{j} \frac{F_i}{\sum_{i_2=1}^{nc} F_{i_2}} \qquad (B.1)$$

where θ_0^j are the intercepts included in order to account for deviations from linearity.

Bayesian estimation (Box and Tiao, 1973) provides a framework in which informative prior parameter distributions can be used. Bayes' theorem states that the posterior distribution of a parameter will be equal to its prior distribution multiplied by the likelihood function, where the latter represents information that originates from experimental data. The inclusion of prior information prevents unnecessarily large experiments in the plant. In the case of gasoline blending, periodic lab samples are taken from the component tanks, and their properties are measured and stored in a database. Therefore, it is thus possible to obtain a good estimate of parameter uncertainty (historical variability) before data is first measured in the process. The parameter

estimation formulation derived from least-squares estimation and Bayesian theory is presented in the following equation (Reilly, 1973).

$$Q^{j}_{i,nom,t} = \left(V(Q)^{-1}\,|_{t-1} + X^{T}_{\exp} \mathrm{V}(z)^{-1} X_{\exp}\right)^{-1} \left(V(Q)^{-1}\,|_{t-1}\; Q^{j}_{i,nom,t-1} + X^{T}_{\exp} \mathrm{V}(z)^{-1} z\right) \qquad (B.2)$$

This formulation assumes zero mean, normal, randomly distributed measurement noise and no structural mismatch between model and plant. In equation (B.2), $V(Q)|_{t-1}$ is the matrix of parameter uncertainty from the previous time step, and $Q^{j}_{i,nom,t}$ and $Q^{j}_{i,nom,t-1}$ are the matrices with parameter estimates of the current and previous time steps (the parameter estimate $Q^{j}_{i,nom,t}$ at $t = 1$ uses the values of initial parameter estimates and their prior uncertainties).

The matrix X_{exp} containing input variables (in this case, flowrates) and the output (measurement) vector z are defined as:

$$z = \begin{bmatrix} Q^{oct}_{blend,meas} \\ Q^{RVP}_{blend,meas} \end{bmatrix}$$

And

$$X_{\exp} = \begin{bmatrix} 1 & \mathbf{NF} & 0 & \mathbf{0} \\ 0 & \mathbf{0} & 1 & \mathbf{NF} \end{bmatrix}$$

$$\mathbf{NF} = \begin{bmatrix} \dfrac{F_{Ref,\exp}}{\sum_i F_{i,\exp}} & \dfrac{F_{LSR,\exp}}{\sum_i F_{i,\exp}} & \dfrac{F_{nBut,\exp}}{\sum_i F_{i,\exp}} & \dfrac{F_{FCC,\exp}}{\sum_i F_{i,\exp}} & \dfrac{F_{Alk,\exp}}{\sum_i F_{i,\exp}} \end{bmatrix}$$

The ones in the X_{exp} matrix correspond to the intercepts θ_0^j that are included in the octane and RVP equations in the parameter estimation step. Since the "perfect" model is not known for the blending of octane and RVP properties, an intercept can be included in order to account for slight model mismatch. The effect of including the intercept in the quality equations is discussed through case studies in Chapter 5. The measurements (z) considered were the blend qualities. The remaining measured variables (flowrates) were

assumed to be known perfectly, which is reasonable for gasoline blending because the flows are measured using turbine meters or other highly accurate flow sensors (Mudt, 2005; Omega, 2005). V*(z)* is the variance-covariance matrix of the output variables (*z*). When using the method in equation (B.2), the parameter uncertainty can be shown to decrease with the experiments according to the following equation (Reilly, 1973).

$$V(Q) = \left(V(Q)|_{i-1} + X_{\exp}^{T} V(z)^{-1} X_{\exp}\right)^{-1} \qquad (B.3)$$

The judicious use of prior knowledge about the parameter distribution may reduce the number and/or magnitude of experimentation in the plant, especially in situations where not enough data points exist for a reasonable initial estimate of parameter uncertainty. By using the method in equation (B.3), parameter variance can only decrease at each update. If a parameter is assumed to have a much smaller variance than the measurement errors around an incorrect initial value, its estimate will likely not change considerably with the new updates (Box and Tiao, 1973). As a safeguard against underestimating prior parameter variance, a larger variance than estimated by prior historical data can be used.

Appendix C

Solution Details for Section 3.5

This appendix presents the solution details of Problem 3.6 for the CLRTO performance monitoring method based on the Expected Value of the Largest Profit Gap (Section 3.5). All of these solutions were obtained using IPOPT-C, with 10^{-8} tolerance. Note that the solution details for the case with $\alpha = 0.95$ is shown in Chapter 3 (Tables 3.11 – 3.13).

For all cases, $Q_i^{j,0} = Q_{i,nom}^j$. The following starting points for the flowrates were used:

Table C.1. Flowrate Starting Points

	$F_{i,1}^0$ $= (1/5)*F_{blend,max}$ (bbl/day)	$F_{i,2}^0$ = current CLRTO operation (bbl/day)
Reformate	1,400.0	5,695.6
LSR Naphtha	1,400.0	942.5
n-Butane	1,400.0	361.0
FCC Gas	1,400.0	0.0
Alkylate	1,400.0	0.0

C.1. Solution with $\alpha = 0.25$ and $dof = 10$ ($\chi^2_{0.25,10} = 6.737$)

Table C.2. Solution of Problem 3.6 - α = 0.25 and dof = 10

	Q_i^{oct} (octane numbers)	Q_i^{RVP} (psi)	$F_{i,BC}$ (bbl/day)	$F_{i,nom}$ (bbl/day)
Reformate	92.86	2.91	2,807 9	5,593.4
LSR Naphtha	64.20	10.98	0.0	1,061.0
n-Butane	92.50	138.00	317.0	345.6
FCC Gas	85.01	6.11	3,875.1	0.0
Alkylate	96.60	6.70	0.0	0.0
	$Maxgap_{ell}$	\$ 740.9 / day		
	Pr_{BC}	\$ 11,538.1 / day		
	$Pr_{nom,CL}$	\$ 10,797.2 / day		

Table C.3. Computational Results for Problem 3.6

Starting Points	CPU sec	# func. eval	# restarts	Solution
$F^0_{i,BC} = F^0_{i,nom} = F^0_{i,1}$; $\lambda^0_{BC} = \lambda^0_{nom} = \mathbf{0}$	3.781	8,056	4	Good
$F^0_{i,BC} = F^0_{i,nom} = F^0_{i,1}$; $\lambda^0_{BC} = \lambda^0_{nom} = \lambda_{nom}$	1.593	639	2	Good
$F^0_{i,BC} = F^0_{i,nom} = F^0_{i,2}$; $\lambda^0_{BC} = \lambda^0_{nom} = \mathbf{0}$	0.297	169	0	Bad
$F^0_{i,BC} = F^0_{i,nom} = F^0_{i,2}$; $\lambda^0_{BC} = \lambda^0_{nom} = \lambda_{nom}$	1.370	494	1	Good

C.2. Solution with $\alpha = 0.50$ and $dof = 10$ ($\chi^2_{0.50,10} = 9.342$)

Table C.4. Solution of Problem 3.6 - α = 0.50 and dof = 10

	Q_i^{oct} (octane numbers)	Q_i^{RVP} (psi)	$F_{i,BC}$ (bbl/day)	$F_{i,nom}$ (bbl/day)
Reformate	92.83	2.94	2,780.7	5,602.0
LSR Naphtha	64.18	10.99	0.0	1,053.6
n-Butane	92.50	138.00	317.0	344.4
FCC Gas	85.09	6.06	3,902.3	0.0
Alkylate	96.60	6.70	0.0	0.0
	$Maxgap_{ell}$	\$ 894.4 / day		
	Pr_{BC}	\$ 11,606.4 / day		
	$Pr_{nom,CL}$	\$ 10,711.9 / day		

Table C.5. Computational Results for Problem 3.6

Starting Points	CPU sec	# func. eval	# restarts	Solution
$F^0_{i,BC} = F^0_{i,nom} = F^0_{i,1}$; $\lambda^0_{BC} = \lambda^0_{nom} = \mathbf{0}$	12.217	48,733	7	Good
$F^0_{i,BC} = F^0_{i,nom} = F^0_{i,1}$; $\lambda^0_{BC} = \lambda^0_{nom} = \lambda_{nom}$	8.892	37,517	9	Good
$F^0_{i,BC} = F^0_{i,nom} = F^0_{i,2}$; $\lambda^0_{BC} = \lambda^0_{nom} = \mathbf{0}$	6.578	29,252	1	Bad
$F^0_{i,BC} = F^0_{i,nom} = F^0_{i,2}$; $\lambda^0_{BC} = \lambda^0_{nom} = \lambda_{nom}$	0.297	108	0	Bad

C.3. Solution with $\alpha = 0.75$ and $dof = 10$ ($\chi^2_{0.75,10} = 12.55$)

Table C.6. Solution of Problem 3.6 - $\alpha = 0.75$ and dof = 10

	Q_i^{oct} (octane numbers)	Q_i^{RVP} (psi)	$F_{i,BC}$ (bbl/day)	$F_{i,nom}$ (bbl/day)
Reformate	92.79	2.98	2,749.2	5,610.6
LSR Naphtha	64.17	11.00	0.0	1,046.2
n-Butane	92.50	138.00	317.0	343.2
FCC Gas	85.18	6.01	3,933.8	0.0
Alkylate	96.60	6.70	0.0	0.0
	$Maxgap_{ell}$	\$ 1,059.0 / day		
	Pr_{BC}	\$ 11,684.1 / day		
	$Pr_{nom,CL}$	\$ 10,625.2 / day		

Table C.7. Computational Results for Problem 3.6

Starting Points	CPU sec	# func. eval	# restarts	Solution
$F^0_{i,BC} = F^0_{i,nom} = F^0_{i,1}$; $\lambda^0_{BC} = \lambda^0_{nom} = \mathbf{0}$	2.687	7,181	2	Bad
$F^0_{i,BC} = F^0_{i,nom} = F^0_{i,1}$; $\lambda^0_{BC} = \lambda^0_{nom} = \lambda_{nom}$	0.313	178	0	Good
$F^0_{i,BC} = F^0_{i,nom} = F^0_{i,2}$; $\lambda^0_{BC} = \lambda^0_{nom} = \mathbf{0}$	5.781	20,974	3	Good
$F^0_{i,BC} = F^0_{i,nom} = F^0_{i,2}$; $\lambda^0_{BC} = \lambda^0_{nom} = \lambda_{nom}$	0.641	894	0	Bad

C.4. Solution with $\alpha = 0.90$ and $dof = 10$ ($\chi^2_{0.90,10} = 15.99$)

Table C.8. Solution of Problem 3.6 - $\alpha = 0.90$ and dof = 10

	Q_i^{oct} (octane numbers)	Q_i^{RVP} (psi)	$F_{i,BC}$ (bbl/day)	$F_{i,nom}$ (bbl/day)
Reformate	92.76	3.02	2,717.1	5,618.4
LSR Naphtha	64.15	11.01	0.0	1,039.6
n-Butane	92.50	138.00	316.9	342.0
FCC Gas	85.26	5.97	3,966.0	0.0
Alkylate	96.60	6.70	0.0	0.0
	$Maxgap_{ell}$	\$ 1,216.1 / day		
	Pr_{BC}	\$ 11,762.7 / day		
	$Pr_{nom,CL}$	\$ 10,546.6 / day		

Table C.9. Computational Results for Problem 3.6

Starting Points	CPU sec	# func. eval	# restarts	Solution
$F^0_{i,BC} = F^0_{i,nom} = F^0_{i,1}$; $\lambda^0_{BC} = \lambda^0_{nom} = \mathbf{0}$	2.797	4,409	3	Good
$F^0_{i,BC} = F^0_{i,nom} = F^0_{i,1}$; $\lambda^0_{BC} = \lambda^0_{nom} = \lambda_{nom}$	0.310	189	0	Good
$F^0_{i,BC} = F^0_{i,nom} = F^0_{i,2}$; $\lambda^0_{BC} = \lambda^0_{nom} = \mathbf{0}$	0.812	333	1	Bad
$F^0_{i,BC} = F^0_{i,nom} = F^0_{i,2}$; $\lambda^0_{BC} = \lambda^0_{nom} = \lambda_{nom}$	1.577	2,408	1	Bad

C.5. Solution with $\alpha = 0.99$ and $dof = 10$ ($\chi^2_{0.99,10} = 23.21$)

Table C.10. Solution of Problem 3.6 - $\alpha = 0.99$ and dof = 10

	Q_i^{oct} (octane numbers)	Q_i^{RVP} (psi)	$F_{i,BC}$ (bbl/day)	$F_{i,nom}$ (bbl/day)
Reformate	92.71	3.08	2,653.0	5,631.3
LSR Naphtha	64.13	11.03	0.0	1,028.7
n-Butane	92.51	138.00	316.7	339.9
FCC Gas	85.41	5.89	4,030.3	0.0
Alkylate	96.60	6.70	0.0	0.0
	$Maxgap_{ell}$	\$ 1,505.3 / day		
	Pr_{BC}	\$ 11,917.8 / day		
	$Pr_{nom,CL}$	\$ 10,412.5 / day		

Table C.11. Computational Results for Problem 3.6

Starting Points	CPU sec	# func. eval	# restarts	Solution
$F^0_{i,BC} = F^0_{i,nom} = F^0_{i,1}$; $\lambda^0_{BC} = \lambda^0_{nom} = \mathbf{0}$	2.516	4,350	1	Good
$F^0_{i,BC} = F^0_{i,nom} = F^0_{i,1}$; $\lambda^0_{BC} = \lambda^0_{nom} = \lambda_{nom}$	0.984	418	1	Good
$F^0_{i,BC} = F^0_{i,nom} = F^0_{i,2}$; $\lambda^0_{BC} = \lambda^0_{nom} = \mathbf{0}$	3.109	3,858	10	Bad
$F^0_{i,BC} = F^0_{i,nom} = F^0_{i,2}$; $\lambda^0_{BC} = \lambda^0_{nom} = \lambda_{nom}$	0.250	87	0	Bad

Appendix D

Summary of Optimization Technology

In order to assess, diagnose and enhance the closed-loop performance of RTO systems, this thesis relies heavily on optimization theory and specific software implementations. In this appendix, optimization methods that are the most relevant to this work are presented.

Small linear programming (LP) problems were solved in the closed-loop RTO simulations. To solve these problems, the (default) primal simplex algorithm in CPLEX was used in the GAMS modeling environment. The primal simplex algorithm is one in which the simplex tableau is generated for the primal optimization problem.

The formulations in this work generated different types of nonlinear programming (NLP) problems. A very efficient algorithm to solve NLPs is Sequential Quadratic Programming (SQP). SQP is used in this thesis (in Matlab's *fmincon* function). Therefore, Section D.1 presents an introduction to this optimization method.

In optimization literature, there is a class of optimization problems called Mathematical Programs with Equilibrium Constraints (MPECs). These problems contain constraints of the form $x.y = 0$, also known as *complementarity* constraints. This type of constraint poses a significant challenge to active-set optimization methods, since they render the feasible region nonconvex and even disjoint, and they cause the problem to be ill-conditioned (Raghunathan and Biegler, 2003). Due to the combinatorial nature of active-set methods (such as the one used within standard SQP methods), active set methods do not usually perform well for MPECs. Therefore, interior-point solvers such as IPOPT are more appropriate for this class of problems. Section D.2 presents IPOPT

and its version tailored to handle MPECs (IPOPT-C), which are based on an interior path-following, interior-point method.

The experimental design formulations in Chapter 4 contained gradient evaluations that did not have smooth properties. These formulations required the solution of three-level optimization problems. While the solutions of bilevel optimization were achieved using the IPOPT-C, this software did not reliably solve the three-level problems. Hence, a direct search method was used to solve the outer problem. The selected approach was the Derivative-Free Optimization (DFO) method developed by Conn *et al.* (1996) and implemented in MATLAB by Fan (2002). An overview of this method can be seen in Section D.3.

A Pentium 4, 1700MHz, 523 Gb was used in the simulations. All problems in the thesis were solved to the 10^{-8} tolerance levels of IPOPT-C (version 2.0.1) solver. In *fmincon* (Mathworks, 1999) (in Matlab version 6.5.0.180913a Release 13), tolerances of 10^{-3} for constraint violations and absolute values of the variables and objective function values were set. AMPL was used for the modeling environment for problems solved using IPOPT-C. It provides first and second derivatives through symbolic processing. An overview of the software structure used in the various simulations can be see in Section D.4.

D.1. Sequential Quadratic Programming

Sequential Quadratic Programming (SQP) has been successfully applied to nonlinear constrained optimization problems with continuous first- and second-order derivatives. It is based on solving a quadratic program, i.e., an optimization problem with a quadratic objective function and linear constraints. Consider the following nonlinear optimization problem (Nash and Sofer, 1996):

$$\begin{aligned} &\min f(x) \\ &\text{s.t} \quad h(x) = 0 \end{aligned} \tag{D.1}$$

where $f(x)$ and $h(x)$ are nonlinear functions. The Lagrangian $L(x,\lambda)$ for problem **(D.1)** is given by:

$$L(x,\lambda,\mu) = f(x) - \lambda^T h(x) \qquad (D.2)$$

The first-order optimality conditions of problem (D.1) can be expressed as a function of the derivatives of the Lagrangian, as can be seen below.

$$\nabla_x L(x,\lambda) = \nabla_x f(x) - \lambda \nabla_x h(x) = 0 \qquad (D.3)$$

$$\nabla_\lambda L(x,\lambda) = -h(x) = 0 \qquad (D.4)$$

Newton's method can be applied to find a solution to equations (D.3) and (D.4). This method can be expressed as:

$$\begin{pmatrix} x_{k+1} \\ \lambda_{k+1} \end{pmatrix} = \begin{pmatrix} x_k \\ \lambda_k \end{pmatrix} + \begin{pmatrix} \Delta x_k \\ \Delta \lambda_k \end{pmatrix} \qquad (D.5)$$

The updates Δx_k and $\Delta \lambda_k$ are obtained as follows. For a problem of the form:

$$\min f(x) \qquad (D.6)$$

The (full) Newton step is given by

$$x_{k+1} = x_k - \frac{\nabla f(x)}{\nabla^2 f(x)} \qquad (D.7)$$

Therefore, when applying the Newton step in equation (D.7) to the system of equations (D.5), the following relationship is obtained:

$$\nabla^2 L(x_k, \lambda_k)\begin{pmatrix}\Delta x_k \\ \Delta \lambda_k\end{pmatrix} = -\nabla L(x_k, \lambda_k) \qquad (D.8)$$

This is equivalent to expressing the linear system as:

$$\begin{pmatrix}\nabla^2_{xx} L(x_k, \lambda_k) & -\nabla h(x_k)^T \\ -\nabla h(x_k)^T & 0\end{pmatrix}\begin{pmatrix}\Delta x_k \\ \Delta \lambda_k\end{pmatrix} = \begin{pmatrix}-\nabla_x L(x_k, \lambda_k) \\ h(x_k)\end{pmatrix} \qquad (D.9)$$

The system of equations in (D.9) corresponds to the first-order optimality conditions of the following optimization problem.

$$\min_{\Delta x_k} \frac{1}{2}\Delta x_k^T\left[\nabla^2_{xx} L(x_k, \lambda_k)\right]\Delta x_k + \Delta x_k^T\left[\nabla_x L(x_k, \lambda_k)\right] \qquad (D.10)$$
$$\text{s.t} \quad \left[\nabla h(x)\right]^T \Delta x_k + h(x_k) = 0$$

In problem (D.10), it is possible to see that the objective function is a Taylor series approximation of the Lagrangian at (x_k, λ_k), and the constraints are linear approximations of the original constraints in problem (D.1). The vector $\Delta\lambda_k$ corresponds to the Lagrange multipliers of problem (D.10). At each SQP iteration, problem (D.10) is solved using a quadratic programming approach (QP) with an active set or barrier method, and yields the updates (Δx_k, $\Delta\lambda_k$). In the case of a problem with inequality constraints $g(x) \geq 0$, problem (D.10) can be expressed as:

$$\min_{\Delta x_k} \frac{1}{2}\Delta x_k^T\left[\nabla^2_{xx} L(x_k, \lambda_k)\right]\Delta x_k + \Delta x_k^T\left[\nabla_x L(x_k, \lambda_k)\right] \qquad (D.11)$$
$$\text{s.t} \quad \begin{aligned}&\left[\nabla h(x)\right]^T \Delta x_k + h(x_k) = 0 \\ &\left[\nabla g(x)\right]^T \Delta x_k + g(x_k) \geq 0\end{aligned}$$

SQP is the basis of the nonlinear solver *fmincon* found in Matlab (Mathworks, 1999). An active-set method is used to solve the QP; *i.e.*, only the equality constraints

and active inequality constraints (at the current iterate) from problem (D.11) are considered in the iteration. In active-set methods, an equality-constrained problem based on the current active set is solved at each iteration. If a constraint is encountered during the course of a line search when optimizing this problem, it is added to the constraint set for the following iteration. After optimizing the equality-constrained problem, the Lagrange multipliers for all constraints in the active set of the current iteration are computed at the solution. If there are no negative multipliers, the solution is also deemed to be a solution to the original inequality-constrained problem. If there is a negative Lagrange multiplier, the corresponding constraint is removed from the active set for the following iteration (Nash and Sofer, 1996).

The *fmincon* line search uses a merit function, which is described in Han (1977). The basic idea is to find a step size that leads to a point that will both improve the objective function value and reduce the constraint violations (expressed as exact penalty functions) in the QP. In this particular implementation, the exact penalty function is defined as the l_∞-norm. The Hessian information in *fmincon* is obtained from BFGS updates.

D.2. Interior-Point Methods

Interior-point methods have been developed since the 1980's in order to provide an efficient polynomial-time method for solving mathematical programming problems (Nash and Sofer, 1996). A crucial aspect of these methods is that all points generated by interior-point methods leading to the optimal solution are strictly feasible; i.e., they satisfy all model constraints.

Barrier functions are very useful for solving constrained optimization problems, and they are sometimes adopted in interior-point algorithms. Consider the following constrained optimization problem.

$$\begin{aligned} &\min f(x) \\ &\text{s.t} \quad g(x) \geq 0 \end{aligned} \qquad (D.12)$$

The constrained problem is replaced by an approximate unconstrained problem; this is achieved by replacing the constraints $g(x) \geq 0$ with additional terms in the objective function that become very large as the functions $g(x)$ approach their bounds and are unbounded in the limit of attaining a bound from the interior of the set. Two common types of barrier functions are (1) the logarithm and (2) the inverse of $g(x)$. The reformulation of problem (D.12) using the logarithmic barrier function is seen below.

$$\min_x \left[f(x) - \mu \sum_{i=1}^{nc} \log(g_i(x)) \right] \qquad \text{(D.13)}$$

In problem (D.13), *nc* is the number of constraints and μ is called the barrier parameter. An option in solving the original problem (D.12) is to reduce μ after each solution of the unconstrained optimization problem (D.13) until μ is sufficiently close to zero. As μ decreases, a differentiable solution trajectory $x(\mu)$ (also known as *barrier trajectory*) is formed.

The existence of this barrier trajectory $x(\mu)$ enables the development of central path-following algorithms. In these methods, iterates stay close to the barrier trajectory. The steps of the path-following interior-point algorithm with a barrier sub-problem can be summarized as follows (Nash and Sofer, 1996):

Step 1. Update the barrier parameter $\mu_k \rightarrow \mu_{k+1}$

Step 2. Solve the barrier subproblem (D.13) so that the point x_k is close enough to the path (given a stopping criterion)

Step 3. Use a damped Newton Method to update $x_k \rightarrow x_{k+1}$

Step 4. Go to Step 1 until a convergence criterion is met for the path-following method.

In this thesis, IPOPT (Wächter, 2002) was used to solve several of the nonlinear formulations in Chapters 3, 4 and 5. In IPOPT, the primal-dual interior-point barrier method is used. It is based on finding feasible solutions for both the primal and the dual optimization problem equations simultaneously using a Newton-type approach (Wächter, 2002). The existence of the barrier parameter in the original problem relaxes the complementarity constraints to the form $x.\lambda = \mu$, where x and λ are the primal and dual variables, respectively.

After a search direction has been found by the primal-dual method, it is necessary to determine the size of the step that should be taken by the iterate in that direction, since a full Newton step may be too large and render the next iterate infeasible. Merit functions can be used in determining the step length. The underlying strategy in this method is to extend the original objective function to include an additional term that penalizes infeasibility in the constraints. This penalty term may be, for instance, exact penalty functions such as the l_1-, l_2- or l_∞-norms. Another method for finding step lengths are filter line searches. The filter line search in IPOPT ensures that the new point improves the original objective function *or* the constraint violations (instead of requiring both, as in merit function approaches). With this filter line search procedure, IPOPT has been proven to be globally convergent to a stationary point (Wächter, 2002).

More recently, Raghunathan and Biegler (2003) developed IPOPT-C, an enhancement to IPOPT that handles complementarity constraints. In their work, Raghunathan and Biegler (2003) relaxed the complementarity constraints to $x.\lambda \leq \delta\mu$, where $\delta > 0$ is a fixed constant and $\mu > 0$ is the barrier parameter which was successively tightened until sufficiently close to zero (within a user-specified tolerance). It was shown that the conditioning of the overall problem was greatly improved by this reformulation.

D.3. Derivative-Free Optimization (DFO)

DFO is based on approximating the objective function by a (simpler) smooth, quadratic surrogate model within a trust region, and then optimizing the surrogate model to obtain an improved point. Fitting a surrogate model smoothes the discontinuities in the derivatives of the function, while retaining the dominant local characteristics of the response surface of the original problem.

Given a set of interpolation points $Y=\{y_j\}, j = 1..p$, the surrogate function $Q(x)$ can be considered an interpolation of the original function $f(x)$ if the following holds (Scheinberg, 2000):

$$Q(y_j) = f(y_j), \qquad j = 1..p \tag{D.14}$$

Suppose that $\phi(x)$ is a basis in the space of quadratic polynomials (in the one-dimensional space, $\phi(x)$ could be equal to $\{1, x, x^2\}$). The equality in equation (D.14) can then be expressed as

$$Q(y_j) = \sum_{i=1}^{q} \alpha_i \phi_i(y_j) = f(y_j), \quad j = 1..p \tag{D.15}$$

where q is the number of terms in the basis for the n-dimensional space. The coefficient matrix of the system of equations (D.15) is:

$$\Phi(Y) = \begin{bmatrix} \phi_1(y_1) & \cdots & \phi_q(y_1) \\ \vdots & & \vdots \\ \phi_1(y_p) & \cdots & \phi_q(y_p) \end{bmatrix} \tag{D.16}$$

The linear system of equations (D.15) has a unique solution for $\alpha = (\alpha_1, \ldots, \alpha_q)$ if the coefficient matrix in equation (D.16) is square and nonsingular. The procedure for implementing DFO can be summarized as follows (Conn *et al.*, 1997; Scheinberg, 2000):

Step 1. Build a surrogate model around the current point using the current interpolation set Y_k and the current trust region radius Δ_k. Determine which of the original starting points has the best objective function value by evaluating:

$$f(x_0) = \min_{yi \in Y} f(y_i)$$

Step 2. Build the surrogate model $Q_k(x)$ from the interpolation set Y and solve the optimization problem using the surrogate model within the trust region ($\| \hat{x}_k - x_k \| \leq \Delta_k$) to obtain $\hat{x}_k$. Then, compute the ratio:

$$\rho_k = \frac{f(x_k) - f(\hat{x}_k)}{Q_k(x_k) - Q_k(\hat{x}_k)}$$

Step 3. Update the interpolation set $Y_k \rightarrow Y_{k+1}$. Depending on the value of ρ_k and the number of points currently available in the set, $\hat{x}_k$ is included into the interpolation set Y and one of the existing points is dropped from the set, if necessary.

Step 4. Update the trust-region radius $\Delta_k \rightarrow \Delta_{k+1}$. Also depending on the value of ρ_k, the trust region may be expanded, contracted, or remain the same. If the iteration generated a large enough ratio ρ_k, accept the new point and increase the size of the trust region. If the ratio ρ_k was too small, reject the iterate and decrease the size of the trust region.

Step 5. Update the current iterate. Determine the new point $\underline{x}_k$ with the best objective function value $f(\underline{x}_k) = \min_{yi \in Y,\ yi \neq xk} f(y_i)$, and recalculate

$$\underline{\rho}_k = \frac{f(x_k) - f(\underline{x}_k)}{Q_k(x_k) - Q_k(\hat{x}_k)}$$

If the improvement in is deemed sufficient ($\underline{\rho}_k$ is large enough), $x_{k+1} = \underline{x}_k$. If not, $x_{k+1} = x_k$.

Step 6. Set $k = k+1$ and return to Step 1 until convergence

The main challenge in the DFO algorithm is in Step 3: updating the interpolation set Y that is used to obtain the polynomial surrogate model. This is because, depending on which point is removed from the interpolation set, the coefficient matrix in equation (D.16) may become ill-conditioned.

Two of the approaches for maintaining or improving the poisedness of the interpolation set Y are by using the Lagrange interpolation polynomials (LIP) or the Newton fundamental polynomials (NFP). A poised set X is defined for a given subspace of polynomials if, at the points X, the original function can be interpolated uniquely by polynomials from this subspace. A well-poised set is defined as one that remains poised under small perturbations; i.e., one that will yield a well-conditioned coefficient matrix for the surrogate model (Fan, 2002).

The idea behind both approaches is to maintain or improve the geometric properties of the set Y even when modifications are made to it. The LIP approach is based on comparing the determinant of the coefficient matrix in equation (D.16) using the current interpolation set with the one using the new iterate. The geometry of Y is deemed adequate when all the points in Y are within $2\Delta_k$ of the new iterate x_k, and when the determinant of (D.16) cannot be doubled by replacing one of the points in the set with another which is distant from x_k by a value of Δ_k. This approach is a trust-region problem in itself, and therefore is computationally very demanding (Conn *et al.*, 1997).

The NFP approach, on the other hand, does not require an optimization subproblem, and therefore is not as computationally intensive as LIP. It is based on creating or updating a polynomial basis function and checking if the normalization step within the procedure generates a zero pivot for the current iterate. If no zero pivots exist, the iterate is included, and the set is deemed well-poised. Another main difference between LIP and NFP is that the first requires the entire set of polynomials to be built at each iteration, whereas the latter enables the user to simply update the polynomial set (Conn *et al.*, 1997).

DFO has been shown to be globally convergent to a local optimum and to be computationally cheaper than other direct search methods, such as the Parallel Direct Search method (Torczon, 1991) and Nelder Mead simplex methods (Wright, 1996; Conn *et al.*, 1996). Because it is not a derivative-based optimization method, DFO is very robust to process noise, which is very common in process-related problems, until the trust region radius approaches the noise levels. Because of its better performance with respect to other direct-search methods, DFO was applied to the experimental design formulations in this thesis.

DFO addresses unconstrained optimization of continuous variables. Since constraints are not considered in the algorithm, they were included by using introducing (external) penalty functions in the objective for constraint violations. Care should be taken when choosing penalty weights for a particular problem, since ill-conditioning can result when the penalty weights are too large (Nash and Sofer, 1996). In this work, values for these weights were found by trial and error that gave reasonable optimization performance.

D.4. Software Structure

This section gives an overview of the software structure used to solve the formulations in this thesis.

Closed-Loop RTO Simulations

The simulations for CLRTO were done within GAMS using the "LOOP" function. For Monte Carlo simulations, the GAMS/MATLAB interface was used. (Figure D.1).

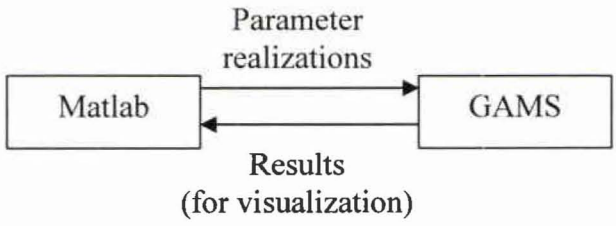

Figure D.1. Framework for Monte Carlo Simulations

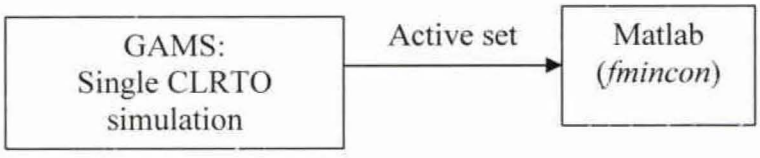

Figure D.2. Framework for Monitoring: Number of Corner Points

Monitoring: Approach Based on the Number of Corner Points

The monitoring approach based on the number of corner points used the Matlab/GAMS interface to automatically provide the active set based on the nominal parameter values to determine active set (Figure D.2).

Monitoring: $MaxGap_{int}$, $MaxGap_{ell}$, $E(MaxGap_{ell})$, $E(Gap)$

All monitoring approaches based on the profit gap were calculated in AMPL, using IPOPT-C as a solver. The approaches based on expected value consisted in solving the $MaxGap_{ell}$ problem in AMPL a few times, which was done manually.

Performance diagnostics / Ranking parameters

The CLRTO performance diagnostics method was solved in AMPL, using IPOPT-C as a solver.

Experimental Design:

The experimental design calculations for the model-based method were done in AMPL, using IPOPT-C as a solver. A Matlab implementation of the DFO method (Fan, 2002) was used for the other experimental design strategy.

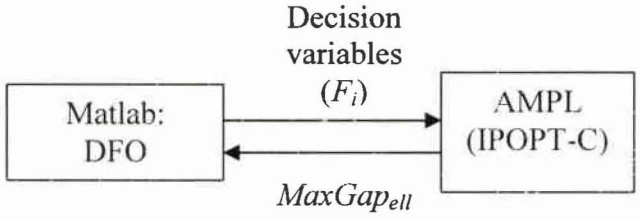

Figure D.3. Framework for Experimental Design Using DFO

Since the "expensive" function evaluation, in this case, consisted of the $MaxGap_{ell}$ problem, a Matlab/AMPL interface was used. A schematic can be seen in Figure D.3.

Appendix E

Open-Loop Optimization Results

Methods developed in Chapter 3 on CLRTO monitoring can be applied to other problem classes. In this appendix, we investigate one important issue in optimization of uncertain systems: the range of possible outcomes when the system is subject to measured disturbances. In this case, the term disturbance is used to indicate a realization of an uncertain variable. In a process plant, a typical disturbance is feed composition, which will vary about an average or nominal value. We assume that the model structure is correct and disturbances are characterized by parameter uncertainty described by intervals or an ellipsoid. We seek the range of objective function values (e.g., profit) that would be achieved by optimizing each realization when we know the parameter values without error during each optimization. Thus, we consider a sequence of realizations in which (1) we measure the feed composition disturbance (without error), (2) we optimize the model, which is perfect when the uncertain parameters have been measured, and (3) we implement the results of the optimization perfectly.

The best and worst cases considered in the open-loop problems are due solely to the variation of the disturbances when the best possible response is made to each disturbance in a perfect feedforward (open-loop) manner. This is in contrast to the monitoring method in Chapter 3, which determines the loss due to model mismatch in CLRTO when the disturbances are not measured and a specific feedback control system acts upon the process. The idealized scenario considered in this appendix would be useful in many engineering analyses. For example, we would be able to determine if a proposed plant would be profitable under the best and worst feed composition conditions. If the profit for both scenarios were greater than the corporate minimum acceptable rate of

return on investment (MARR), the project would be deemed acceptable. If the profit for both scenarios were less than the corporate minimum acceptable rate of return on investment (MARR), the project would be deemed unacceptable. If the worst-case profit were less and the best case greater than the MARR, the expected value would have to be evaluated. Naturally, the sensitivity of the results to model error would have to be investigated as well before a final decision was made.

In this appendix, a method for determining the effect of parameter uncertainty on the objective function of open-loop systems will be introduced. Then, it will be applied to several problems that have been published by other authors. For linear programs, the uncertain parameters appear in the objective function, right hand side of constraints and left hand side (technological) coefficients multiplied by the variables. Finally, we apply the method to a simple nonlinear problem to demonstrate the generality of the method.

E.1. Description of Method

Consider the maximization optimization problem in Problem E.1.

Problem E.1

$$
\begin{aligned}
z = \max_{x} \quad & J(c,x) \\
\textit{subject to} \quad & \\
& g(\theta_{in}, x) \leq 0 \\
& h(\theta_{eq}, x) = 0
\end{aligned}
$$

In Problem E.1, c and θ are the model parameters for the objective function and constraints. The subscripts "in" and "eq" correspond to inequality and equality constraints, respectively. Note that the inequality constraints can also be bounds on x. The following problem will be solved to determine the best and worst cases resulting from disturbances that are perfectly measured.

Problem E.2

$$MaxGap_{OL} = \max_{x_{BC}, z_{WC}, c_{BC}, c_{WC}, \theta_{in,BC}, \theta_{in,WC}, \theta_{eq,BC}, \theta_{eq,WC}} (J(c_{BC}, x_{BC}) - z_{WC})$$

subject to

$$\left.\begin{aligned} g(\theta_{in,BC}, x_{BC}) &\leq 0 \\ h(\theta_{eq,BC}, x_{BC}) &= 0 \end{aligned}\right\}$$ Constraints of best-case realization for Problem E.1

$$\left.\begin{aligned} z_{WC} = \max_{x_{WC}} & J(c_{WC}, x_{WC}) \\ s.t. \quad & \\ g(\theta_{in,WC}, x_{WC}) &\leq 0 \\ h(\theta_{eq,WC}, x_{WC}) &= 0 \end{aligned}\right\}$$ Worst-case realization for Problem E.1

$$\left.\begin{aligned} & c_{\min} \leq c_{BC}, c_{WC} \leq c_{\max} \\ & \theta_{in,\min} \leq \theta_{in,BC}, \theta_{in,WC} \leq \theta_{in,\max} \\ & \theta_{eq,\min} \leq \theta_{eq,BC}, \theta_{eq,WC} \leq \theta_{eq,\max} \end{aligned}\right\}$$ Interval bounds

In order to solve Problem E.2, the optimality conditions of the inner maximization problem z_{WC} are substituted into the formulation, similarly to in the bilevel formulations in Chapter 3. Since the parameter values in Problem E.2 are completely independent for the best- and worst-case scenarios, it is not necessary to derive the optimality conditions of the best-case scenario: the original best-case constraints are placed directly in the outermost optimization layer of the bilevel problem, thus easing the computational burden of Problem E.2.

Given an optimization problem of the form:

$$\begin{aligned} & \min_{x} f(x) \\ & s.t. \\ & \quad g(x) \geq 0 \end{aligned}$$

the Karush-Kuhn-Tucker (KKT) optimality conditions can be stated as (Nash and Sofer, 1996):

$$\nabla_x L(x,\lambda) = \nabla_x f(x) - \lambda \nabla_x g(x) = 0 \qquad (E.1a)$$

$$g(x) \geq 0 \qquad (E.1b)$$

$$\lambda^T g(x) = 0 \qquad (E.1c)$$

$$\lambda \geq 0 \qquad (E.1d)$$

$$\nabla^2_{xx} L(x,\lambda) \text{ is positive semi-definite} \qquad (E.1e)$$

For linear programming problems, the first-order optimality conditions (E.1a-d) are sufficient to ensure optimality. For nonlinear problems, however, the first-order optimality conditions used in the monitoring approach are not sufficient to ensure that a local optimal solution has been found. In order to check for local optimality, one may check if the Hessian of the Lagrangean function is positive semi-definite at the solution found (Clark and Westerberg, 1990). Another option is to make a grid search around the solution in order to determine if there are "better" solutions in the vicinity (Forbes *et al.*, 1994). In the nonlinear case study with independent parameter variations, the formulation using first order optimality conditions was used and the results were confirmed by Monte Carlo simulations.

E.2. Linear Programming Problems

E.2.1. Uncertain RHS and LHS of Constraints

In some situations, the user may wish to determine the effect of uncertainty in the parameters appearing in the right-hand side (RHS) and left-hand side (LHS) of the constraints. The goal of the formulation shown in this appendix is to calculate the maximum objective function values for the best-case and worst-case optimization scenarios given this uncertainty. Since the uncertain parameter values are different in Problem E.2, both the best- and worst-cases are determined in the solution, along with the parameter values.

Problem E.3 was taken from Chinneck and Ramadan (2000). In this problem, there are uncertain parameters in the LHS coefficients and in the RHS coefficients of both equality and inequality constraints simultaneously.

Problem E.3

$$
\begin{aligned}
&\min_{x_1, x_2} && (x_1 + x_2) \\
&\textit{subject to} \\
& && -x_1 + x_2 \geq \theta_1 \\
& && \theta_2 x_1 + x_2 = \theta_3 \\
& && x_1 \geq 0 \\
& && 0 \leq x_2 \leq 3
\end{aligned}
$$

where the interval uncertainty regions are given in the following (with the symbol θ used for uncertain parameters to be consistent with the original paper):

$$
\begin{aligned}
-2 &\leq \theta_1 \leq -1 \\
2 &\leq \theta_2 \leq 3 \\
3 &\leq \theta_3 \leq 4
\end{aligned}
$$

The formulation in Problem E.2 was used to solve Problem E.3. The worst-case scenario sub-problem was replaced by its KKT conditions (first-order optimality conditions), and the overall problem was then solved with IPOPT-C. Since Problem E.3 is a minimization problem, $Maxgap_{OL}$ was calculated as worst case minus best case. At the solution given in Table E.1, $Maxgap_{OL}$ is 1.33, where the best case objective is 1.0 and the worst case objective is 2.33. The values obtained for the parameter and variable values at the best- and worst-case solutions agree with the results in Chinneck and Ramadan (2000). The different starting points used for this case study can be seen in Table E.2.

Table E.1. Solution of Problem with Uncertain LHS and RHS Coefficients

	Best-Case Scenario	Worst-Case Scenario
$(x_1 + x_2)$	1.0	2.33
x_1	1.0	1.67
x_2	0.0	0.67
θ_1	-1.67	-1.0
θ_2	3.0	2.0
θ_3	3.0	4.0

This example has demonstrated the application of the method to a system with uncertainty in right- and left-hand side coefficients in equality and inequality constraints.

E.2.2. Uncertain Objective Function Coefficients

Another application of the method is to systems with uncertain objective function coefficients. This situation is common in process applications where the costs of feed and energy and the sales price are uncertain, or when evaluating projects that will begin operation in months to years in the future. Another problem taken from Chinneck and Ramadan (2000) is used to illustrate this situation.

Table E.2. Starting Points for the Problem with Uncertain LHS and RHS Coefficients

Starting Points	CPU sec	# func. eval	# restarts	Solution
$x_{BC} = x_{WC} = \mathbf{0}$; $\theta^0 = \theta_{nom}$*; $\lambda^0_{BC} = \lambda^0_{WC} = \mathbf{0}$	1.281	2,969	0	Good
$x_{BC} = x_{WC} = x_{nom}$; $\theta^0 = \theta_{nom}$*; $\lambda^0_{BC} = \lambda^0_{WC} = \lambda_{nom}$	1.562	3,129	0	Good

* θ_{nom} was taken as the average value of the interval for each θ_i

Problem E.4

$$\begin{aligned} &\min_{x_1, x_2} && (\theta_1 x_1 + \theta_2 x_2) \\ &\textit{subject to} \\ &&& 3x_1 - 5x_2 \geq -15 \\ &&& 4x_1 - 2.5x_2 \geq -10 \\ &&& -x_1 + 0.5x_2 \geq -1 \\ &&& x_1 \leq 2 \\ &&& x_2 \geq -3 \end{aligned}$$

where:

$-1 \leq \theta_1 \leq 1$

$-1 \leq \theta_2 \leq 1$

The worst-case scenario subproblem was replaced by its KKT conditions, and the overall problem was then solved with IPOPT-C. In the solution (Table E.3), $Maxgap_{OL}$ was equal to 7.38, where the best case objective is -7.38 and the worst case objective is 0.0. These results are consistent with the values reported by Chinneck and Ramadan (2000).

In Chinneck and Ramadan (2000), optimal values for x1, x2, θ1 and θ2 are not reported. The authors point out that the challenge associated with this test problem is that the worst-case scenario of cost coefficients lies in the center of the uncertainty region, at (0,0), which coincides with the results in Table E.3. The computational experience can be seen in Table E.4.

Table E.3. Solution of the Problem with Uncertain Cost Coefficients

	Best-Case Scenario	Worst-Case Scenario
x_1	-4.38	-0.74
x_2	-3.0	-0.46
θ_1	1.0	0.0
θ_2	1.0	0.0
$(\theta_1 x_1 + \theta_2 x_2)$	-7.38	0.0

Table E.4. Starting Points for the Problem with Uncertain Cost Coefficients

Starting Points	CPU sec	# func. eval	# restarts	Solution
$x_{BC} = x_{WC} = \mathbf{0}$; $\theta^0 = \theta_{nom}$*; $\lambda^0_{BC} = \lambda^0_{WC} = \mathbf{0}$	2.016	3,298	0	Good
$x_{BC} = x_{WC} = x_{nom}$; $\theta^0 = \theta_{nom}$*; $\lambda^0_{BC} = \lambda^0_{WC} = \lambda_{nom}$	2.906	5,729	0	Good

*θ_{nom} was taken as the average value of the interval for each θ_i

E.2.3. Gasoline-Blending Problem

This section presents the application of the method to a linear programming problem with uncertainty in the LHS coefficients. Even though this topic has been covered in Chapter 3, the application of the open-loop method to the gasoline-blending problem is shown to emphasize the difference between finding profit bounds *due to measured disturbances* and closed-loop performance monitoring, which finds the profit loss *due to model mismatch.*

For the gasoline-blending problem, this analysis would be useful for assessing the effect of uncertainty in purchased component properties prior to the purchase; i.e., before the material was delivered and the properties were (exactly) measured. For this case study, intervals of ±1.0 (octane numbers, psi) were assigned to all parameters. After applying Problem E.2 to this case study (without the feedback information), the results in Table E.5 are obtained, where Pr_{BC} = \$ 14,090.4 / day (which is the same value as the *MAP* calculated in Section 3.2.2), and Pr_{WC} = \$ 8,569.3 / day.

Table E.5. Gasoline-Blending Problem: Open-Loop Results

	$Q^{oct}_{i,BC}$ (octane numbers)	$Q^{RVP}_{i,BC}$ (psi)	$F_{i,BC}$ (bbl / day)	$Q^{oct}_{i,WC}$ (octane numbers)	$Q^{RVP}_{i,WC}$ (psi)	$F_{i,WC}$ (bbl / day)
Reformate	94.1	1.7	5,258.2	92.1	3.7	5,815.0
LSR Naphtha	65.3	9.9	1,353.0	63.3	11.9	867.7
n-Butane	93.5	137.0	388.8	91.5	139	314.7
FCC Gas	84.6	6.4	0.0	83.7	7.3	0.0
Alkylate	96.6	6.7	0.0	96.6	6.7	0.0

Due to the nonconvexity of Problem 3.5, it was solved for different starting points in order to attempt to detect better local optima. The starting points can be seen in Table E.6.

All starting points yielded the same objective function value. The difference between best- and worst case scenarios of (\$14,090.4/day - \$8,569.3/day =) \$5,521.1/day obtained in this section is much larger than the closed-loop maximum profit gap ($Maxgap_{int}$) of \$ 3,024.9/day in Chapter 3. However, we recall that the two approaches have very different goals. The goal in Chapter 3 was to determine what would be the largest profit loss for the closed-loop system with nominal parameter values in the CLRTO model. In that case, the uncertain plant parameters were assumed unmeasured, and the two cases were evaluated using the *same* uncertain parameter values. In this problem, the goal is to determine the largest difference between a "perfect" optimization given the best-case plant parameter scenario, and a "perfect" optimization model given the worst-case plant parameter scenario. The two cases involve *different* values of the uncertain parameters. This would be the case if the plant parameters were measured.

$$Q_{i,BC}^{j,0} = Q_{i,WC}^{j,0} = Q_{i,nom}^{j}$$

$$F_{i,1}^{0} = [1{,}400.0 \;\; 1{,}400.0 \;\; 1{,}400.0 \;\; 1{,}400.0 \;\; 1{,}400.0]$$

$$F_{i,2}^{0} = [5{,}695.6 \;\; 942.5 \;\; 361.0 \;\; 0.0 \;\; 0.0]$$

Table E.6. Starting Points for the Open-Loop Gasoline-Blending Problem

Starting Points	CPU sec	# func. eval	# restarts	Solution
$F_{i,BC}^{0} = F_{i,WC}^{0} = F_{i,1}^{0}$; $\lambda_{BC}^{0} = \lambda_{WC}^{0} = \mathbf{0}$	14.500	7,973	0	Good
$F_{i,BC}^{0} = F_{i,WC}^{0} = F_{i,1}^{0}$; $\lambda_{BC}^{0} = \lambda_{WC}^{0} = \lambda_{nom}$	14.594	7.953	0	Good
$F_{i,BC}^{0} = F_{i,nom}^{0} = F_{i,2}^{0}$; $\lambda_{BC}^{0} = \lambda_{nom}^{0} = \mathbf{0}$	15.375	8,849	0	Good
$F_{i,BC}^{0} = F_{i,nom}^{0} = F_{i,2}^{0}$; $\lambda_{BC}^{0} = \lambda_{nom}^{0} = \lambda_{nom}$	14.250	7,976	0	Good

E.2.4. Summary

In the previous sections, the open-loop applications of the monitoring criteria developed in this work to linear problems present some advantages over the best published method to date on evaluating the effects of parameter uncertainty on linear programming problems (Chinneck and Ramadan, 2000).

- First, several cases were solved in a single optimization problem, where no enumeration was required. These cases involved: LHS and RHS parameter uncertainty, uncertain equality constraints, and uncertain cost coefficients in problems where the worst-case values were not at the bounds of the interval.
- Second, the monitoring methods provide objective function and optimization variable values for the best- and worst-case scenarios, as well as their respective parameter realizations.
- Third, uncertainty using deterministic (interval) or stochastic correlation (ellipsoidal) characterizations can be handled. This will be demonstrated in the following section for a nonlinear system, but the method can also be applied to linear problems.

The method for evaluating the effects of measured disturbances on optimal results is applied to a nonlinear system in the following section.

E.3. Nonlinear Programming Problems: Reactor-Separator System

Consider the reactor-separator system shown in Figure E.1, which represents a problem from Grossmann and Sargent (1978). The isothermal continuous flow stirred tank reactor (CSTR) with volume V is fed with fresh feed and a recycle stream with different compositions. The flow and concentration of A in the fresh feed are F_{A0} and C_{A0}. The components leave the reactor with flow F and with molar fractions x_a, x_b, x_r, x_x and x_y. It is assumed that the desired product R only leaves the system through the top of the

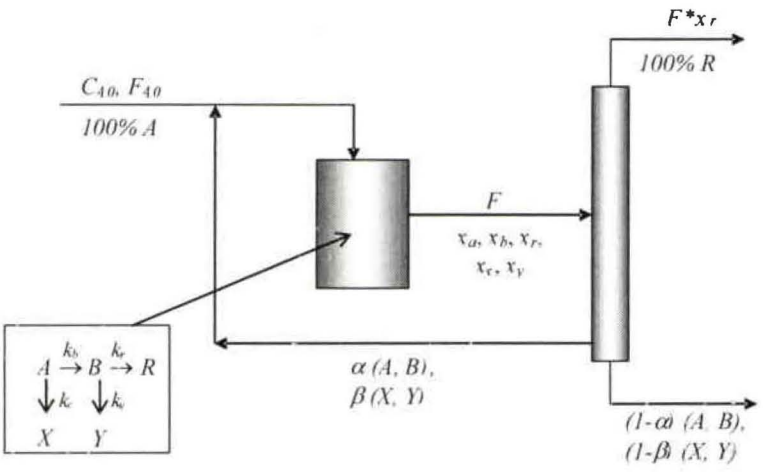

Figure E.1. Reactor-Separator System

distillation column and that pure R is obtained at the rate of F_r. The flowrate at the bottom of the column is the reactor effluent that is not recycled. Fraction α of components A and B and fraction β of components X and Y are recycled back to the inlet stream of the reactor. The separation required by the model would require several stages; however, Figure E.1 does not show the separation units in detail to be consistent with the figure in the original paper from Grossmann and Sargent (1978).

The goal of the nominal optimization problem is to minimize the design and operating costs, which in this case are comprised of the design cost (assumed to be proportional to reactor volume) and the cost for recycle (pumping equipment and operating cost for pumping and heating/cooling). The uncertain optimization problem handles variation in reaction rate constants; therefore, the volume of the reactor V, flow F and fractions x_a, x_b, x_r, x_x, x_y, α and β must be calculated subject to the worst-case realization of the uncertain parameters. The formulation for this problem is simpler than in Problem E.2 since only the set of KKT conditions corresponding to the worst-case scenario needs to be included. The steady-state problem and uncertainty in the rate constants are given in the following problem.

Problem E.5

$$\min_{x_a, x_b, x_r, x_x, x_y, F, V, \alpha, \beta} \quad 10V + 0.125\,[\alpha F(x_a + x_b) + \beta F(x_x + x_y)]$$

subject to

$$\begin{aligned}
& F_{A0} - x_a F\,(1-\alpha) - V\,C_{a0}\,(k_b + k_X)\,x_a && = 0 \\
& -x_b F\,(1-\alpha) + V\,C_{a0}\,[k_b x_a - (k_R + k_Y)\,x_b\,] && = 0 \\
& -x_x F\,(1-\beta) + V\,C_{a0}\,k_x x_a && = 0 \\
& -x_y F\,(1-\beta) + V\,C_{a0}\,k_y x_b && = 0 \\
& -x_r F + V\,C_{A0}\,k_r x_b && = 0 \\
& F_r - x_r F && \leq 0 \\
& x_A + x_B + x_R + x_X + x_Y - 1 && = 0
\end{aligned}$$

where the uncertain parameters have the following ranges.

$$\begin{aligned}
0.32\ h^{-1} &\leq k_b \leq 0.48\ h^{-1} \\
0.08\ h^{-1} &\leq k_r \leq 0.12\ h^{-1} \\
0.016\ h^{-1} &\leq k_x \leq 0.024\ h^{-1} \\
0.008\ h^{-1} &\leq k_y \leq 0.012\ h^{-1}
\end{aligned}$$

The model structure takes advantage of the conservation of moles in the specific reaction stoichiometry in Figure E.1. As a result, the reactor inlet and outlet molar flows rates are equal, and the inlet and outlet total molar concentrations are the same, at C_{A0}. The results for the nominal optimization model (using the nominal parameter values from Table E.7) can be seen in Table E.8.

Table E.7. Fixed Parameters and Nominal Values of Uncertain Parameters for the Reactor-Separator System

Parameter	Nominal Values
F_{a0}	100 mole/h
F_r	70 mole/h
C_{a0}	100 mole/m^3
k_b	0.4 h^{-1}
k_r	0.1 h^{-1}
k_x	0.02 h^{-1}
k_y	0.01 h^{-1}

Table E.8. Results for Reactor-Separator System – Nominal Parameter Values

Objective = $ 151.916	$k_b = 0.40\ h^{-1}$	$x_a = 0.1841$
$V = 12.3477\ m^3$	$k_r = 0.10\ h^{-1}$	$x_b = 0.5669$
$F = 327.506$ mole/h	$k_x = 0.0020\ h^{-1}$	$x_r = 0.2137$
$\alpha = 0.9250$	$k_y = 0.010\ h^{-1}$	$x_x = 0.0139$
$\beta = 9.69e\text{-}10$		$x_y = 0.0214$

In this case study, there was no need to determine the best-case scenario, since the goal was to determine the *overdesign* needed due to parametric uncertainty. By overdesign, we mean the increase in reactor volume (from the nominal value in Table E.8) and changes in plant operating conditions that yields the lowest (optimal) cost when the uncertain parameters are within their uncertainty bounds. Naturally, excessive overdesign of the reactor volume will result in unjustified costs.

Grossmann and Sargent (1978) calculated the gradients of equations numerically in order to simplify the solution strategy. In their work, uncertain coefficients in equality constraints were fixed at the values that were selected to be worst case based on "engineering knowledge" in order to simplify the solution strategy. The method outlined in Section E.1 determines these worst case coefficient values automatically.

The results are consistent with expectations. The recycle of unreacted A and B is nearly maximized ($\alpha \approx 1$), while the recycle of undesired X and Y is essentially zero

Table E.9. Results for Reactor-Separator System – Independent Parameters, Interval Uncertainty

Objective = $ 185.115	$k_b = 0.32\ h^{-1}$	$x_a = 0.1863$
$V = 15.1188\ m^3$	$k_r = 0.08\ h^{-1}$	$x_b = 0.5788$
$F = 371.4$ mole/h	$k_x = 0.0024\ h^{-1}$	$x_r = 0.1885$
$\alpha = 0.9552$	$k_y = 0.012\ h^{-1}$	$x_x = 0.0182$
$\beta = 2.25e\text{-}12$		$x_y = 0.0283$

Table E.10. Starting Points Used for Obtaining the Solution in Table E.9

Starting Points	CPU sec	# func. eval	# restarts	Solution
$x = \mathbf{0.2}$; $V,F = 1.0$; $\alpha, \beta = 0.5$, $k^0 = k_{nom}$*; $\lambda^0 = \mathbf{0}$	0.031	46	0	Good
All parameters and variables at nominal values	0.047	29	0	Good

*k_{nom} was taken as the average value of the interval for each k_i

($\beta \approx 0$). The solution was clearly obtained at the worst-case scenario of the parameter values, which is the most unfavourable to the generation of desired product R (k_b and k_r – reaction rates on the main product route– at their lower bounds, and k_x and k_y – reaction rates on side-reaction routes – at their upper bounds).

The values obtained for the reaction rate constants in Table E.9 match those selected by Grossmann and Sargent (1978), which indicates that their judgements were good. Grossmann and Sargent (1978) reported an objective function of \$185.66 and a volume V=15.5854 m^3. Table E.9 shows a smaller volume (V=15.1188 m^3) and lower cost (\$185.115). Our results were verified by running 10,000 Monte Carlo simulations (optimizations) on uniformly distributed uncertain parameters, which yielded a worst-case objective function of \$185.115 and V = 15.119 m^3. In the next sections, the effect of deterministic and stochastic correlation among the parameters is presented.

E.3.1. Deterministic Parameter Correlation

The approach in Section E.1 can be easily modified to incorporate deterministic knowledge about parameter correlation. In order to illustrate this, we defined a modification to the Reactor-Separator problem that was not defined in the original paper. If reactions A→B and B→R use the same catalyst active sites, the total number of these sites is constant, and the catalyst manufacturing process has variability in the production of the ratio of sites, there would be negative correlation between reaction rate constants k_B and k_R. When adding the deterministic correlation structure given in equation (E.2) as another equality constraint in the original problem, the results in Table E.11 are obtained.

Table E.11. Results for Reactor-Separator System – Worst-Case Scenario with Deterministic Correlation

Objective = \$ 172.4	$k_b = 0.48$ h^{-1}	$x_a = 0.1374$
$V = 14.0522$ m^3	$k_r = 0.08$ h^{-1}	$x_b = 0.6227$
$F = 354.8$ mole/h	$k_x = 0.024$ h^{-1}	$x_r = 0.1972$
$\alpha = 0.9442$	$k_y = 0.012$ h^{-1}	$x_x = 0.0131$
$\beta = 3.2e\text{-}13$		$x_y = 0.0296$

$$\left(k_B - k_{B,nom}\right) = -\frac{\left(k_{B,\max} - k_{B,\min}\right)}{\left(k_{R,\max} - k_{R,\min}\right)}\left(k_R - k_{R,nom}\right) \qquad (E.2)$$

Since the parameters k_B and k_R are negatively correlated, the method identified the worst-case scenario as having k_B at its upper bound and k_R at its lower bound. This indicates that, when compared to the nominal case, A would have a faster conversion to B, while B would take longer to be converted to R. The results in Table E.11 were confirmed by running 1,000 Monte Carlo simulations, in which the largest (worst-case) objective function found was of \$171.9 with a corresponding volume of $V = 14.0321$ m^3.

This would support the fact that the parameter settings in Table E.11 correspond to the worst-case scenario can also be confirmed by simulating the opposite, best-case, scenario (giving the largest k_R and the smallest k_B possible), which yields a much smaller reactor volume ($V = 11.583$ m^3) and a lower cost (\$143.7).

The reason why the best-case reactor volume is smaller than the nominal one (11.583 m^3 versus 12.3477 m^3) is because the negative correlation structure requires one of the reaction rates to be below its nominal value, thus resulting in a faster conversion of reactants. Even though the other rate is above its nominal value, in this case, the reduction in one of the rates made the overall conversion (A $\rightarrow$ R) higher, leading to a smaller residence time.

E.3.2. Stochastic Parameter Correlation

In this case, we introduce ellipsoidal correlation in the uncertain parameters that was not in the original paper. We assume that the four reaction rate constants [k_b k_r k_x

$k_y]^T$ are multivariate normally distributed with the variance-covariance matrix shown below.

$$V(\mathbf{k}) = \begin{bmatrix} 6.746.10^{-4} & -1.670.10^{-4} & 0 & 0 \\ -1.670.10^{-4} & 4.216.10^{-5} & 0 & 0 \\ 0 & 0 & 1.687.10^{-6} & 0 \\ 0 & 0 & 0 & 4.216.10^{-7} \end{bmatrix}$$

In order to obtain the values used in the variance-covariance matrix in this example, the reaction rates were assumed to belong to a multivariate normal distribution with 4 degrees-of-freedom, at 95% confidence levels. The largest deviation allowed for each individual reaction rate was the absolute deviation from the nominal value reported in Problem E.5, which are the interval bounds given by Grossmann and Sargent (1978). Note that the rate constants k_b and k_r have a negative correlation (= -0.99), so that the uncertainty is qualitatively similar to Section E.3.1. In a true plant, the correlation structure in $V(\mathbf{k})$ could be obtained from designed laboratory or plant experiments. This correlation information is included in the problem as the additional inequality constraint (E.3).

$$(\mathbf{k} - \mathbf{k}_{nom})^T \mathbf{V}(\mathbf{k})^{-1} (\mathbf{k} - \mathbf{k}_{nom}) \leq \chi^2_{\alpha,dof} \qquad (E.3)$$

In equation (E.3), $\mathbf{k}$ is the vector of uncertain parameters, α is the confidence level, and *dof* is the number of degrees of freedom, which is equal to the number of uncertain parameters in the ellipsoid (Rooney and Biegler, 2001). In this example, α = 95% and the number of degrees-of-freedom is four.

A projection of the four-dimensional parameter distribution on the k_b, k_r plane can be seen in Figure E.2. The circles correspond to a diagonal matrix V(k), when there is no correlation between k_b and k_r, and the filled dots correspond to the correlated case. The bold rectangle corresponds to the interval description of uncertainty used in Problem E.2.

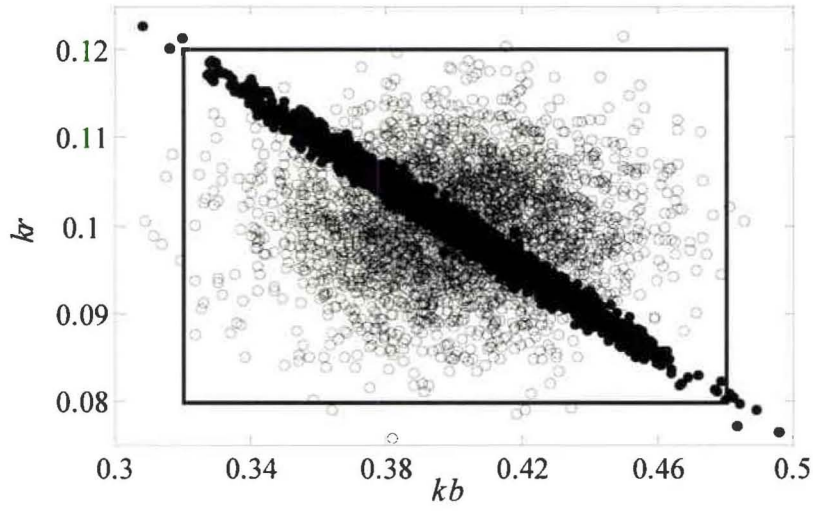

Figure E.2. Parameter Uncertainty Descriptions – Reactor-Separator Case Study (o - no correlation; • - correlation = -0.99)

Table E.12. Results for Reactor-Separator System – Stochastic Correlation

Objective = \$ 171.2	$k_b = 0.4789\ h^{-1}$	$x_a = 0.1385$
$V = 14.0132\ m^3$	$k_r = 0.0800\ h^{-1}$	$x_b = 0.6242$
$F = 348.6$ mole/h	$k_x = 0.020\ h^{-1}$	$x_r = 0.2008$
$\alpha = 0.9350$	$k_y = 0.0100\ h^{-1}$	$x_x = 0.0112$
$\beta = 5.1e\text{-}10$		$x_y = 0.0253$

The solution for the worst-case is given in Table E.12. As can be observed in Table E.12, the directionality of the results was the same as when considering deterministic correlation between k_b and k_r; i.e., k_b was above its nominal value, while k_r was below its nominal value. The design for the system with ellipsoidal uncertainty contains a slightly smaller reactor volume and lower cost than the interval uncertainty with deterministic correlation, thus being less conservative.

The computational experience for the cases with deterministic and stochastic parameter correlation was very similar to the one with no correlation: very short computation times were needed (< 0.1 CPU seconds), no restarts were required, and the same optimal solution was obtained given different starting points for both cases.

E.4. Summary

This appendix demonstrates the application of the monitoring methods developed in Chapter 3 to open-loop systems. In these systems, the method determines the worst-(best-) case scenario of an optimization problem (without feedback) for uncertain parameters described by intervals, deterministic correlation or statistical correlation. There are likely many industrial "open-loop" applications in this category for process design and process operations, where the effects of decisions cannot be measured until the operation has been completed.

Previously published methods for evaluating the effect of uncertainty on the objective function of linear programming problems require multiple enumerations for equality constraints and cannot deal with stochastic parameter correlation. The methods presented in this thesis require only a single solve and provide not only the best- and worst-case objective function values, but also the variable values and uncertain parameter values at the solution. The advantages of the methods developed in this work are achieved by accepting the additional burden of solving a bilevel optimization problem, which is reformulated as a non-convex, single-level problem.

A small nonlinear problem was solved to confirm that the method can be extended to nonlinear systems. However, in this case, first-order conditions are not sufficient to guarantee local optimality. The use of first order conditions is consistent with Clark and Westerberg (1990). After a solution is obtained, the second order conditions must be verified in order to establish that a locally optimal solution has been found.

Appendix F

Full Formulation of $MaxGap_{int}$

This appendix presents the complete formulation of Problem 3.5 ($MaxGap_{int}$) as a single-level optimization. When substituting the inner optimization problems of Problem 3.5 with their optimality conditions, the following optimization problem is obtained:

Problem F.1:

$$Maxgap_{int} = \max_{Pr_{BC}, Pr_{nom,CL}, \varepsilon^j, Q_i^j, \lambda_{nom}, \lambda_{BC}} (Pr_{BC} - Pr_{nom,CL})$$

subject to

$$-\nabla_{F_{i,nom}} Pr_{nom,CL} - \sum_{k=1}^{\#ineq} \lambda_{nom,k} \nabla_{F_{i,nom}} g_{nom,k} = 0$$

$$\lambda_{nom,k} g_{nom,k} = 0 \quad , k = 1 \ldots \#ineq$$

$$g_{nom,k} \geq 0$$

$$\lambda_{nom,k} \geq 0$$

} KKT conditions for Nominal CLRTO

$$-\nabla_{F_{i,BC}} Pr_{BC} - \sum_{k=1}^{\#ineq} \lambda_{BC,k} \nabla_{F_{i,BC}} g_{BC,k} = 0$$

$$\lambda_{BC,k} g_{BC,k} = 0 \quad , k = 1 \ldots \#ineq$$

$$g_{BC,k} \geq 0$$

$$\lambda_{BC,k} \geq 0$$

} KKT conditions for "Best" CLRTO

$$\varepsilon^j \sum_{i=1}^{n} F_{i,nom} = \sum_{i=1}^{n} F_{i,nom} \left(Q_i^j - Q_{i,nom}^j \right) \quad , \quad j = oct, RVP$$

$$Q_{i,\min}^j \leq Q_i^j \leq Q_{i,\max}^j \quad , \quad j = oct, RVP$$

} Interval Bounds

where, for the KKT conditions of the nominal CLRTO model:

$$Pr_{nom,CL} = \sum_{i=1}^{n}(value - cost_i)F_{i,nom} \quad (F.1)$$

$$g_{nom,1} = -\sum_{i=1}^{n} F_{i,nom}(Q_{i,nom}^{oct} + \varepsilon^{oct}) + Q_{blend,max}^{oct}\sum_{i=1}^{n} F_{i,nom} \geq 0 \quad (F.2)$$

$$g_{nom,2} = -\sum_{i=1}^{n} F_{i,nom}(Q_{i,nom}^{RVP} + \varepsilon^{RVP}) + Q_{blend,max}^{RVP}\sum_{i=1}^{n} F_{i,nom} \geq 0 \quad (F.3)$$

$$g_{nom,3} = \sum_{i=1}^{n} F_{i,nom}(Q_{i,nom}^{oct} + \varepsilon^{oct}) - Q_{blend,min}^{oct}\sum_{i=1}^{n} F_{i,nom} \geq 0 \quad (F.4)$$

$$g_{nom,4} = \sum_{i=1}^{n} F_{i,nom}(Q_{i,nom}^{RVP} + \varepsilon^{RVP}) - Q_{blend,min}^{RVP}\sum_{i=1}^{n} F_{i,nom} \geq 0 \quad (F.5)$$

$$g_{nom,5} = -\sum_{i=1}^{n} F_{i,nom} + F_{blend,max} \geq 0 \quad (F.6)$$

$$g_{nom,6} = \sum_{i=1}^{n} F_{i,nom} - F_{blend,min} \geq 0 \quad (F.7)$$

$$g_{nom,7} = -F_{Ref,nom} + F_{Ref,max} \geq 0 \quad (F.8)$$

$$g_{nom,8} = F_{Ref,nom} - F_{Ref,min} \geq 0 \quad (F.9)$$

$$g_{nom,9} = -F_{LSR,nom} + F_{LSR,max} \geq 0 \quad (F.10)$$

$$g_{nom,10} = F_{LSR,nom} - F_{LSR,min} \geq 0 \quad (F.11)$$

$$g_{nom,11} = -F_{But,nom} + F_{But,max} \geq 0 \quad (F.12)$$

$$g_{nom,12}: \quad F_{But,nom} - F_{But,min} \geq 0 \quad (F.13)$$

$$g_{nom,13}: \quad -F_{FCC,nom} + F_{FCC,max} \geq 0 \quad (F.14)$$

$$g_{nom,14}: \quad F_{FCC,nom} - F_{FCC,min} \geq 0 \qquad (F.15)$$

$$g_{nom,15}: \quad -F_{Alk,nom} + F_{Alk,max} \geq 0 \qquad (F.16)$$

$$g_{nom,16}: \quad F_{Alk,nom} - F_{Alk,min} \geq 0 \qquad (F.17)$$

For the KKT conditions of the "best" CLRTO, the equations are very similar to equations (F.1) to (F.17). The only differences are that (1) the subscript *nom* is replaced by the subscript *BC*, and (2) in equations (F.2) to (F.5), there is no feedback term ε, since in this case, there is no mismatch between the model and the plant.